การจำลองเชิงคอมพิวเตอร์สำหรับการฉีดเข้าแบบประยุกต์กับเทอร์โมพลาสติกอะสัณฐานเอบีเอส

นางสาว บุศรินทร์ อินทเศียร

COMPUTER SIMULATION FOR INJECTION MOULDING APPLIED TO AMORPHOUS
THERMOPLASTIC ABS

MISS BUSARIN INTASIAN

A Thesis Submitted in Partial Fulfillment of the Requirements

for the Degree of Master of Science in Petrochemistry and Polymer Science

Program of Petrochemistry and Polymer Science

Faculty of Science

Chulalongkorn University

Academic Year 2000

Thesis Title	COMPUTER SIMULATION FOR INJECTION MOULDING APPLIED TO AMORPHOUS ABS

Thesis Title   COMPUTER SIMULATION FOR INJECTION MOULDING   APPLIED TO AMORPHOUS ABS

By   Miss Busarin Intasian

Department   Petrochemistry and Polymer Science

Thesis Advisor   Professor Pattarapan Prasassarakich, Ph.D.

Thesis Co-Advisor   Frederick H. Axtell, Ph.D.

Accepted by the Faculty of Science, Chulalongkorn University in Partial Fulfillment of the Requirements for the Master's Degree.

………………………………/…………Dean of Faculty of Science

(Associate Professor Wanchai Phothiphichitr, Ph.D.)
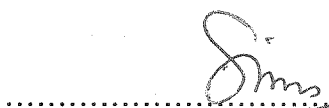
Thesis Committee

………………………………………Chairman

(Associate Professor Supawan Tantayanon, Ph.D.)

………………………………………Thesis Advisor

(Professor Pattarapan Prasassarakich, Ph.D.)

………………………………………Thesis Co-advisor

(Frederick H. Axtell, Ph.D.)

………………………………………Member

(Associate Professor Wimonrat Trakarnpruk ,Ph.D.)

………………………………………Member

(Sim Kock Seng , M.Sc.)

A comparison between the pressure predicted by the Moldflow$\circledR$ simulation software and measured during the injection moulding experiment was made to study the effects of injection moulding parameters on impact performance. The simulation was investigated for the Moldflow standard database and personal database which was prepared by testing of ABS properties. The cavity pressures of rectangular plaque mould were measured by two pressure transducers fitted near the gate and far from the gate. The comparison was made using three grades of amorphous thermoplastic ABS. For the study of the effects of injection moulding parameters on the impact properties, two important influence parameters were the injection speed and melt temperature. Increasing injection speed increased the impact properties which caused by molecular degradation. Low melt temperature gave slightly reduction in impact properties because of higher internal stress.

The simulation which the material information input was Moldflow standard database or personal database showed insignificant difference of the predicted pressure for Lustran 250. For Lustran 440 and Lustran 640, the simulation predicted higher pressure values as personal database was selected. The simulation was done by the selection of Moldflow standard database for ABS 250 to compare with the measurement. The simulation showed disagreement to the measurement. The fill times were different from the measured values. The differences in the prediction were attributed to the over-estimation of the cooling rate of Moldflow. The experimental mould had very simple cooling system which possibly was inefficient in terms of Moldflow software design assumptions. In addition, Moldflow could over-estimate the shear-heating during the injection phase of nozzle, runners and gate system.

สาขาวิชา.ปิโตรเคมีและวิทยาศาสตร์พอลิเมอร์……… ลายมือชื่อ
หลักสูตร..ปิโตรเคมีและวิทยาศาสตร์พอลิเมอร์……… ลายมือชื่ออาจารย์ที่ปรึกษา……………………….
ปีการศึกษา ..2543………………………………. ลายมือชื่ออาจารย์ที่ปรึกษาร่วม………………………

บุศรินทร์ อินทเศียร : การจำลองเชิงคอมพิวเตอร์สำหรับการฉีดเข้าแบบประยุกต์กับเทอร์โมพลาสติก อสัณฐานเอบีเอส. (COMPUTER SIMULATION FOR INJECTION MOULDING APPLIED TO AMORPHOUS THERMOPLASTIC ABS) อ. ที่ปรึกษา : ศ.ดร.ภัทรพรรณ ประศาสน์สารกิจ, อ. ที่ปรึกษาร่วม : ดร.เฟรดเดอริก เอช แอ็กซ์เทล , 175 หน้า. ISBN 974-346-751-3.

งานวิจัยนี้ได้เปรียบเทียบความดันที่ทำนายโดยโปรแกรม Moldflow® สำหรับจำลองแบบงานฉีดพลาสติกกับความดันที่เกิดขึ้นจริงในแม่พิมพ์ โดยศึกษาถึงผลของตัวแปรงานฉีดต่อสมบัติการทนแรงกระแทกของชิ้นงานสำหรับการจำลองแบบด้วยโปรแกรมคอมพิวเตอร์ได้ศึกษาถึงการใช้ฐานข้อมูลสมบัติของวัสดุที่สร้างเองจากการทดสอบสมบัติเม็ดพลาสติกเอบีเอสเป็นข้อมูลป้อนเข้าเปรียบเทียบกับฐานข้อมูลที่มีอยู่แล้วในโปรแกรม สำหรับการวัดความดันในแม่แบบที่เกิดขึ้นจริงทำได้โดยติดอุปกรณ์วัดความดันไว้ที่ตำแหน่งใกล้ทางเข้าพลาสติกหลอมและไกลทางเข้า การเปรียบเทียบนี้จากการใช้เทอร์โมพลาสติกเอบีเอส 3 เกรด สำหรับการศึกษาผลของตัวแปรการฉีดพลาสติกต่อสมบัติการทนแรงกระแทกของชิ้นงานนั้นพบว่าสองตัวแปรที่มีความสำคัญคือ ความเร็วการฉีด และอุณหภูมิพลาสติกหลอม เมื่อความเร็วการฉีดเพิ่มขึ้นสมบัติการทนแรงกระแทกเพิ่มขึ้นเนื่องจากการจัดเรียงตัวของโครงสร้างโมเลกุล เมื่ออุณหภูมิพลาสติกหลอมสูงสมบัติการทนแรงกระแทกลดลงเนื่องจากการสลายตัวของโครงสร้างพลาสติกหลอม เมื่ออุณหภูมิพลาสติกหลอมต่ำสมบัติการทนแรงกระแทกลดลงเนื่องจากความเค้นตกค้างสูงขึ้น

จากผลการจำลองเมื่อเลือกข้อมูลวัสดุจากฐานข้อมูลมาตรฐานของโปรแกรม และจากฐานข้อมูลสร้างเองนั้นให้ผลการทำนายที่ไม่แตกต่างกันสำหรับพลาสติกเกรด Lustran 250 ส่วนการเลือกใช้ฐานข้อมูลสร้างเองโปรแกรมทำนายค่าความดันสำหรับพลาสติกเกรด Lustran 440 และ Lustran 640 สูงกว่าเมื่อเลือกใช้ฐานข้อมูลมาตรฐานของโปรแกรม ในการเปรียบเทียบความดันคำนวณกับความดันที่วัดได้โดยใช้ข้อมูลพลาสติกเกรด Lustran 250 จากฐานข้อมูลมาตรฐานโปรแกรมทำนายค่าความดันไม่สอดคล้องกับความดันที่วัดจริง และการทำนายเวลาการเติมเต็มแม่แบบของพลาสติกหลอมแตกต่างกับเวลาที่วัดได้ ความแตกต่างที่เกิดขึ้นนี้อาจเกิดจากการประเมินอัตราการหล่อเย็นของโปรแกรม Moldflow สูงมากเกิน แม่แบบในการทดลองระบบการหล่อเย็นแบบง่ายซึ่งไม่เพียงพอสำหรับสมมุติฐานของโปรแกรม Moldflow รวมทั้ง Moldflow อาจทำนายความร้อนมากเกินเกิดจากการเฉือนตัวของหัวฉีด ทางวิ่ง และระบบทางเข้าระหว่างช่วงการฉีด

สาขาวิชา.ปิโตรเคมีและวิทยาศาสตร์พอลิเมอร์.......... ลายมือชื่อนิสิต ....
หลักสูตร..ปิโตรเคมีและวิทยาศาสตร์พอลิเมอร์.......... ลายมือชื่ออาจารย์ที่ปรึกษา ....
ปีการศึกษา.. 2543............................ ลายมือชื่ออาจารย์ที่ปรึกษาร่วม ....

ACKNOWLEDGEMENTS

CONTENTS

CONTENTS (Continued)

CONTENTS (Continued)

CONTENTS (Continued)

CONTENTS (Continued)

LIST OF TABLES

LIST OF FIGURES

FIGURE   PAGE

LIST OF ABBREVIATIONS

Moldflow	:	Moldflow®
Exp. No.	:	Experimental Number
ABS L250	:	ABS Lustran 250
BS L440	:	ABS Lustran 440
BS L640	:	ABS Lustran 640
mm	:	millimeter
°C	:	degree Celsius
rpm	:	revolution per minute
mm/s	:	millimeter per second
sec	:	second
min	:	minute
h	:	hour
MPa	:	mega Pascal
pp.	:	page
ppm	:	part per million
standard dev.	:	standard deviation
displ.	:	displacement

CHAPTER I

INTRODUCTION

1.1 SCIENTIFIC BACKGROUND AND RATIONALE

Injection moulded plastic parts are more and more used for high quality technical purposes today. The consumer electronics industry and the automotive industry are the main customers in this business. [1 , 2] The parts made for these industry have to withstand high thermal, mechanical and chemical loadings. Together with good dimensional accuracy and surface quality of the moulding which mostly being the complex shapes have to be guaranteed. The produced parts must include final material properties at an optimum quality level as well as structural and aesthetic consideration for a given level of economic production volume.

The essential prerequisites for high quality production are the design
of moulds, constant conditions on the part of machines and the utilization of process control system as well as homogeneous material properties. It is still the quality of the moulds that is the major influence on the economic efficiency of the entire production process in order to deliver successfully the moulded products at the lowest possible cost.

In recent years, Computer Aided Design (CAD) , Computer Aided Engineering (CAE) and Computer Aided Manufacturing (CAM) software are becoming important for designing plastic parts to be manufactured by the injection moulding process. [3 , 4] CAD program should have two and three-dimensional capabilities to advance all relevant design in the mould making

industry for example, a mould cooling system; a runner system ; and associated gate locations ; type and size ; and cavity design. By using a CAD system tied together with some CAE software such as an analysis program which is combined with mathematical modeling and combined numerical procedures to simulate the injection moulding process. The engineering properties of injection moulded parts are dependent upon their thermomechanical history which in turn is greatly influenced by the processing conditions and part geometry [5]. Therefore, simulation programs require the input of data such as rheological, thermal and physical characteristics of the materials, processing parameters such as melt temperature, injection rate, etc., including the geometric model of the mould for calculation. The moulding problems can be solved by investigating theresults of the flow analysis such as the filling time, pressure, temperature and cooling time distribution which affecting the end-use properties of the part.

CAE software should approximate the real conditions as closely as possible. Any simulation is only of use if there is good agreement between the simulated data and the real situation [6]. Therefore, it is necessary to have a reliable material database especially important to use accurate rheological data and data from physical equation of state including mathematical models as well as methods of calculation which each simulation program uses.

1.2 Objectives of the Research Work

To verify the simulation software by comparison between the pressure predicted by Moldflow® simulation software and pressure cavity measured by experiment.

1. To study the effects of moulding conditions on mechanical properties of the moulded parts.

1.3 Scopes of the Research Work

In this research work , the focus is the comparison between the pressure predicted by Moldflow® flow analysis with existing Moldflow® standard database and a personal database for the inputs of material properties and the pressure measured experimentally. As well as the effect of injection moulding parameters on parts impact property were studied. The necessary process to achieve the goal may be as follows.

1. Literature survey and in-depth study of this research work.

2. Testing the ABS properties for the input of a personal database of the material properties.

3. Comparing the pressure predicted by Moldflow® to the cavity pressure measured experimentally at various injection moulding conditions.

4. Testing the impact property of the moulded parts to study the effect of injection moulding parameters by changing the following parameters.

- The effect of injection speed
- The effect of holding pressure
- The effect of holding time
- The effect of melt temperature

5. Analyzing the relevance of molecular orientation, internal stress and molecular degradation of the moulded parts to support the causes of impact property changed resulting from the effect of injection moulding parameters by testing tensile strength, glacial acetic acid immersion and melt flow index respectively.

6. Summarizing the results and writing up the thesis.

CHAPTER II

THEORY AND LITERATURE REVIEW

2.1 INJECTION MOULDING

2.1.1 Basic Principle of Injection Moulding Process [7]

The important elements of injection moulding are given in a simplified schematic diagram of the screw injection unit (Fig. 2.1). A typical sequence of an injection moulding operation involves the following stages is shown in Fig. 2.2.
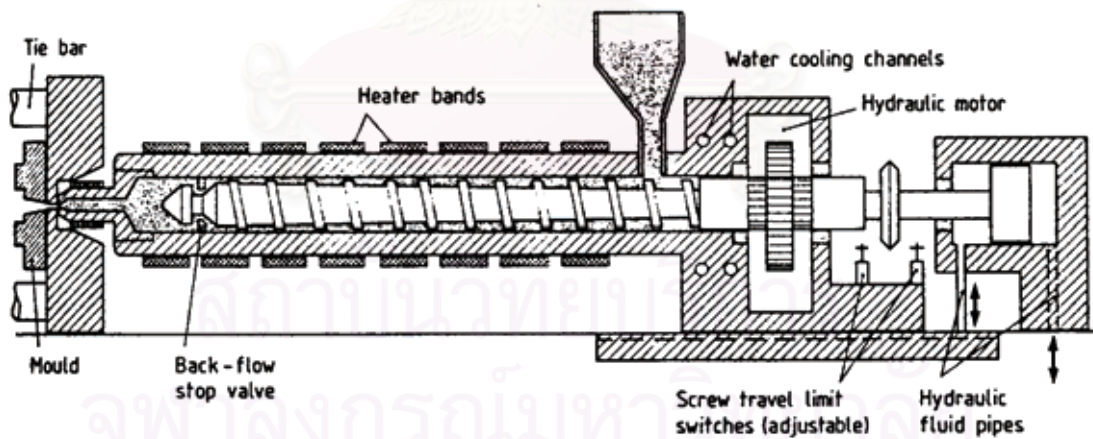
Figure 2.1 Single screw injection moulding machine : the injection unit [8] .

a. Screw Plasticizing

b. Injection

c. Holding & Cooling

c. Holding&Cooling
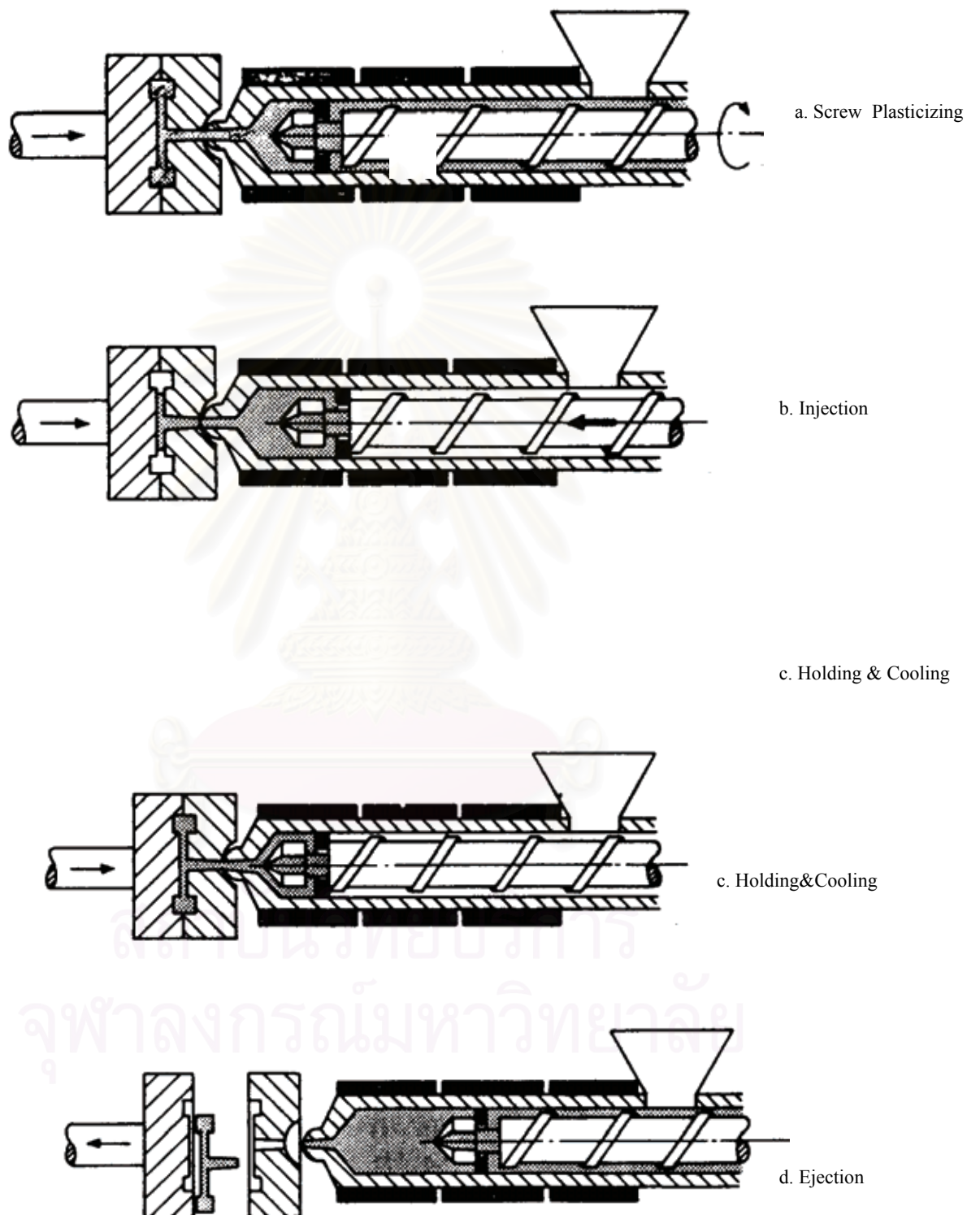
d. Ejection

Figure 2.2 Typical cycle in reciprocating screw injection moulding machine[9]

- The locking device of the machine presses the moving mould half to the stationary mould part, thus closing the mould.

- The screw is powered by a hydraulic motor as it rotates, the polymeric resin, in the form of powder or pellets, is drawn from the hopper to be heated and compressed in the extruder screw channel. Rotation of the screw conveys the material forward along the barrel where it is transformed to a viscous melt by a combination of external heat sources and the rotary shear action of the screw. The molten material accumulating at the front of the screw generates a positive pressure in front of the screw tip, which (once it exceeds the back pressure set in the hydraulic cylinder at the rear of the injection unit) forces the screw back down the barrel (whilst still rotating) to a pre - set limit which determines the swept - volume available for the next shot, the stroke. The screw rotation phase is usually termed screwback. (a)

- Soon after screwback is completed , the injection unit is activated. The screw moves forward like a ram and causes the melt to flow through the flow channels of the mould (i.e.; the sprue, the runner and the gate) into the mould cavity, usually at a constant volumetric displacement rate (injection speed). The time taken for this operation is called injection time. (b)

- As soon as the melt strikes the relatively cool surface of the mould it begins to solidify and contract. After the mould cavity is filled, additional material is packed into the mould under high pressure immediately following injection, to counterbalance the thermal shrinkage which would otherwise occur as the moulded part cools toward ambient temperature. The screw maintains pressure for the packing time (alternatively termed the holding time or dwell time) which is effectively terminated when the flow path to the mould cavity becomes sealed due to material solidification in the gate region. (c)

7

● Whilst the moulding is cooled enough to be extracted, the screwback phase is reinitiated for the next cycle. (a)

● The machine opens the mould allowing the removal of the moulding from between the two parts.

● Finally, the ejector mechanism of the machine lifts the finished moulding out of the mould cavity. The machine is now ready to start the next cycles of operations. (d)

2.1.2 The Injection Cycle

Comparison of a typical injection cycle when separated as the time for each stage briefly is illustrated in Fig 2.3 .
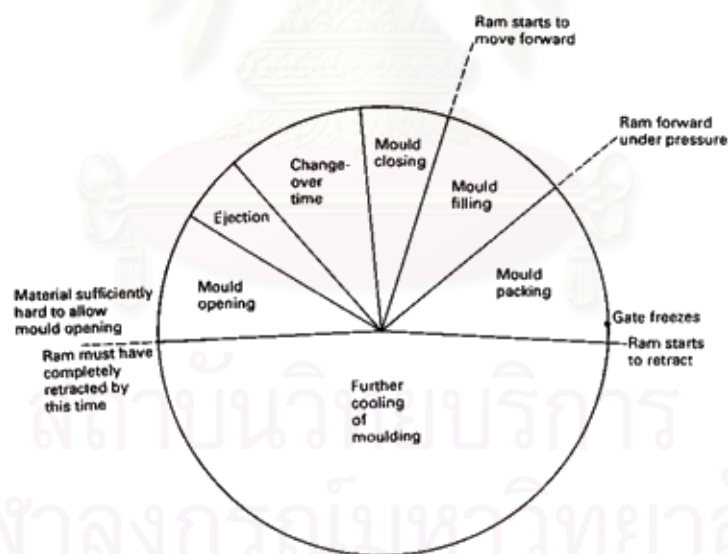
Figure 2.3 The injection moulding cycle [10] .

The first stage [11] , *mould closing* should be as fast as possible consistent with the final part of the closing operation not being so fast as to cause damage to the mould. There should also be time for any safety switches to become effective if necessary. As soon as the mould is closed the screw can start to move forward and the *mould filling* stage commences.

When the ram is fully forward and the mould cavity is filled the pressure on the melt will increase and this will help to consolidate the material in the cavity. This is known as the *mould packing* stage. During this stage the gate freezes. When this happens , any activity in the injection cylinder has no bearing on what is happening in the mould cavity.

Once the gate has frozen, the screw is rotated and retracted to prepare molten material for the next cycle which is called *plasticization stage* whilst further cooling of the moulding occurs. Whilst this is often known as the *mould cooling stage* the melt is actually beginning to cool from the moment that it leaves the injection cylinder.

When the moulding is sufficiently solidified *mould opening* can take place, and the *moulding ejected*.

2.2 CAVITY PRESSURE

2.2.1 Cavity Pressure during a Moulding Cycle

Typical cavity pressure curve comes from each stage of injection cycle as shown in Fig. 2.4 .

a. Plasticizing
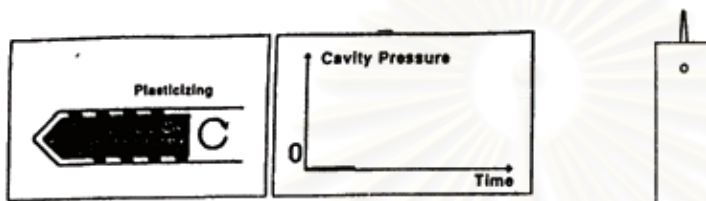
b. Injection

c. Switching to Holding Pressure at volumetric filling
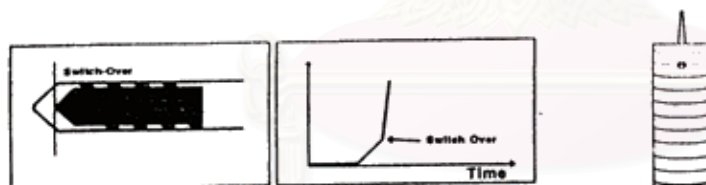
d. Compression

Holding Pressure

Figure 2.4 Typical cavity pressure curve during a moulding cycle [7] .

a. Plasticizing : During plasticizing the rotating screw in the barrel retracts, while the plasticized raw material gets transported in front of the screw. During this period no cavity pressure can be measured, because the plastic melt is not injected yet.

b. Injection : Cavity pressure can only be measured as soon as the melt passesby at the sensor position. A cavity pressure sensor at the end of the flow path will therefore detect a pressure increase later than a sensor near the gate.

c. Switching to Holding Pressure at volumetric filling : Only proper position for switching - over to holding pressure is when the cavity is just volumetrically filled. Switching - over too early causes warpage due to undefined filling, switching - over too late causes internal stress due to overpacking. Overpacking means less strength and easy cracking of the moulded parts.

d. Compression , Holding Pressure : After switching - over cavity pressure rises very fast due to compression of the injection melt. Immediately after injection the melt starts to cool down and gets contracted. This volume change must be compensated by the holding pressure through additional material supply. The cavity pressure curve indicates the actual condition of the moulded part, which is a result of many different influences like temperatures, viscosities and material properties, at any time.

2.2.2   Typical Pressure Curve of Amorphous and Semi – Crystalline
         Thermoplastics

         In the range of thermoplastic materials there are basically two
typical groups of materials : amorphous plastics and semi - crystalline
plastics.

         2.2.2.1 Amorphous Plastics

         Amorphous plastics which usually are transparent (such as
Polystyrene : PS, Polycarbonate : PC) consist of a homogeneous chemical
structure, which continuously changes its physical condition during heating up
or cooling down. Cavity pressure is therefore continuously decreasing during
the cooling of amorphous melt in the cavity. Figure 2.5 shows a typical
pressure curve of amorphous thermoplastics.

Figure 2.5 Typical Pressure Curve of Amorphous Thermoplastics [7] .

2.2.2.2 Semi-crystalline plastics

Semi - crystalline plastics which are non - transparent (such as Polyoximethylene : POM, Polypropylene : PP, Polyamide : PA) consist of an amorphous and a crystalline part. During heating up of the material there is one certain temperature, where the crystals melt, and during cooling down there is one certain temperature, where the crystals solidify. This phenomenon causes a very sudden pressure difference in the P , V, T-diagram and therefore in the cavity pressure curve. A typical cavity pressure curve of a semi - crystalline material usually shows a sharp bend during the cooling respectively the holding pressure phase , which is caused by the solidification of the crystal part. Figure 2.6 shows a typical pressure curve of semi-crystalline thermoplastics.

Typical Cavity Pressure Curve
of Semi Crystalline Plastics

Cavity Pressure

Ⓐ　　Ⓑ　A) Radius depends on Geometry of Molded Part
　　　　　and on Molding Parameters

B) Significant Pressure Decrease due to Freezing
of the Crystals

Time (sec)
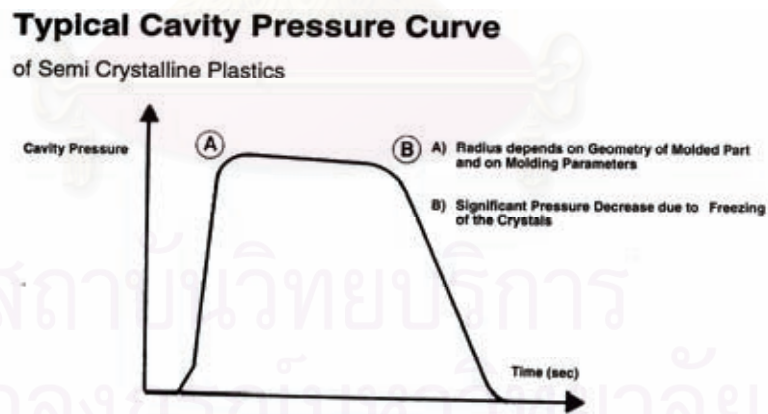
Figure 2.6 Typical Pressure Curve of Semi-Crystalline Thermoplastics [7] .

2.2.3 Cavity Pressure Characteristics

The course of different cavity pressure curves always reflects certain physical conditions in the mould cavity. As all moulded parts are different, an ideal cavity pressure curve does not exist. Furthermore each specific moulded part has its own specific *ideal cavity pressure curve* , which should be optimized first , and reproduced afterwards. It is possible , however, to analyze certain process tendencies out of any cavity pressure curve. Figure 2.7 shows the cavity pressure characteristics.
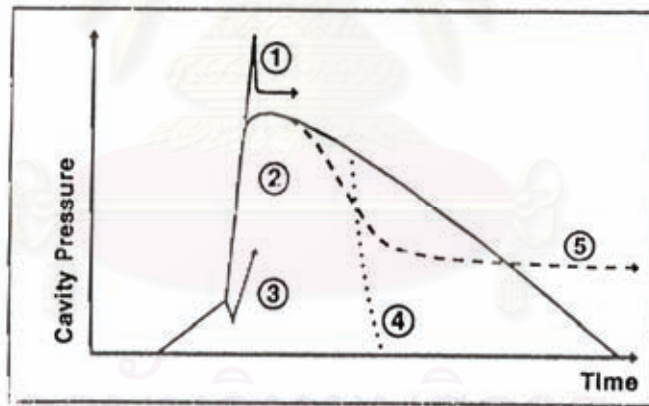
Figure 2.7 Cavity Pressure Characteristics [7] .

1. A pressure peak right after filling of the cavity indicates that switching - over happened too late. The moulded part is overpacked, which results in internal stress.

2. Ideal course of a cavity pressure curve.

3. A pressure decrease after switching - over to holding pressure indicates that the cavity was not filled completely at this time. The moulded part will be filled under holding pressure, which usually causes warpage.

4. In case of sudden cavity pressure drops at the end of holding pressure, holding pressure time was too short. The gate of the moulded part has not solidified yet, so that melt can flow back out of the cavity. This will cause sinkmarks or even incomplete filling.

5. Cavity pressure does not decrease back to atmospheric pressure. This can be caused either by overmoulding (e. g. switching-over too late) or by deformation of the mould platen during injection. If the mould platen are not dimensioned well enough, they will get deformed due to the injection forces. The injected melt will solidify and disable the platen to relax. The result will be a so- called " residual pressure " in the mold cavity.

2.2.4 Effects On Sensor Positions

The location of the pressure transducer in the cavity also affects what can be deduced from this sensor. Plastics have a structure - viscous or non - Newtonian behaviour as a consequence there is a pressure drop from the gate to the end of the cavity, which of course influences the choice of the sensor position. A sensor, which is positioned near the gate, measures a higher cavity pressure for a longer period than a sensor, which is positioned far from the gate at the end of filling. A lot more information concerning the filling and cooling of the moulded part is therefore obtained close to the gate instead of far from the gate.

15

A sensor position far from the gate is only recommended for the monitoring of complete filling, e.g. in case of very long flow distance or in case of 100 % control of multi - cavity moulds. In general, a pressure transducer should be installed close to the gate, because the most useful information about the injection moulding process can be collected there, but for switching, a sensor position far from the gate at the end of the flow path is more useful for monitoring the degree of filling.

The selected pressure for switching by a pressure transducer close to the gate should be changed if there are slight fluctuations in the melt temperature, because the pressure drop (indicating the degree of filling) towards the end of the flow path varies. If the switching pressure is not changed, there are changes in the switching point and therefore in the pressure curves. Such fluctuations in melt temperature cause smaller variations in the pressure signal if a sensor far from the gate is used. Therefore a pressure transducer at the end of the flow path is better suited to controlling the degree of filling and to initiating the switching.

The course and the actual size of a pressure curve depends on the position of the pressure measurement. In injection moulding there is a continuous loss from the end of the injection unit (e.g. the hydraulic system) to the end of the moulded part ($P_{far\ from\ the\ gate}$). The most important difference however is the fact that only pressures measured within the moulded part itself are related to the part quality.

- Pressures measured in the hydraulic system or in the melt in front of the screw can only reflect the machine adjustment.

- Pressures measured within the moulded part (cavity pressure) show the result of all machine settings including the cooling behaviour.

16

2.2.4.1 Pressure Curves from Different Sensor Positions
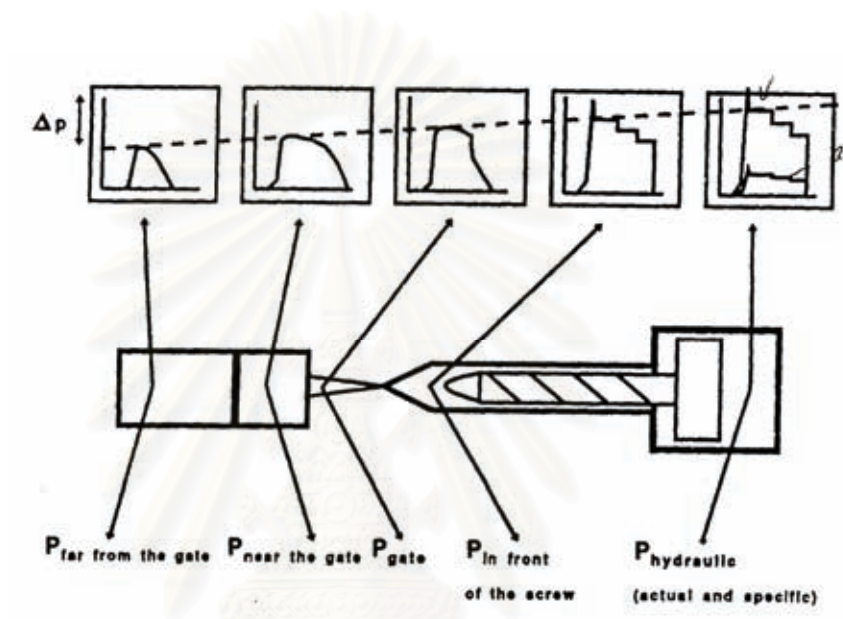
Figure 2.8 shows pressure curves from different sensor positions [7]

a. Cavity Pressure far from the gate.

Cavity pressure far from the gate is mainly used for 100 % control (0 % ppm rejects).

b. Cavity Pressure near the gate

Cavity pressure measurement near the gate is the only way to determine and indicate all part related quality influences

c. Pressure Measurement within the sprue

Pressure measurement within the sprue can be used for quality monitoring purposes. The monitoring of the cooling behaviour and the sealing point however is not possible.

d. Melt Pressure in front of the screw

Melt pressure in front of the screw is the only reliable measurement for machine control and rheological purposes.

e. The Actual Hydraulic Pressure

The actual hydraulic pressure is far lower than the calculated specific pressure due to the different diameters of piston and screw. The calculated values are only approximate, because of influencing friction in the injection barrel.

2.3 VARIOUS EFFECTS ON MOLTEN PLASTIC FLOW PROPERTIES IN MAIN PHASES Of THE INJECTION MOULDING CYCLE [12].

2.3.1 Injection Phase

The term injection phase is used to describe the part of the process between the beginning of mould filling and the point at which the machine is switched to holding pressure. At higher injection speeds, the pressure course is steeper and the compression phase is reached sooner. The pressure course in the holding phase is independent of injection speed. Figure 2.9 shows the effect of injection velocity on cavity pressure curve.
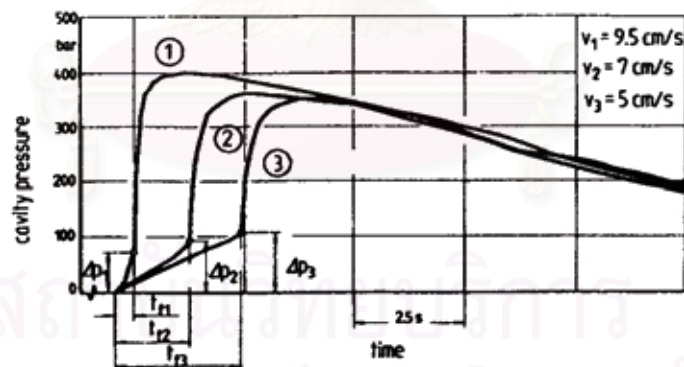
Figure 2.9 Cavity pressure for different injection velocities [12] .

Usually the injection phase is performed under velocity –controlled conditions. This means that the screw forces the plasticated material into the cavity with a velocity profile that can change in 5 to 10 steps. The velocity profile has to be adjusted to suit the material and the moulding, as well as other process parameters. Generally the injection of material starts with a low

velocity, which is increased so that the mould can be filled in a shorter time. Before the cavity is completely filled the velocity is decreased, to achieve a smooth transition from filling to packing. Velocities at the beginning and end of the filling phase are low, in order to treat the mechanical elements of the injection machine and mould gently. For each combination of material, machine setting, and moulding, there is an optimum injection time span (Fig. 2.10).
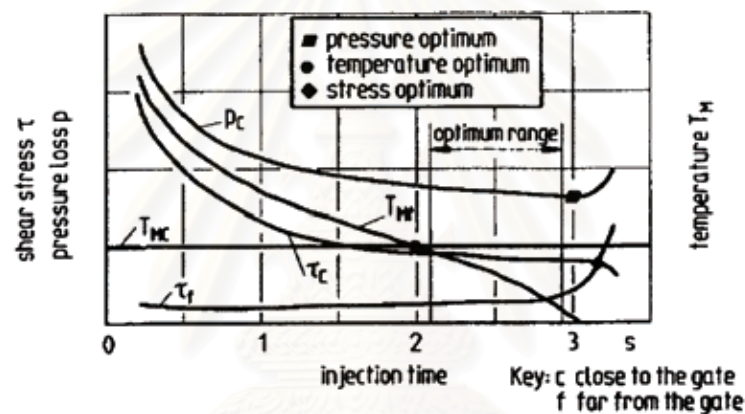
Figure 2.10 Optimizing the injection time $[12]$.

Very short injection times result in high - pressure losses, due to the high volume flow. However, extremely long injection times lead to a reduction of the free channel cross section, due to solidification of the melt close to the wall, and thus also to higher pressure losses. The injection time should be within the range of minimum pressure. For reasons of quality the average material temperature should be constant over the moulding. Although the temperature of the injected melt is almost independent of injection time, the average temperature is less at the end of the flow path, because the melt has cooled longer.

20

For short injection times, the temperature at the end of the flow path may be higher than the injection temperature, because of heating through dissipation (internal friction); with long injection times, it may be lower. There is an intermediate injection time for which there is no difference between the temperatures at the beginning (injection temperature) and the end of the flow path. The stress resulting from the flow process should be low and constant all along the flow path, so that possible degradation of mechanically sensitive materials is avoided. An optimum injection time can be determined based on all the points above , but the time depends chiefly on the type of moulding and the material involved.

2.3.2 Holding Pressure Phase

The most important aspect of the holding pressure phase is the addition of fresh melt to compensate for the effects of the thermal contraction of the melt during cooling . The result is that air bubbles and sink marks in the moulding are prevented, and shrinkage and warpage are minimized [13]. The holding pressure phase starts at the switchover point and ends at the end of holding pressure exerted by the machine, and thus includes both the packing phase and the holding phase. The holding pressure phase is performed under pressure control. Usually this means that the screw is loaded with a pressure that can be adjusted in 5 to 10 different steps. The amount of holding pressure and the pressure profile must be adjusted to the material, the moulding, and other process parameters. The pressure profile has to be used to optimize shrinkage and warpage behavior of the part. Switching to holding pressure is an important factor in avoiding pressure peaks and thus the consequent overloading of the mould.

21

There are three different procedures for switching over from the filling to the holding phase :

● time - dependent switchover

● screw - position - dependent switchover, and

● pressure - dependent switchover, including hydraulic pressure switchover and cavity pressure switchover

The switching may be initiated by time. If so, the change to holding pressure takes place, regardless of any other factors, after a certain time has elapsed. This procedure is inflexible and does not consider the formation of the moulding in the mould, and therefore is rarely used nowadays. If switching over depends on screw position, holding pressure is applied as soon as the screw has reached a certain point. If the particular moulding requires only a little melt to be forced into the mould, an entirely position - related switchover procedure may cause problems, and small fluctuations in the plasticated volume, the valve response times, or the material itself, may have a significant effect on the pressure course (Fig. 2.12). The result is that slight fluctuations in the switching point can cause significant changes in the pressure course.

Figure 2.11   Cavity pressure for different switching points

22
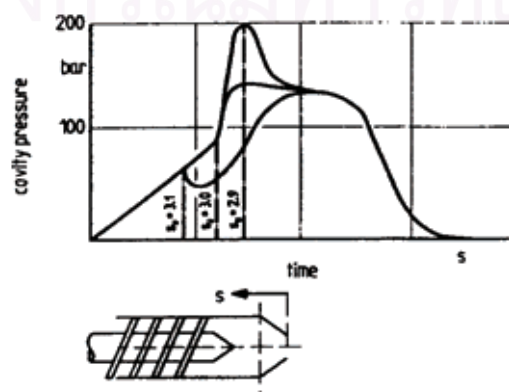
(different screw positions) [12] .

If switching is triggered by pressure, holding pressure is applied as soon as the selected pressure is reached. There are two different types of pressure - related switching strategies. In the first, the hydraulic pressure is used as a reference pressure, and in the second, a pressure transducer in the cavity measures pressure. In the first method only a pressure transducer in the machine is required, whereas for pressure measurement within the cavity a separate sensor is required for each mould used. However, the second alternative offers the advantage of measuring the actual pressure in the cavity and using this information to further optimize the process. The purpose of correct switching is to perform a smooth transition from the filling phase to the holding pressure phase. The switchover to holding pressure should as a rule take place only after volumetric filling is finished, to ensure that the cavity is filled completely. Figure 2.12 shows the cavity pressure for different times of switching to holding pressure.

a   b   c

- dimensions too small   - dimensions too large
- danger of stress cracks   - danger of stress cracks
- unfavorable orientations   - unfavorable orientations
- sink marks   - demolding problems
- vacuoles   - flash
- surface marks
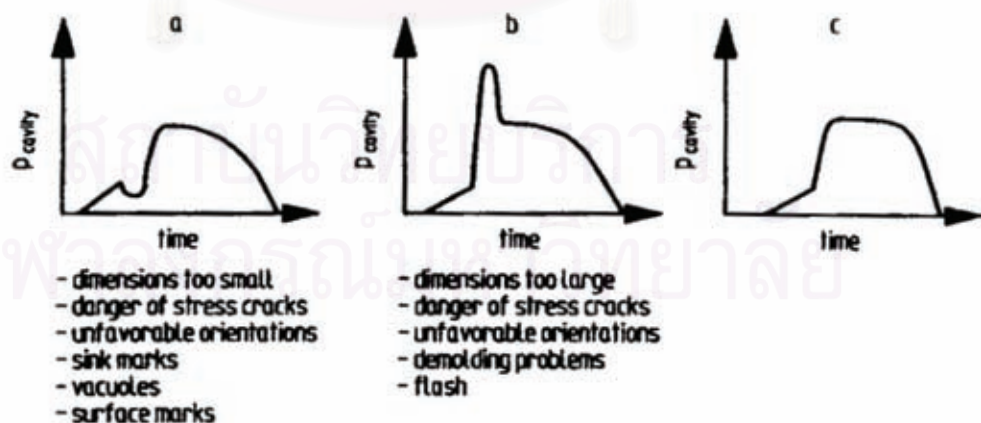
Figure 2.12 Cavity pressure for different times of switching to holding pressure [12].

23

If the switchover occurs too early, some filling takes place under holding pressure. This causes a noticeable decrease in the pressure course (Fig. 2.12 a). If switching over is too late, the result is a pressure peak above the holding pressure (Fig. 2.12 b). When this pressure peak is relieved, some melt flows back into the runner system. This additional motion of melt should be avoided because it is not reproducible and can cause additional orientations in the moulding. Marked pressure peaks in the packing phase are also undesirable because the mould may be forced open briefly and flash may be produced. A correct switchover to holding pressure ensures a smooth transition in the pressure course (Fig. 2.12 c).

The holding pressure value is the factor with the largest influence on the pressure curve during the holding pressure phase (Fig. 2.13). A rise in the holding pressure causes a rise in the cavity pressure and an increase in the effective holding pressure time.
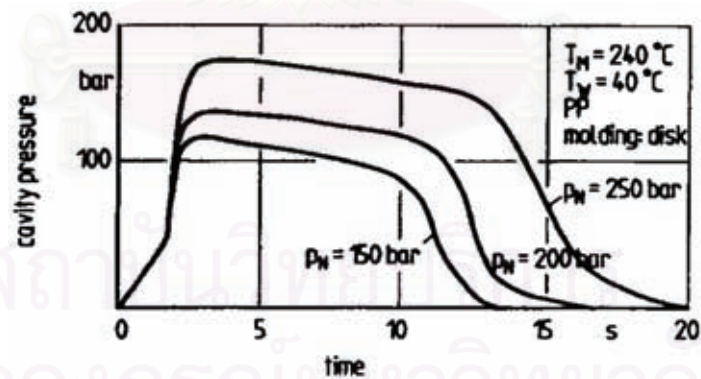
Figure 2.13 Cavity pressure for different holding pressures [12] .

The duration of the holding pressure also has a decisive influence on the pressure course (Fig. 2.14). If the duration is too short, the melt may flow out of the cavity into the runner system and back into the screw chamber; these non - reproducible events lead to additional orientation as well as to fluctuations in part weight and consequently to a variety of defects. Switching the holding pressure off too soon results in a noticeable drop - off in the pressure curve ; the drop - off shifts with increasing duration of holding pressure and becomes less and less marked.
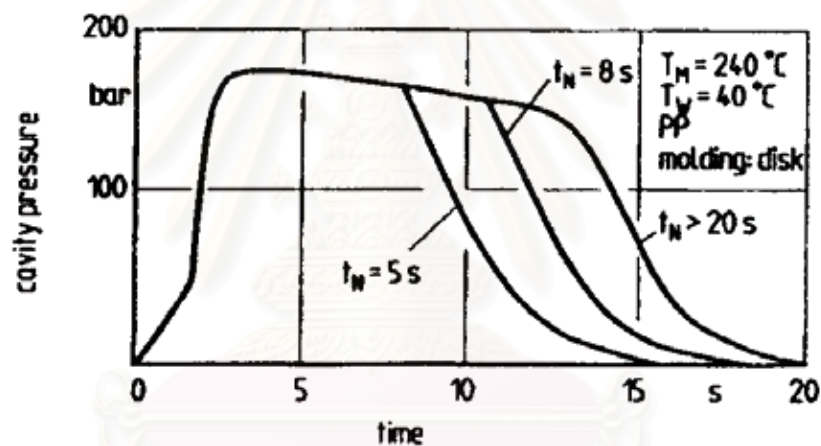
Figure 2.14 Cavity pressure for different duration times of holding pressure [12].

If the holding pressure lasts longer than the sealing time, no further change occurs in the pressure curve. At the sealing time the gate is solidified, so no further melt can enter the cavity to compensate for shrinkage. Thus it does not make sense to prolong the holding pressure beyond that time. The sealing time can be found by inspection of the pressure curves or by measurement of the part weight as a function of the holding pressure time (Fig. 2.15).
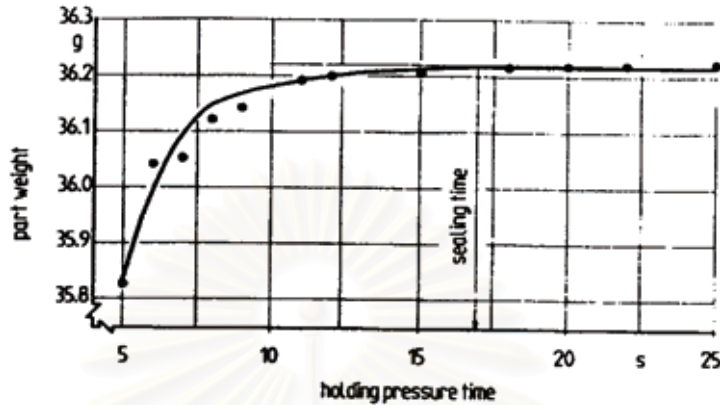
Figure 2.15 Determination of sealing time by measurement of part weight [12]
.

There is an initial steady increase in weight with increasing holding pressure time. After the sealing time has passed, no more melt can be pushed into the cavity, and the weight of the moulding remains constant regardless of the duration of the holding pressure.

Melt temperature can also exert a strong influence on the pressurecourse within the mould (Fig. 2.16). Higher melt temperatures lead to larger free cross sections. The melt in the core, which is still fluid, has a higher temperature and thus a lower viscosity. The effects of both temperature and viscosity reduce the pressure drop and therefore result in a higher pressure at the pressure transducer. Furthermore, the hotter melt causes the gate to stay open longer before sealing, so the duration of the holding pressure must be increased too.
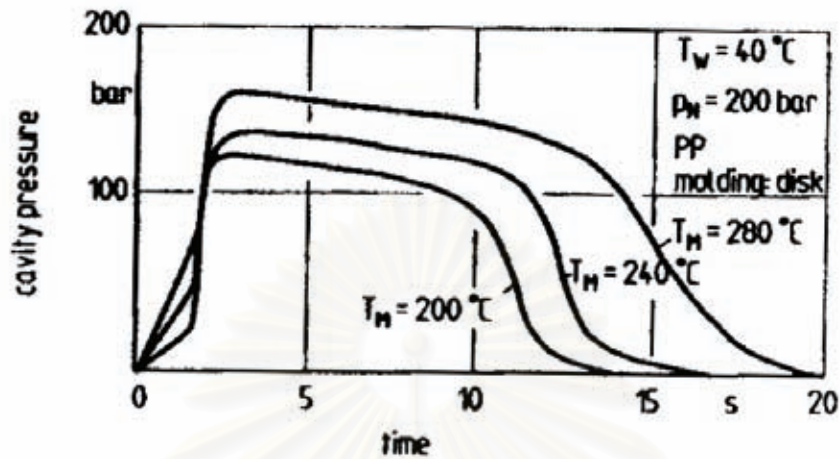
Figure 2.16 Cavity pressure for different melt temperatures [12] .

The temperature of the mould wall has only a slight influence on the pressure course in the filling phase (Fig. 2.17), because of the short cooling times in the filling phase. But there is a strong influence on the pressure course in the holding pressure phase, because wall temperature influences the cooling behavior. If the wall temperature is higher, the moulding cools more slowly, has larger flow cross sections, and thus has a slightly higher - pressure level in the holding phase. Slower cooling also causes the sealing time to lengthen.
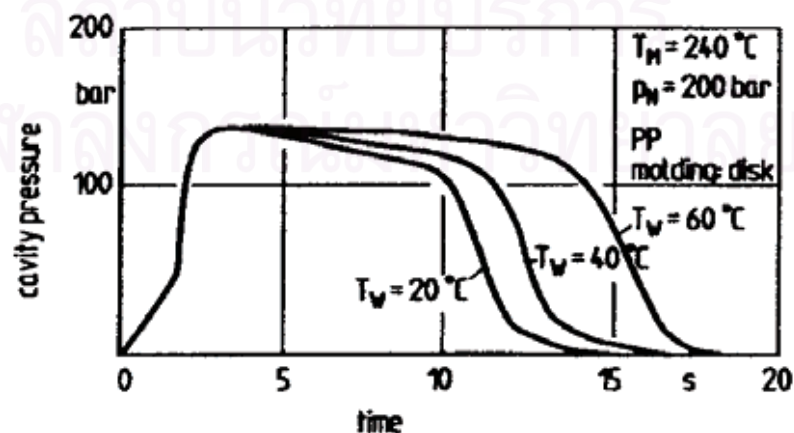
Figure 2.17 Cavity pressure for different mold wall temperatures [12] .

2.3.3 Cooling Phase

The cooling phase starts immediately after the injection of the material and includes both the injection and holding pressure phases. However, the cooling time must be extended beyond the holding phase, as the moulding has not yet cooled down sufficiently and is not stable enough for de - moulding (ejection). Parameters that govern the injection and holding pressure phases therefore also affect the cooling of the moulding. Apart from such factors as injection time , temperature , and holding time, the cooling time can have a significant effect on the properties of the moulding. Following the holding pressure phase, the moulding remains in the mould for continued cooling. It is removed from the mould only when the danger of deformation is past.

After its removal from the cavity, the moulding is exposed to a completely new set of thermal and mechanical boundary conditions. As long as the moulding remains in the cavity, shrinkage and warpage are inhibited mechanically by the surrounding walls of the mould. Instead of deformation, residual stresses are built up within the moulding during cooling. After the moulding is ejected from the cavity, some of the generated stress is relieved by deformations, and the contraction process that follows takes place without any external constraints. There are also changes in the thermal conditions. Within the mould, the mould wall temperature determines the temperature of the molding. Outside, however, cooling takes place by convective heat transport, and is considerably slower. Because of stress relaxation, the cooling time can be used to influence the shrinkage of the moulding, as long as it is still in the mould. Extending the cooling time generally has the effect of reducing the amount of shrinkage.

28

2.4 SIMULATION SOFTWARE $[14]$.

The relationship between processing and part quality has long been realized. However , due to the complexity of the interplay between the various processing factors and quality, injection moulding remained something of an art for many years.

Many persons worked on this field in the 1960 's and 70 's. There are a lot of empirical studies cited, each adding to the general knowledge on the relationships between processing and part quality. Despite the obvious interest, attempts to formulate an approach to plastic part design with a sound theoretical foundation were thwarted by the non-Newtonian nature of polymer melts and the complex heat transfer experienced in injection moulding. However, ever increasing demands for higher quality in the 1970 's saw increased interest in mathematical modeling of the moulding process.

During this time , pioneering studies were published. These focused on rather simple geometry and while of academic interest, offered little assistance to engineers involved with the day to day design of plastic parts and moulds. In 1974 Moldflow Pty. Ltd offered commercial software on a worldwide computer time sharing system. This software allowed users to determine processing conditions (melt temperature , mould temperature and injection time) and to balance flow in cavities and runner systems. A considerable break through was made with the introduction of finite element methods. In 1983 Moldflow released a finite element flow analysis program for analysis of three dimensional geometry. This was the first commercial available package. Early versions of the software modeled only the filling phase. Analysis of the packing phase was developed to predict shrinkage and warpage. Generally speaking , the equations governing the flow of the

polymer melt, can not be solved in any but the simplest of geometry. Since injection moulds have different geometry, a general method of solution is required. The finite element method is particularly well suited to this type of problem. The Finite Element Method (FEM) is a general method for solving engineering problems. Historically, finite element analysis began in structural analysis. Soon, however, it was realized that the method could be applied to a very wide class of problems.

2.4.1 Different Simulation Programs

Several software packages are at this time on the market such as

- Moldflow Dynamic-Series
- TM-Concept
- IDEAS for plastics
- C-Mold
- Cadmould
- STRIM-Flow

2.4.2 Moldflow® Dynamic-Series

Supplier

                :   Moldflow Pty Ltd.

Subprogram

MF/VIEW	:	Geometry and mesh generation
MF/FLOW	:	Calculation of the filling and packing phase
MF/COOL	:	Calculation of the cooling phase

MF/SHRINK	:	Calculation of the shrinkage
MF/WARP	:	Calculation of the warpage
MF/GAS	:	Simulation of the GID method
MF/TSETS	:	Calculation of thermosets

Program Specifications

FEM-Mesh	:	Triangular elements
Max. Element number	:	10000
Element types	:	Cold runner
		Hot runner
		Insulated runner
		Shell element
		Gas element

The simulation program package consists of five parts of the program :

MFVIEW : **Model creation and meshing**

MFL : Mould filling and Packing/holding phase (injection moulding)

WARPIN : Final shape prediction (shrinkage, warpage-injection moulding)

MFLG : Gas internal pressure moulding and Packing / holding phase (Gas assisted moulding)

BEMCL : **Mould cooling**

2.4.3 Moldflow® Flow Analysis

The basic idea is to create a model of the mould geometry to be analyzed. This can be done by using either a module in the package itself or one of the CAD computer programs. The model is then meshed by creating triangular elements on its surfaces. The vertices of these elements are called nodes. The next step is to carry out a mould filling simulation using a cavity filling module. In this module, fluid mechanics and heat transfer calculations are conducted using finite element (or finite difference) analysis. Information about important variables are stored at each element and node. The 3-D version of the mould filling module allows the calculation of some variables at different fluid layers (mould thickness). The filling module is followed by a packing module and a cooling module. Finally, some packages have modules for conducting shrinkage and warpage analysis.

2.4.3.1 Geometry Generation

A calculation of the filling phase can be carried out, a solution domain must be available. A calculation can then in this domain. A solution domain is a region of space throughout which the mathematical model is defined and solution are sought. Often the solution domain also includes the period of time over which changes in the system take place. In the flow analysis the solution domain is the physical space in which the molten polymer flows (the model of the mould cavity) and the time during which filling and packing takes place. The physical space of the solution domain is defined by the user when preparing a FEM model of the cavity geometry.

There are three ways to build a geometry :

- Use native MFVIEW geometry commands to build geometry.
- Use a compatible FEM program to model the part and import it.
- Use a CAD system to design and draw a part and transfer it.

MFVIEW divides the generation of the cavity geometry into two steps. Firstly, creating of points by coordinates and then creating of lines or surfaces by points. Surfaces and lines which the user creates only contain graphical attributes. For example, surfaces contain no indication of the wall thickness. The non graphic attributes must be assign to the surfaces and fill out the graphical representation. These non graphical attributes are called element properties. The program allows to define multiple properties (plate , gate , cold , hot , insulated). The better way for creating geometry is to transfer geometry from a CAD program because geometry is to be manufactured very difficult in the pre-processor (MFVIEW).   The corresponding interfaces are available (IGES) .

2.4.3.2 Mesh Generation

MFVIEW is its automatic mesh generation capabilities by entering the desired dimension of the elements (length of the side), the program will automatically mesh all lines and surfaces in the model. If the specified element size is too big for any curve or surface, it uses the largest element possible. If during automatic mesh generation, there is a surface that have been previously meshed , it will automatically adjust the element density to insure connectivity.

2.4.3.3 Material Selection

Before a calculation can be started , material data must be available. The necessary material data are :

- Viscosity data
- Specific heat capacity
- Thermal conductivity
- Density
- No Flow Temperature
- Ejection Temperature
- Range of Melt Temperature
- Range of Mould Temperature
- Maximum shear stress
- Maximum shear rate

Material selection can be input from existing a standard Moldflow database or creating a personal database.

2.4.3.4 Analysis of Filling Phase

The first step is to determine the cavity geometry and the mesh element where flow will begin (boundary condition). Once this element is determined , the moulding conditions and other calculation parameters can then be entered and the calculation performed.

The following inputs are necessary :

Configuration options

- Analysis Aim : *multi laminate filling / fast filling*

- Restart file : *None / fill (result file)*

Input / Output files

- Model file : *Filename of the mould geometry*

- Boundary conditions file : *Injection location (file required)*

- Results name : *Name of the result file*

- Cooling interface file : *yes / no (Name of a cooling result necessary)*

Material Information

- Material Supplier : *Name of the material database*

- Material grade : *Selection of a required material from the database*

- Fill compressed by : *PVT / factor (use PVT-data or constant factor)*

Processing Conditions

- Maximum injection pressure : *Limit of the injection pressure*

- Maximum clamp force : *Limit of the clamp force*

- Mould temperature : *The real mould temperature*

- Melt temperature : *The melt temperature*

- Injection : *Time / flow rate / automatic*

  (injection time or flow rate required)

2.4.3.5 Analysis of Packing Phase

The following inputs are necessary (similar to the filling phase).

Configuration options

- Analysis Aim   : *multi laminate   packing*
- Restart file   : *None / fill (result file)*

Input / Output files

- Model file   : *Filename of the mould geometry*
- Boundary conditions file : *Injection location (file required)*
- Results name   : *Name of the result file*
- Cooling interface file : *yes / no (Name of a cooling result necessary)*

Material Information

- Material Supplier   : *Name of the material database*
- Material grade   : *Selection of a required material from the database*
- Fill compressed by : *PVT / factor (use PVT-data or constant factor)*

Processing Conditions

- Maximum injection pressure   : *Limit of the injection pressure*
- Maximum clamp force   : *Limit of the clamp force*
- Mould temperature   : *The real mould temperature*
- Melt temperature   : *The melt temperature*
- Injection   :   *Time/ flow rate / automatic(injection time or flow rate required)*

Before entering the inputs for the holding phase calculation, the results of the filling phase must be carefully examined. It is necessary to look at the no-flow and cooling data of the filling phase analysis.

Another value is the maximum pressure at the end of filling. This will be the starting pressure for optimization of the holding pressure.

2.4.3.6 Analysis of Shrinkage and Warpage

Configuration Options

- Analysis type   : *Small deflection analysis / large deflection analysis / buckling anlysis*

- Analysis description   : *Yes / no (description)*

- Exclude cold runners : *Yes / no*

- Cut-off angle (corner) : Limit angle for corners

Input / Output files

- Model Name : *Filename of the mould geometry*

- Boundary conditions file : *Fixing location (file required)*

- Cooling elemental file   : *yes / no (Name of a cooling result necessary)*

- Results name   : *Name of the result file*

Material Information

- Material supplier   : *Name of the material database*

- Material grade   : *Selection of a required material from the database*

- Mechanical data source : *Use material data / result of fiber option calculation*

- Shrinkage data source : *Packing restart file (file required)*

2.4.4 Moldflow$^®$ Flow Analysis Results

2.4.4.1 Filling Results

The program MFVIEW is used to view the results in terms of melt temperature , pressure distribution , shear stress , frozen skin for each short shot requested during the calculation. The holding and cooling times

are available only for the last shot. Followings are the explanation of filling analysis results.

- Fill Time

This option offers the best capability and flexibility in viewing isochrome images. This is a multicoloured picture of the advancing flow front. Each colour corresponds to a different short shot.

- Temperature

This displays the temperature distribution which represents the average temperature of the material across the thickness in each element. It can be obtained at each time step (short shot) and at the end of filling. To obtain high quality parts, the differences in all regions of the part should be in a narrow range (in general : 15 to 20 degree).

- Pressure

The pressure distribution all over the part is displayed. The values indicate areas of the overpacking which can cause differential shrinkage and warpage.

- Stress

The stress displayed is the maximum shear stress across the thickness of the part. During cooling, part of stress at the end of filling relaxes, but a residual stress remains frozen and will be one of the causes tending to distort the part. The shear stress should not exceed specific value. These value is a function of the different materials.

- Shear Rate

The shear rate is the difference in velocity between adjacent laminar layers within the flow channel, divided by the layer thickness (derivation of the velocity profile). The maximum shear rate across the wall thickness is the shown value.

- Frozen Skin

The frozen skin shows the percentage of material frozen during the filling phase. For example, 10 % frozen skin on a 3 mm thick part means that the frozen layer in each side is 0.3 mm. This value is important to optimize the moulding conditions. The allowable amount depends on the type of material. The value of the frozen skin is very important for parts with very thin wall moulded with crystalline materials. For the best part quality and for most of resins , it is recommended that the frozen skin should be maintained below 10 %.

- Flow Angle

The flow angle shows the orientation of the flow in each element. It is used to understand the filling pattern in order to predict weld lines and to judge potential causes of warpage.

● Clamp Tonnage

This force is necessary by moulding machine clamping force. It is generated by the filling pressure acting on the projected area of the part. The considered

projected area is the projection of the part geometry on the x-y plane of the screen.

● Cooling Time

This time is required for the center of each element to reach the freezing temperature of the resin. It normally represents the maximum cooling time until

the part can be ejected.

2.4.4.2 Packing Results

Followings are the explanation of packing analysis results.

● Temperature

No precise rule can be applied to know the best value at each time , only uniformity is important . The best quality is achieved if all temperature values are below the no-flow temperature at the end of holding phase.

● Pressure

The pressure distribution all over the part is displayed. Excessive pressure drop

 during packing should be avoided , this will generate different density.

● Shear Stress

The values should be kept at a lower level than in filling. The uniformity of the values is very important.

● Frozen Skin

At the end of the holding time, the value should be 100 % all over the part.

● Density / Volumetric Shrinkage

These values are connected to the entering mass during holding phase. Uniformity of density are essential to avoid potential warpage. It should be noted that the density displayed is the value at the considered temperature. However, the computed volumetric shrinkage considers cooling of the part to room temperature with relaxation of the pressure.

2.4.4.3 2 - D Graph Results

Both of the filling and packing results can be represented as 2 D line graphs which are the change in a given property with respect to time. This is called " Time Series " showing result. For example, for a flow analysis some of the time series results available include :

● pressure (nodal)

● temperature (nodal)

● frozen layer thickness (elemental and for multi-laminate analysis only)

● clamp tonnage (global)

Time series results are available for all nodes and elements in the model. The primary use for these results is to obtain a history of the value of a moulding property at a specific position in the model.

2.4.4.4 Shrinkage and Warpage Results

WARPIN computes the direction and the amount of deformation that occurs in a part as a result of the accumulated residual stress left after packing phase. To display the calculations results , it is necessary to enter MFVIEW again. Following is the explanation of shrinkage and warpage analysis results.

● Deformation / Undeformation

The final shape of the part is displayed. In order to see better the distortion , a scale factor can be used. The undeformed option allows to redraw the actual model over the deformed part.

● Displacement

This option evaluates the displacement for each node as a solid contour plot for the global or any of cartesian axes.

2.5 LITERATURE REVIEW

Axtell, F.H. and Haworth, B.[6] compared the pressure drops arising during injection moulding as predicted by a simulation software package named SIMPOL$^{®}$ and as measured during moulding trials to study the effects of moulding variables. The comparison was made using amorphous thermoplastic polyesters, PET and PCTG. The moulding trials were conducted using a mould fitted with a cavity transducer and a machine fitted with a hydraulic pressure sensor. The simulation showed qualitative agreement to the observations made in practice. The difference in pressure drop values was attributed to the software's dependence on crystalline PET physical properties for calculation and an overestimation of the frozen layer thickness by the simulation model.

Cox, H.W. and Mentzer, C.C. [15] studied the effect of fill time on the mechanical properties, surface appearance, and part dimensions of ABS, PP, Nylon 6,6 and GF-Nylon 6,6 injection moulded parts. The fill time was varied from 0.8 to 20 seconds in order to cover both the viscous flow controlled region (short fill times) where laboratory samples are ordinarily moulded and the heat transfer controlled region (long fill times) where production parts are commonly moulded. Testing as a function of fill time were tensile properties (tensile modulus, peak stress and peak strain) , scanning electron micrographs of tensile bar fracture surfaces, flexural properties, shrinkage measurements of tensile bars in both the length and thickness directions, part weight and surface appearance from micrographs. The results being observed for polypropylene or nylon were no large variations in tensile properties, but a 10 % increase in peak tensile stress and strain for ABS did indicate that molecular orientation increased with increasing fill time. However , significant differences did occur in the properties of glass reinforced nylon. Peak tensile stress increased 15 % and flexural strength decreased 10 % as the fill time was increased. These properties variations could be attributed to differences in glass fiber orientation of the skin and core regions of the part. The measurement of moulded tensile bar dimensions on the shrinkage of the various polymers except for shrinkage in the length direction for PP. The shrinkage increased from 13 to 15.4 mm / m over the fill time range. The most dramatic change with fill time was the surface appearance of the glass reinforced nylon. The surface of samples moulded at short fill times had a dark uniform colour and smooth appearance while samples moulded at long fill times had a lighter colour and a porous surface. This surface porosity was due to crystallization prior to complete pressurization of the mould.

43

Dairanieh, I.S., Haufe, A., Wolf , H.J. and Mennig , G. [16] examined the sensitivity of Moldflow[®] computer simulation package 's weld-line prediction algorithm to variations in material properties and processing conditions applied to injection moulded Poly (Methyl Methacrylate). Parameters studied included : die (melt) temperature , mould temperature, injection time , and material properties. The model prediction was then compared with experimental tensile strength in the weld-line area. The algorithm was successful in predicting the influence of variations in the injection time on weld line strength. Qualitatively, the algorithm correctly predicted the effect of changes in material viscosity, density and PVT relationship on the weld-line strength. However, the algorithm predictions of changes in weld-line severity with variations in die and mould temperature were not in accordance with experimental measurements. The variation in the predicted weld-line severity value was small.

Seow, L.W. and Lam, Y.C. [17] worked on optimization design for quality mould and part design by balancing the cavity. The injection moulding software, Moldflow[®] was used for controlling the plastic flow in the filling phase such that the melt front reached the boundaries of the mould at the same time. This was done by adjusting the thickness of various sections by using the simulation of the software which can be automated the thickness-adjustment to generate the thickness necessary to balance the mould cavity. Good results were obtained for several basic geometric models.

44

Gao, F. , Patterson, W.I. , and Kamal, M.R. [18] evolved cavity pressure control during a cooling phase through the manipulation of coolant temperature

by self-tuning controller for achieving the ideal cavity pressure profiles and its repeatability due to very strong influencing on the quality of the moulded part,

particularly its dimensions, dimensional stability, mechanical behaviour and surface quality. A coolant temperature control system was designed for the control of cavity pressure during the cooling phase. Alternative variables were defined to describe changes in cavity   pressure during the cooling phase. The

concept of controlled pressure cooling time (CPCT) was defined and selected

as the most appropriate controlled variable. The control system for CPCT was implemented and tested using coolant temperature as the manipulated variable.

Cavity pressure during the cooling phase could be controlled effectively by using CPCT control.

CHAPTER III

EXPERIMENTAL

3.1 MATERIAL

Acrylonitrile-Butadiene-Styrene , ABS Lustran was supplied by Bayer Polymers Co.,Ltd. Table 3.1 shows the properties data of ABS 3 grades with differences in viscosity and impact strength. ABS Lustran 250 , Lustran 440 and Lustran 640 are the high flow , medium impact and high impact injection moulding grade , respectively.

3.2 EQUIPMENTS

3.2.1 Equipments For ABS properties Test

- Gradient Column
- Twin Bore Capillary Rheometer
- Differential Scanning Calorimeter
- Heat Distortion Temperature Tester
- Vicat Softening Point
- Thermal Conductivity Tester

Table 3.1   The properties data of ABS Lustran 250 , Lustran 440 and Lustran 640

Property	Unit	Test Condition	Test Method	Lustran 250 High Flow	Lustran 440 Medium Impact	Lustran 640 High Impact
Mechanical						
Tensile Strength @ Yield	MPa					
Tensile Strength @ Break	MPa	Speed	ISO527	46	44	42
Tensile Elongation @ Break	%	50 mm / min	ISO527	34	33	32
Flexural Strength	MPa	"	ISO527	25	17	17
Flexural Modulus	GPa	Speed	ISO178	72	70	66
Izod Impact Strength	KJ/m^2	2 mm / min	ISO178	2.5	2.2	2.0
(notched)		$23^{\circ}C$	ISO180	12.1	17.3	21.3
Thermal	$^{\circ}C$	5 Kg	ISO306	96	95	96
Vicat Softening Temperature	%	-	ASTM D955	0.4 – 0.6	0.4 – 0.6	0.4 – 0.6
Mould Shrinkage						
Flow	g/10min	$220^{\circ}C$, 10 Kg	ISO 1133	40.0	21.4	12.4
Melt Flow Index						
Other Properties	-	-	UL94	HB	HB	HB
UL Flame Class Rating	g/cm^3	Natural	ISO 1183	1.05	1.05	1.05
Density						
Gloss	%	20° reflectance	-	94	94	94

3.2.2 Equipments For Injection Moulding

- Injection Machine , 50 kN ENGEL, model EC 88
- Thermometer
- Mould fitted with the cavity pressure transducers , Kistler type 6157 BA
- A charge amplifier , Kistler type 5039A232
- An adapter for DAS-16 type 2851
- A data acquisition card type CIO-DAS 1602-330
- DataflowPlus acquisition program

3.2.3 Equipments For Mechanical Property Test

- High Speed Instrumented Impact Tester , Radmana ITR-2000 : ASTM D3763

3.2.4 Equipments for Molecular Orientation and Degradation Test

- Tensile Tester , Lloyd LR 10K : ASTM D 638
- Melt Flow Indexer , Kayeness : ASTM D 1238

3.3 EXPERIMENTAL PROCEDURES

3.3.1 ABS Properties Test

ABS properties were tested for the input of a personal database which is as the material information for flow analysis. The followings are the items of testing.

(a) Density was tested by Gradient Column according to ASTM D 3835 ASTM 1505

(b) Viscosity vs. Shear Rate and Temperature was measured by Twin Bore Capillary Rheometer , Rosand RH7-2 for according to ASTM D 3835

(c) Specific Heat was measured by Differential Scanning Calorimeter according to ASTM Proposed Test Method (Project TM-01-06 A in Committee E37)

(d) Vicat Softening Point was determined by Heat Distortion Temperature Tester according to ISO 306

(e) Thermal Conductivity was measured by Thermal Conductivity Tester according to JIS R 2618

3.3.2 Injection moulding of Experimental Plaques

The experimental plaques of three ABS grades were moulded by varying injection speed, holding pressure , holding time and melt temperature to determine the effect of injection moulding parameters on mechanical property and their pressure cavity.

The injection machine , 50 kN ENGEL, Model EC 88 used for this work is shown in Fig. 3.1. Figure 3.2 shows the mould cavity of dimension

100 x 125 x 3 mm rectangular plaque, with film type gate. The mould was instrumented with the cavity pressure transducers from Kistler type 6157 BA, ϕ 4 mm, sensitivity -9.4 pC / bar , positioned near the gate and far from the gate as shown in Fig. 3.3. The transducers was connected to a charge amplifier type 5039A232 and an adapter of DAS-16 type 2851 as shown in Fig. 3.4. The signal was passed through a data acquisition card type CIO-DAS 1602-330 to DataflowPlus program for the output shown between cavity pressure (bar) vs. filling time (sec).

Figure 3.1 The injection machine , 50 kN ENGEL, Model EC 88.
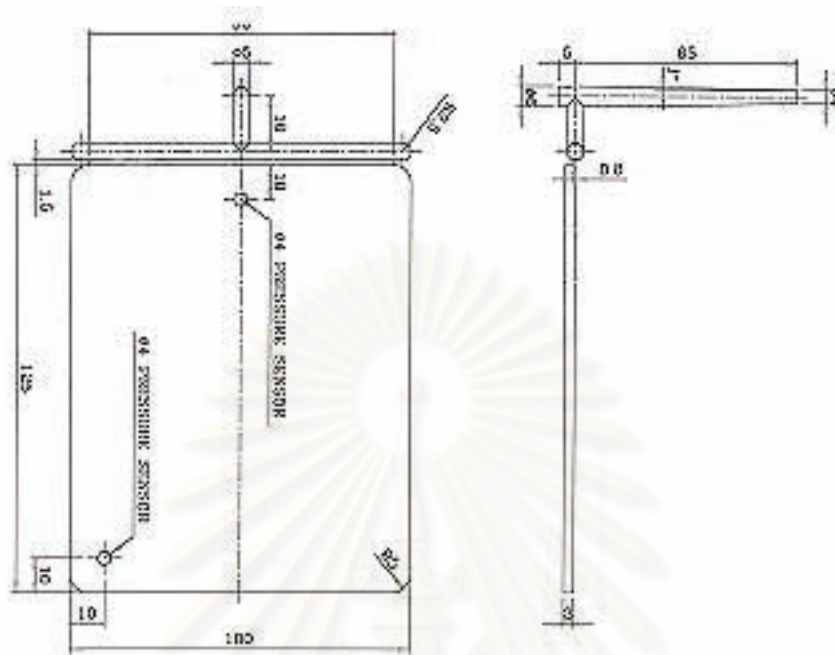
Figure 3.2 Drawing of the part .
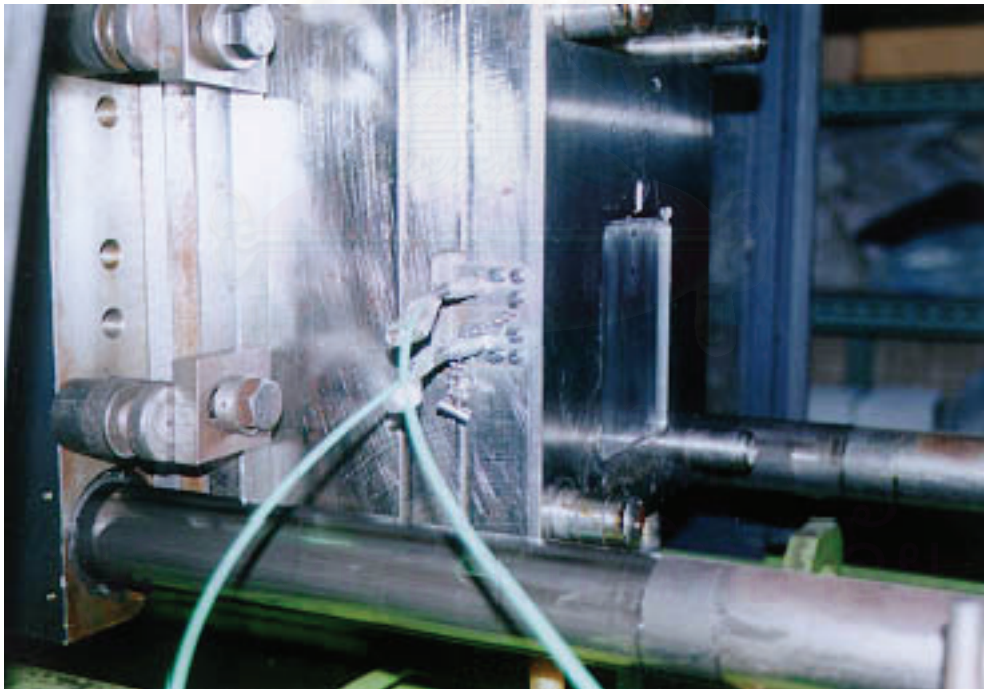
Figure 3.3 The mould fitted with the cavity pressure transducers near the gate
and far from the gate .
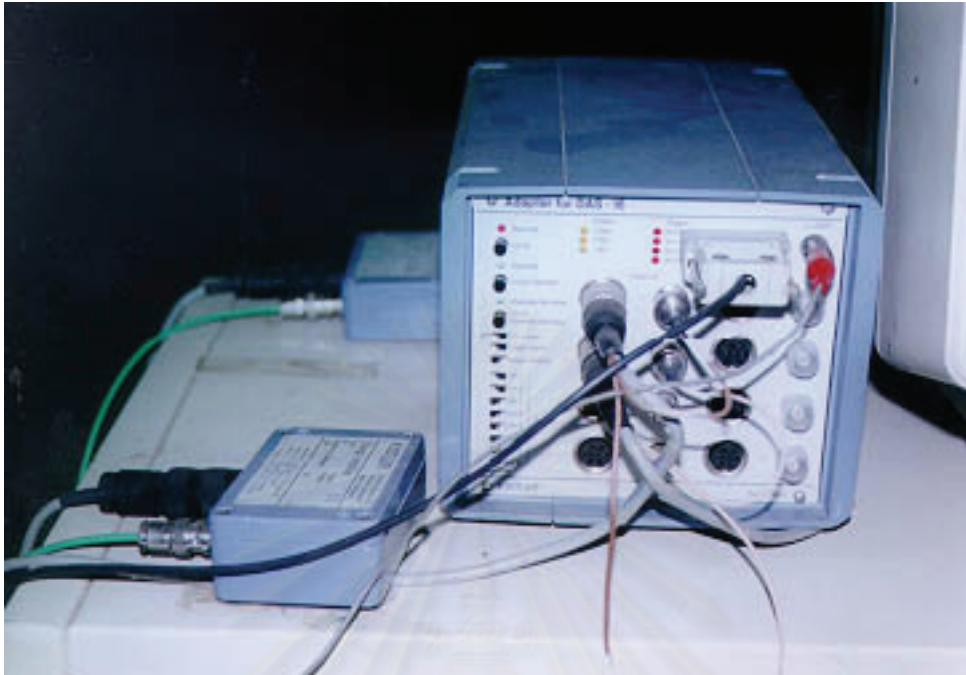
Figure 3.4   Charge amplifiers   type 5039A232   connected to an adapter of
             DAS-16 type 2851 .

3.3.2.1 Injection Moulding Conditions

(a) Injection   moulding   parameters   were   adjusted   until the ideal   cavity pressure curves were achieved   for ABS Lustran 250 , Lustran 440 and Lustran 640.

(b) The   parameters   were   recorded   for   using   as   the reference conditions.

(c)   The   only   one   parameter   was   varied   while   the   other parameters   were   maintained constant. Injection speed, holding pressure, holding time and melt temperature were varied one by one to be higher and lower conditions from the reference condition. All conditions were recorded and the cavity pressure curves were obtained.

The fixed parameters during all of the experiments were as follows.

Plasticizing Stroke   51 mm

Screw Rotation Speed   29 mm / s

Back Pressure   5 bar

Cooling Time   25 sec.

The mould temperature was maintained at 50 $^{\circ}$C by the cooling water. The mould surface temperature was measured by a thermometer as shown in Fig. 3.5 . The moulded parts as well as the cavity pressures were kept and recorded after operated 1 hour already to make the machine and temperature stable.

Figure 3.5 Thermometer used for the mould surface temperature measurement.

Table 3.2   The experimental injection moulding conditions.

Exp. No.	Exp. Description	Injection Parameters for Lustran 250			
		Injection Speed (mm/s)	Holding Pressure (bar)	Holding Time (sec)	Melt Temperature ($^{\circ}$C)
1	Reference Condition (Ideal P Curve)	40	15	1.5	230
2	Injection Speed Increment	75	15	1.5	230
3	Injection Speed Increment	100	15	1.5	230
4	Injection Speed Decrement	25	15	1.5	230
5	Injection Speed Decrement	10	15	1.5	230
6	Holding Pressure Increment	40	20	1.5	230
7	Holding Pressure Increment	40	70	1.5	230
8	Holding Pressure Increment	40	100	1.5	230
9	Holding Pressure Decrement	40	10	1.5	230
10	Holding Pressure Decrement	40	5	1.5	230
11	Holding Pressure Decrement	40	0	1.5	230

Table 3.2   The experimental injection moulding conditions. (Continued)

Exp. No.	Exp. Description	Injection Parameters for Lustran 250			
		Injection Speed (mm/s)	Holding Pressure (bar)	Holding Time (sec)	Melt Temperature (C)
12	Holding Time Increment	40	15	2	230
13	Holding Time Increment	40	15	20	230
14	Holding Time Decrement	40	15	1	230
15	Holding Time Decrement	40	15	0	230
16	Melt Temperature Increment	40	15	1.5	240
17	Melt Temperature Increment	40	15	1.5	250
18	Melt Temperature Increment	40	15	1.5	270
19	Melt Temperature Increment	40	15	1.5	280
20	Melt Temperature Decrement	40	15	1.5	210
21	Melt Temperature Decrement	40	15	1.5	190

Table 3.2   The experimental injection moulding conditions. (Continued)

Exp. No.	Exp. Description	Injection Parameters for Lustran 440			
		Injection Speed (mm/s)	Holding Pressure (bar)	Holding Time (sec)	Melt Temperature (^{o}C)
22	Reference Condition (Ideal P Curve)	38	29	1.0	230
23	Injection Speed Increment	50	29	1.0	230
24	Injection Speed Increment	75	29	1.0	230
25	Injection Speed Increment	100	29	1.0	230
26	Injection Speed Decrement	20	29	1.0	230
27	Injection Speed Decrement	5	29	1.0	230
28	Holding Pressure Increment	38	50	1.0	230
29	Holding Pressure Increment	38	100	1.0	230
30	Holding Pressure Decrement	38	20	1.0	230
31	Holding Pressure Decrement	38	10	1.0	230
32	Holding Pressure Decrement	38	0	1.0	230
33	Holding Time Increment	38	29	15	230

Table 3.2 The experimental injection moulding conditions. (Continued)

Exp. No.	Exp. Description	Injection Parameters for Lustran 440			
		Injection Speed (mm/s)	Holding Pressure (bar)	Holding Time (sec)	Melt Temperature (^{o}C)
35	Melt Temperature Increment	38	29	1.0	280
36	Melt Temperature Decrement	38	29	1.0	200
37	Melt Temperature Decrement	38	29	1.0	180

Exp. No.	Exp. Description	Injection Parameters for Lustran 640			
		Injection Speed (mm/s)	Holding Pressure (bar)	Holding Time (sec)	Melt Temperature (^{o}C)
38	Reference Condition (Ideal P Curve)	30	60	2.0	230
39	Injection Speed Increment	60	60	2.0	230
40	Injection Speed Decrement	20	60	2.0	230
41	Injection Speed Decrement	10	60	2.0	230
42	Holding Pressure Increment	30	80	2.0	230
43	Holding Pressure Decrement	30	40	2.0	230
44	Holding Pressure Decrement	30	10	2.0	230

Table 3.2   The experimental injection moulding conditions. (Continued)

Exp. No.	Exp. Description	Injection Parameters for Lustran 640			
		Injection Speed (mm/s)	Holding Pressure (bar)	Holding Time (sec)	Melt Temperature (^{o}C)
45	Holding Pressure Decrement	30	0	2.0	230
46	Holding Time Increment	30	60	20	230
47	Holding Time Decrement	30	60	1	230
48	Holding Time Decrement	30	60	0	230
49	Melt Temperature Increment	30	60	2.0	230
50	Melt Temperature Increment	30	60	2.0	270
51	Melt Temperature Increment	30	60	2.0	280
52	Melt Temperature Decrement	30	60	2.0	210
53	Melt Temperature Decrement	30	60	2.0	190

3.3.3 Mechanical Property Test

The injection moulded rectangular plaque samples of 3 mm thickness were tested on Radmana ITR-2000 high speed instrumented impact tester as shown in Fig. 3.6. The tester was set at 4 ms^{-1} velocity , 500 kPa clamping force , 600 kPa air control circuit and 400 kPa air supply. The samples (Lustran 250, Lustran 440 and Lustran 640) of each varied injection moulding parameters according to Table 3.2 were tested by sampling of 30 specimens per experiment. Normally, the large scatter in impact result would be given, so the use of a minimum sample of 10 was recommended to resolve the problems associated with comparing the impact performance of material[19] .

The effect of injection moulding parameters on the impact property and the pattern of fracture for each ABS grades were analyzed.

Figure 3.6 Radmana ITR-2000 instrumented impact tester.

3.3.4 Moldflow® Flow Analysis Program

The Moldflow® flow analysis program needed the input data for injection moulding simulation. The details of the rectangular plaque mould , the ABS material database , the injection conditions such as the mould and the melt temperatures, injection time , packing pressure and time were entered into the program as the following steps.

Details of the rectangular plaque mould were entered into the program. The model of the mould geometry was created using the Moldflow pre-processing module. The model was meshed as triangular elements divided into 1265 elements and 685 nodes. The node which was the starting point of injection was fixed and saved as the Boundary Condition File. Figure 3.8 shows the mould geometry after meshed by MFVIEW pre-processor of the Moldflow ®.

Figure 3.7 The mould geometry and meshing.

Mould-filling   simulation   was   then   carried   out   using   the
Moldflow 3D flow analysis for thermoplastics by the following steps.
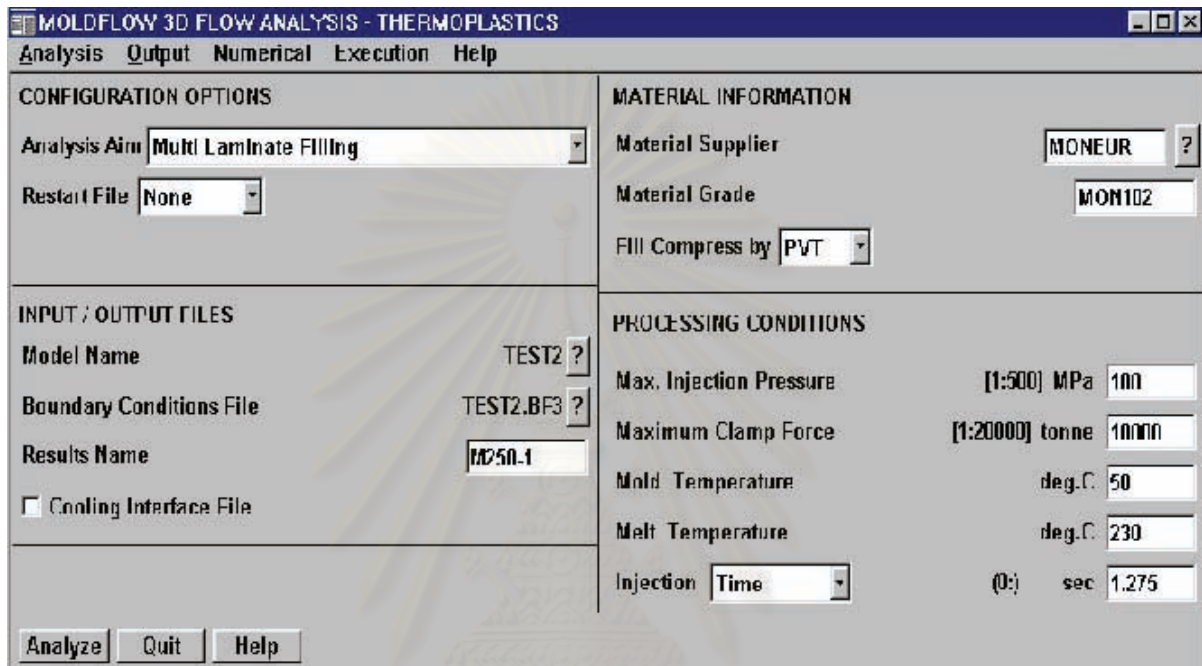
Figure 3.8 Input page of the filling analysis stage.

(a) Analysis   Aim   was   selected   as   Multi Laminate Filling   then
the   Model   Name , Boundary   Conditions   File   and   the   Result   name   were
entered. Figure 3.9 shows   the   input   page   for   the   filling   stage of Moldflow 3D
flow analysis.

(b) The   material   information was   selected   from   Moldflow® standard
database   as   grade   MON 102 [1] for ABS Lustran 250 , MON 105 for   ABS Lustran
440   and   MON 106   for ABS Lustran 640 or the ABS material information   from
the prepared personal database was selected.

[1] MON 102 was the material properties of   Lustran 240 , existing in Moldflow
standard database , which was the same impact property but lower melt flow for

61

Lustran 250. ABS Lustran 250 was used for the actual injection moulding experiments.

(c) The various injection moulding conditions were entered into the program as same as the injection moulding experiments.

(d) Mould - Packing Simulation was analyzed by selection the analysis aim as Multi Laminate Packing then the Packing Profile was entered as same as the actual injection moulding experiments. Figure 3.10 shows the input page for the packing stage of Moldflow 3D flow analysis.

(e) The output results of the pressure with respect to time (Time Series) were plotted as 2 D line graphs by determination of the node numbers as conforming to the pressure transducers positions fitted in the mould.

(f) The result of pressure prediction by the Moldflow® and cavity pressure measured by pressure transducers fitted in the mould were compared for verification of the Moldflow® simulation software.
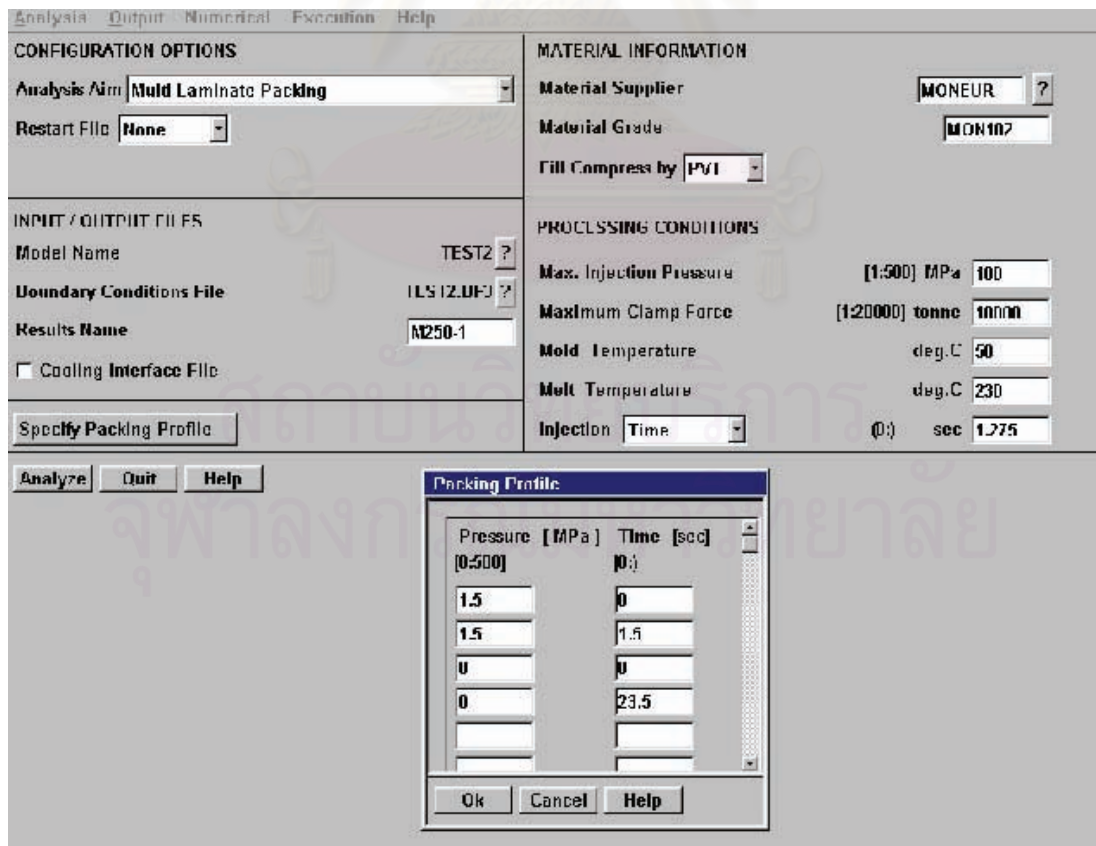
Figure 3.9 Input page of the packing analysis stage.

3.3.5 Testing the Internal Structure to Verify the Effect of Injection Moulding Parameters

The injection moulding parameters caused the changes of moulded part internal structure affecting to the impact property. Therefore, some simple test method done to verify there were different in the internal structure of moulded parts as the following.

(a) Molecular Orientation testing by tensile test according to ASTM D 638.

The specimens were prepared by cutting the tensile bars according to the Fig. 3.10 . One group of tensile bar specimens was annealed at 80 $^{\circ}$ C , 4 h in an oven. The specimens were tested for tensile strength with and without annealing. The tensile properties were tested on a Lloyd LR 10K tensile tester at a strain rate of 5 mm/min.
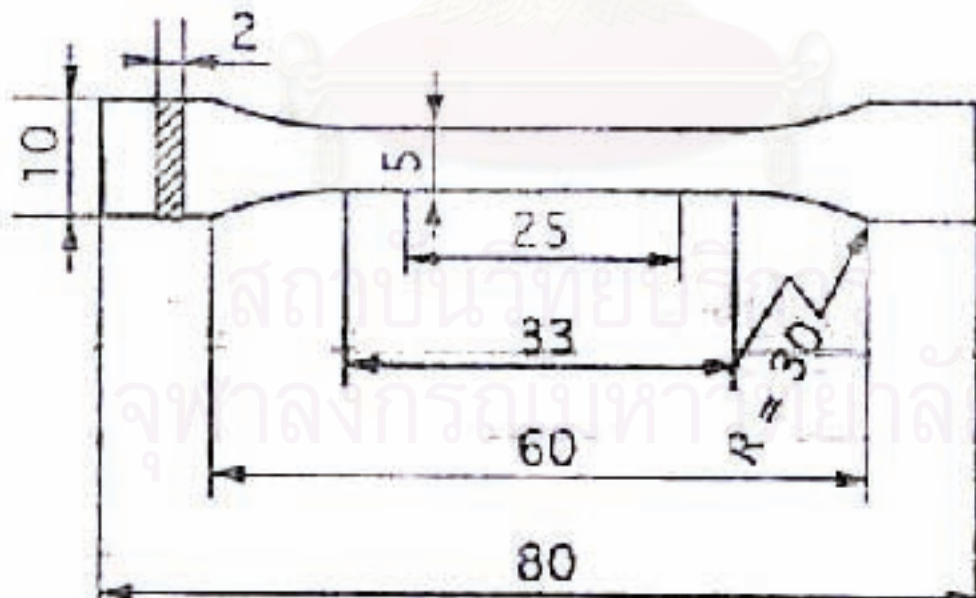
Figure 3.10 Dimensions of milled tensile bar in mm [16] .

(b) Residual stress testing [20] by Glacial Acetic Acid (AA) Immersion Test for stress visualization. Specimens were tested for internal stresses by using the glacial acetic acid test. This test was done by immersion the plastic specimens in anhydrous glacial acetic acid. The first step was to immerse the specimens for 30 seconds followed by rinsing in water and drying at room temperature. In the second step, the specimens were re-immersed in the acid for 2 minutes, followed by rinsing and drying. The specimens were then visually inspected.

(c) Molecular Degradation test by comparing the melt flow index

The specimens moulded at 280 $^\circ$C , 230 C and 190 C melt temperature were crushed then tested melt flow index according to ASTM 1238 at 230 $^\circ$C , 2.16 kg . The virgin granules were tested at the same condition. The experimental flow chart of this work is shown in Fig. 3.11 .
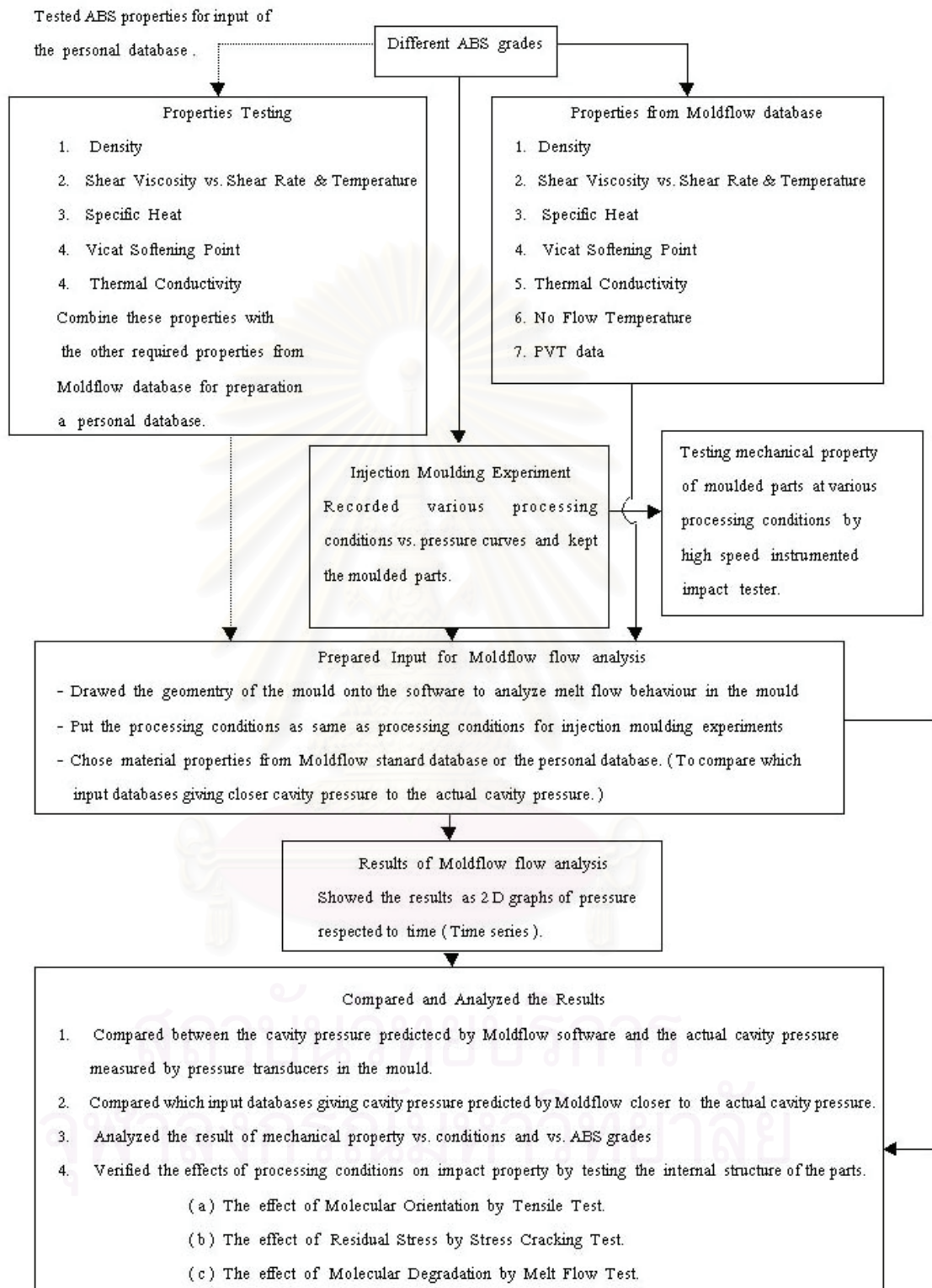
Figure 3.11 Experimental Flowchart.

CHAPTER IV

RESULTS AND DISCUSSION

4.1 MATERIAL PROPERTIES

Some material properties data were needed for database requirements in order to use the complete simulation program [3].

Some properties of the chosen three grades of ABS , Lustran 250 , Lustran 440 and Lustran 640 , are presented in Table 4.1. The testing results were used for preparing the personal database.

Table 4.1 Properties data (by measurement) for ABS Lustran 250, Lustran 440 and Lustran 640

Test Items	Lustran 250	Lustran 440	Lustran 640
1. Density at 23°C (Kg / m^3)	1054.5	1054.7	1054.8
2.Thermal Conductivity (W/m$^{\circ}$C) at 23°C at 200°C	0.1767 0.2958	0.1841 0.3045	0.1835 0.3030

Table 4.1   Properties data (by measurement) for ABS Lustran 250, Lustran 440
and Lustran 640 (Continued)

Test Items	Lustran 250	Lustran 440	Lustran 640
3. Viscosity (Pa.s) at Temp. 200°C			
Shear Rate (1 / s) 100	1285.71	2937.5	3200
300	1140	1400	1500
1000	450	557.14	571.43
3000	220	236.67	253.33
10000	91.43	87.5	81.25
Viscosity (Pa.s) at Temp. 230°C			
Shear Rate (1 / s) 100	1060	1640	1720
300	600	800	850
1000	290	354.55	327.73
3000	144	165.39	187.5
10000	54.29	60	63
Viscosity (Pa.s) at Temp. 260°C			
Shear Rate (1 / s) 100	530	800	900
300	337.5	425	266.67
1000	178.95	218.18	231.82
3000	90	103.95	113.16
10000	38.44	42.5	43.33
4. Specific Heat (J / Kg$^{\circ}$C)	2100	2100	2100
5. Vicat Softening Point ($^{\circ}$C)	97.84	99.4	99.56
6. Glass Transition Temperature ($^{\circ}$C)	103.83	104.76	105.14

4.2 COMPARISON OF PREDICTED AND MEASURED PRESSURE

A simulation program is useful if it gives a good agreement with the actual processing output. This section illustrates a practical verification results of the Moldflow® simulation for various injection moulding parameters.

4.2.1 Measurement of Cavity Pressure Curves

4.2.1.1 Effect of Injection Speed on Pressure Curve

The effect of injection speed on the pressure curve was investigated by varying injection speeds while other parameters were kept constant as follows :

Holding Pressure   :   15   bar
Holding Time   :   1.5   sec
Melt Temperature   :   230   ° C

In the filling phase , the strong influences on thepressure curve were the injection speed and melt temperature [12]. At high injection speed , the pressure curve was steeper. When the phase started , the melt was pushed into the cavity. The melt reached pressure transducer near the gate (P_1) then passed through the pressure transducer far from the gate (P_2). The fill time decreased with increasing injection speed. The compression phase was reached sooner. Figure 4.1 shows the pressure curves of ABS Lustran 250 at various injection speeds. It can be seen that the pressure increased with the increase of injection speed and there was a pressure peak (Exp. No.2 and No.3) which indicated overpacking of the moulded parts. It was corresponded to the flashed parts produced from Exp. No. 3 . As the injection speed

decreased, the pressure curve decreased (Exp. No. 4 and 5) which indicated that the cavity was not filled completely . No or low pressure value was detected by P_2 if the injection speed was very low. In this case, little melt was pushed through P_2 and the melt could solidify before it reached P_2 so the plastic parts produced from Exp. No. 5 were short shot.

4.2.1.2 Effect of Holding Pressure on Pressure Curve

The effect of holding pressure on the pressure curve was investigated by varying holding pressure while other parameters were kept constant as follows :

Injection Speed   :   40   mm/s

Holding Time   :   1.5   sec

Melt Temperature   :   230 $^{\circ}$ C

The holding pressure was the important factor which had strong influence on the pressure curve during the holding pressure phase [12]. An increase in the holding pressure caused a rise in the cavity pressure and an increase in the effective holding pressure time as shown in Fig. 4.2 . The pressure curve of Exp. No. 8 (370 bar) was higher than Exp. No. 7 (250 bar) and Exp. No. 1 (210 bar) respectively due to higher holding pressure. In addition, an increase in the effective holding pressure time was shown in the pressure curves of Exp. No.7 and Exp. No. 8 as increasing holding pressure. Very high holding pressure (Exp. No. 8) also caused the flash parts of plastic specimens. Decreasing the holding pressure even at 0 bar (Exp. No. 11) did not affect the pressure curve. The pressure curve of Exp. No. 11 (high holding pressure) was as same as that of Exp.No. 1 (reference condition).

4.2.1.3 Effect of Holding Time on Pressure Curve

The effect of holding time on the pressure curve was investigated by varying holding time while other parameters were kept constant as follows :

Injection Speed : 40 mm/s

Holding Pressure : 15 bar

Melt Temperature : 230 $^\circ$C

The holding time also had a decisive influence on the pressure curve [12]. In the case of too short holding time , the melt might flow out of the cavity into the runner system and back into the screw chamber ; these non – reproducible events led to sink marks , fluctuations in part weight and consequently to a variety of defects. Zero holding time , the holding pressure removed too soon resulted in a drop – off in the pressure curve as shown in the Exp. No. 15 of the Fig. 4.3 . The parts of the Exp. No. 15 had sink marks at the end of flow and a little short shot. If the holding time was longer than the gate freeze off time, no further change occurred in the pressure curve as shown in Fig. 4.3 the Exp. No.13 . When the gate was solidified, so no further melt could flow into the cavity to compensate for shrinkage during the holding phase.

4.2.1.4 Effect of Melt Temperature on Pressure Curve

The effect of melt temperature on the pressure curve was investigated by varying melt temperature while other parameters were kept constant as follows :

Injection Speed	:	40	mm/
Holding Pressure	:	15	bar
Melt Temperature	:	230	$^{\circ}$C

The other strong influence on the pressure curve in the injection phase was melt temperature. High melt temperature led to the large free cross section. The melt in the core , which was still fluid , had a higher temperature and thus a lower viscosity. Therefore, the high melt temperature and low viscosity caused the pressure drop reduction and resulted in a higher pressure at the pressure transducers both of the P_1 near the gate and the P_2 far from the gate. Furthermore, the hotter melt caused the gate to open longer before freeze off , the duration of the holding pressure also increased. Figure 4.4 shows the pressure curves at various melt temperature. The ABS parts produced from high melt temperature (Exp. No. 18 and No. 19) had silver streaks and discolouration.
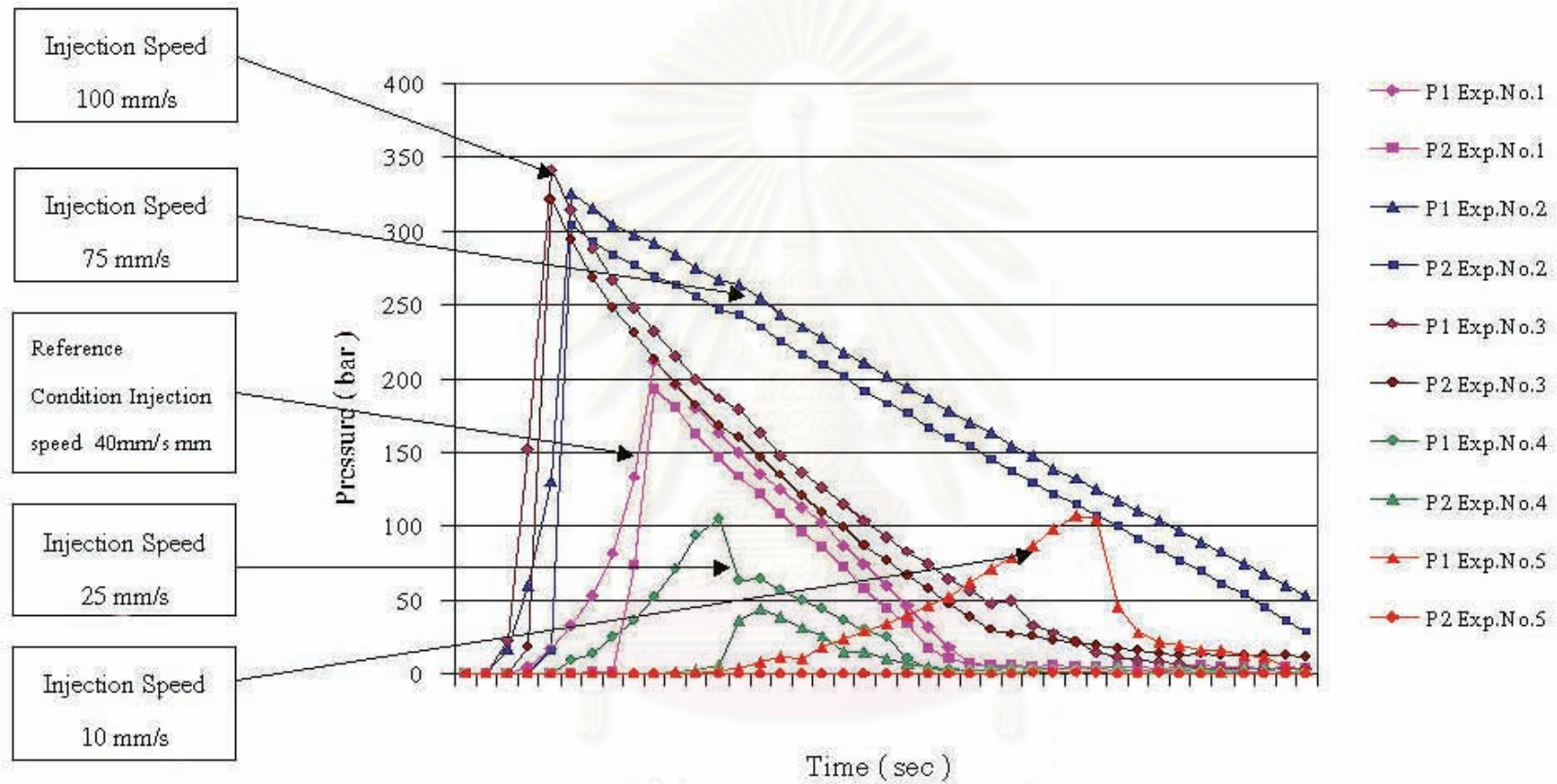
Figure 4.1   The pressure curves of ABS Lustran 250 as injection speed was varied.
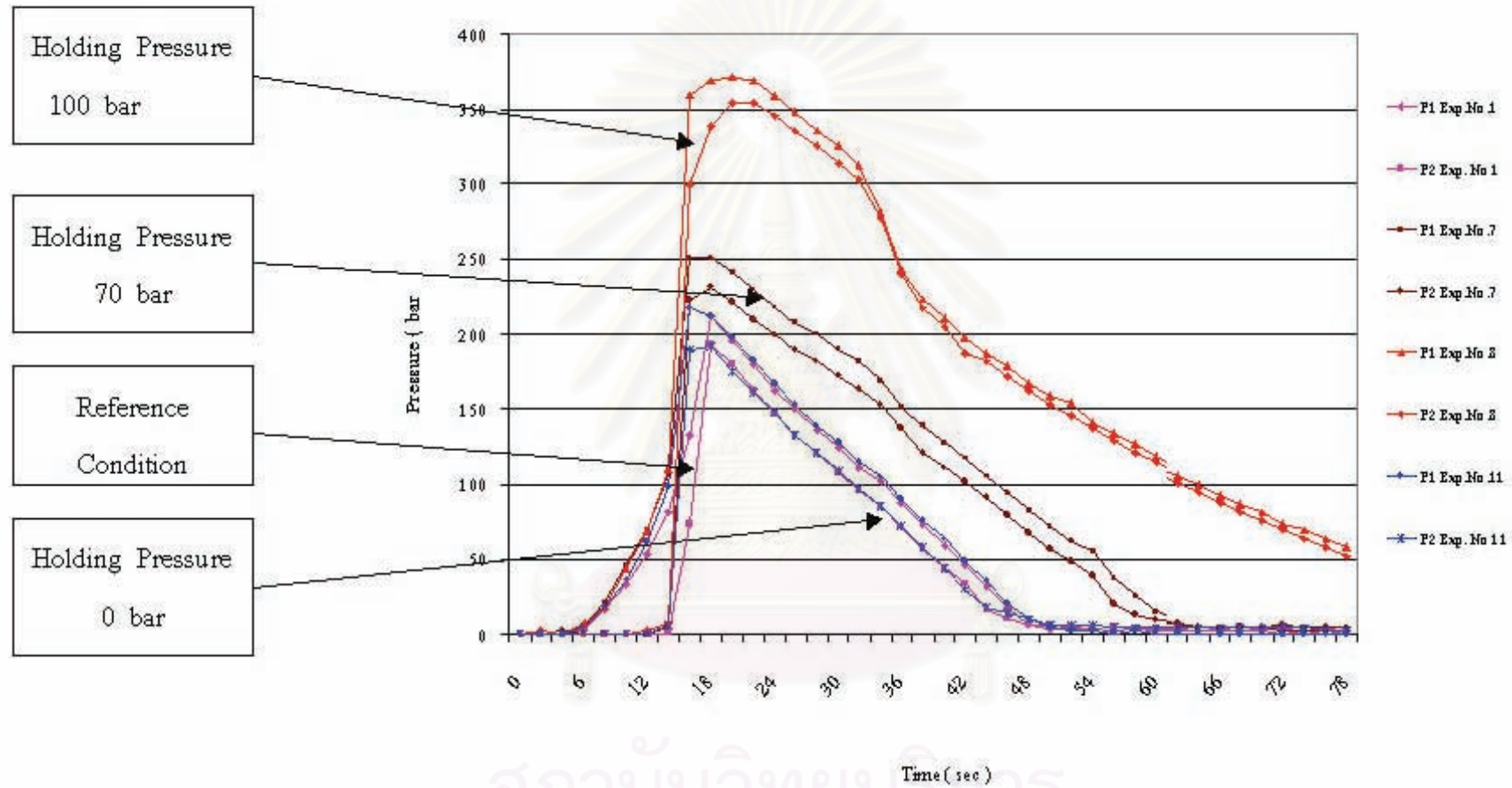
Figure 4.2   The pressure curves of ABS Lustran 250 as holding pressure was varied .
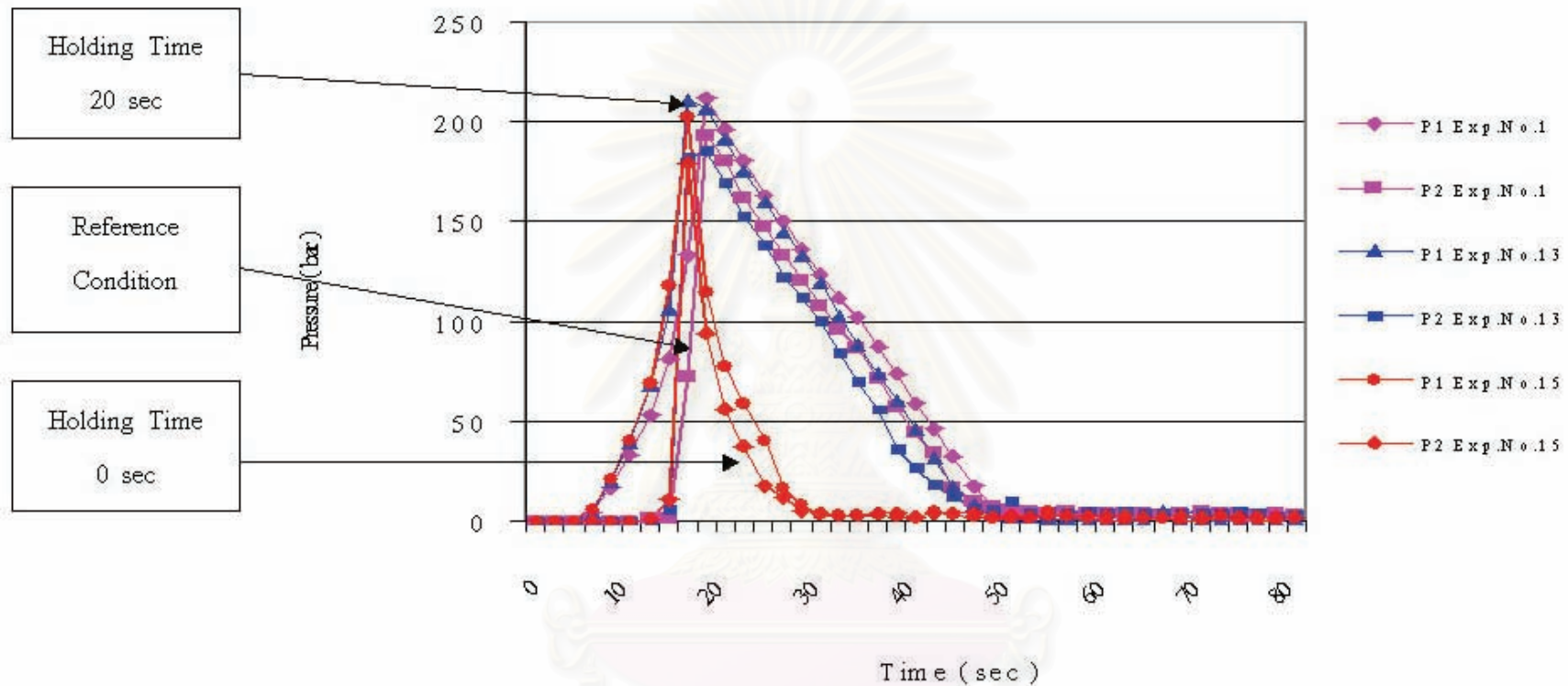
Figure 4.3   The pressure curves of ABS Lustran 250 as holding time was varied.
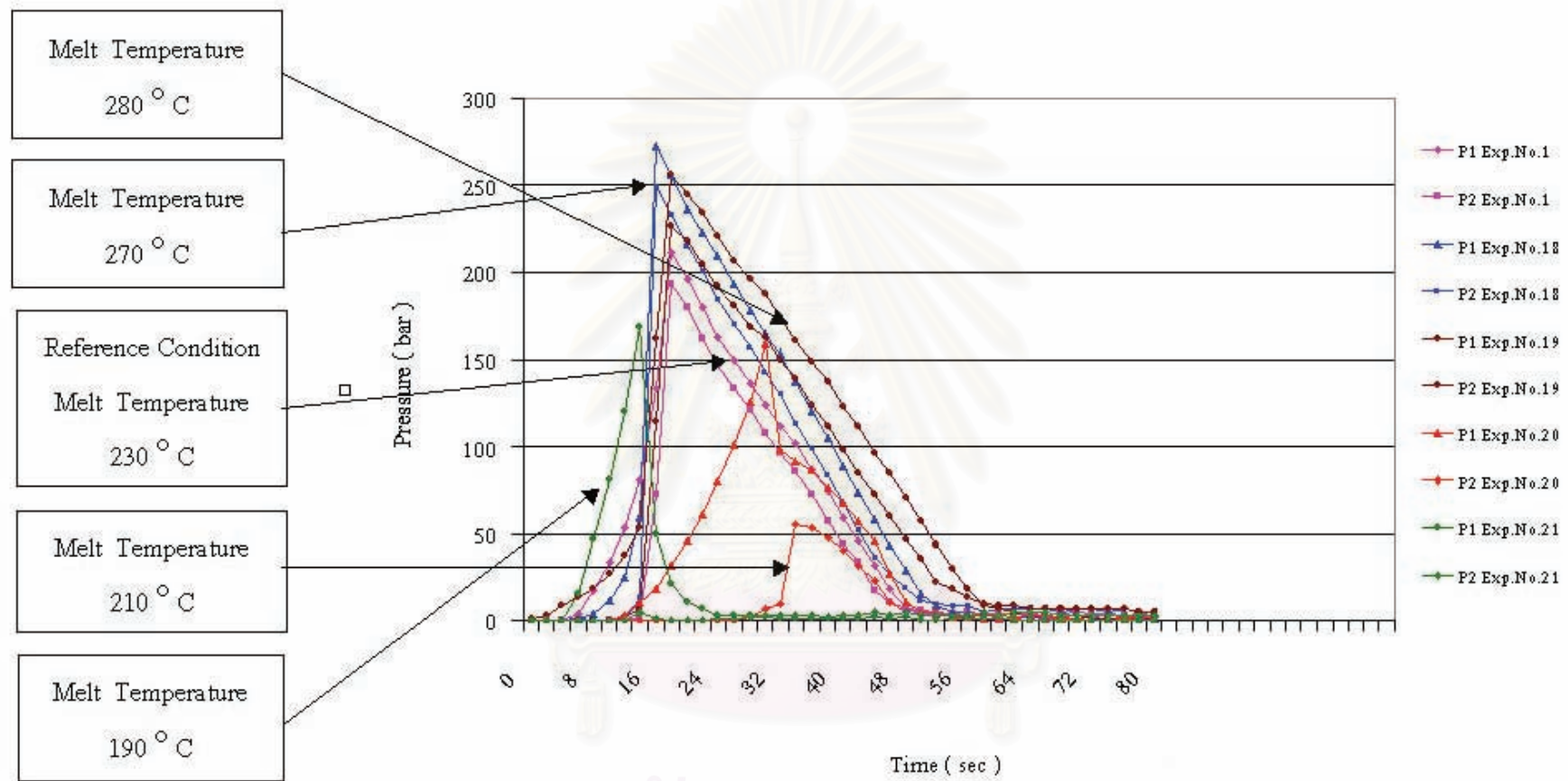
Figure 4.4   The pressure curves of ABS Lustran 250 as melt temperature was varied.

4.2.2 Pressure Curves Predicted by Moldflow Ⓡ Software

Pressure predicted by   the Moldflow Ⓡ simulation program (ABS properties was selected from existing Moldflow standard database or the personal database to compare the results for different material information input) and cavity pressure measured experimentally   by pressure transducers fitted in the mould.

The quality and accuracy of the input determines the utility and usefulness of the simulation output[14]. Therefore, a personal database was also prepared and compared the output results with the existing Moldflow standard database in this work.

The pressure predicted by selection the existing Moldflow standard database and a personal database were quite similar features given at various injection moulding parameters. The example of pressure curves for each reference conditions (Exp. No.1 , Exp. No.22 and Exp.No.38) of ABS Lustran 250 , Lustran 440 and Lustran 640 were shown in Fig. 4.5. The maximum pressure of Exp.No. 1 for Moldflow standard database and a personal database were approximate the same value (250 bar) but the curves showed the effective holding pressure time predicted for a personal database was shorter than that for Moldflow database. It has been observed the higher pressure values were predicted when a personal database was selected for ABS Lustran 440 and Lustran 640 (Exp. No. 22 and Exp. No. 38).
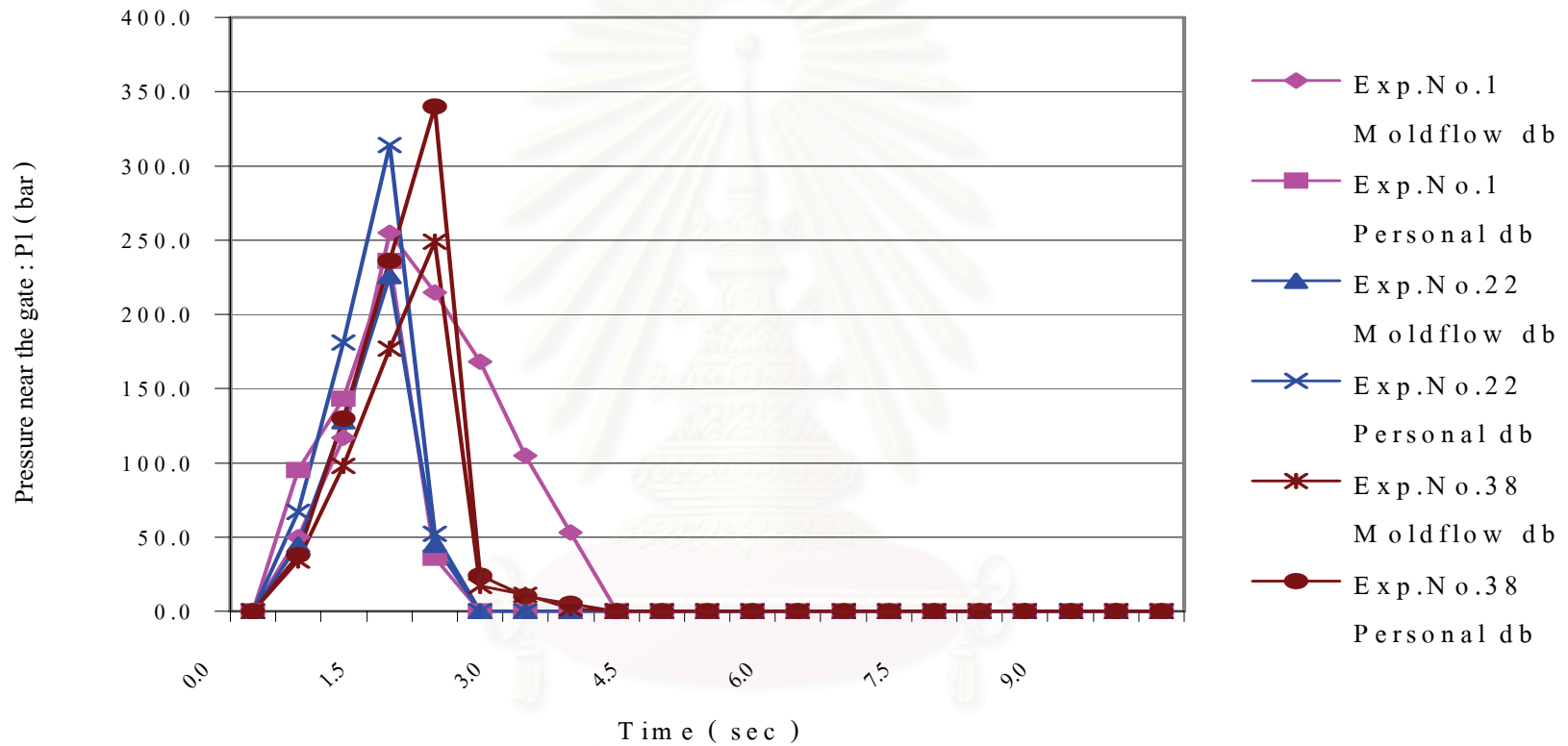
Figure 4.5 Comparison pressure curves between Moldflow standard database and a personal database select at reference conditions of ABS Lustran 250 , Lustran 440 and Lustran 640.

4.2.2.1 Effect of Injection Speed on Pressure Curve

Figure 4.6 (a) shows the pressure curve predicted by Moldflow ® flow analysis at various injection speeds. The material information of ABS Lustran 250 for the input of flow analysis was selected from the Moldflow ® standard database. Figure 4.6 (b) also shows the pressure curve predicted by Moldflow® program at various injection speeds as a personal database was selected.

For prediction from Moldflow ® standard database and a personal database at higher injection speeds, the pressure curves were steeper. The pressure curve of Exp. No. 3 was steeper than that of Exp. No. 2 , Exp. No. 1 , Exp. No. 4 and Exp. No. 5 . The maximum pressure value of Exp. No. 2 at high injection speed was higher than that of Exp. No. 1 and Exp. No. 4. However , the pressure value of very high injection speed (Exp. No. 3) was lower and the fill time was very short due to the higher volume flow. The maximum pressure value for low injection speed of Exp. No. 5 was higher again because the low injection speed led to a reduction of the free channel cross section. This is as due to the solidification of the melt close to the wall and the higher pressure.
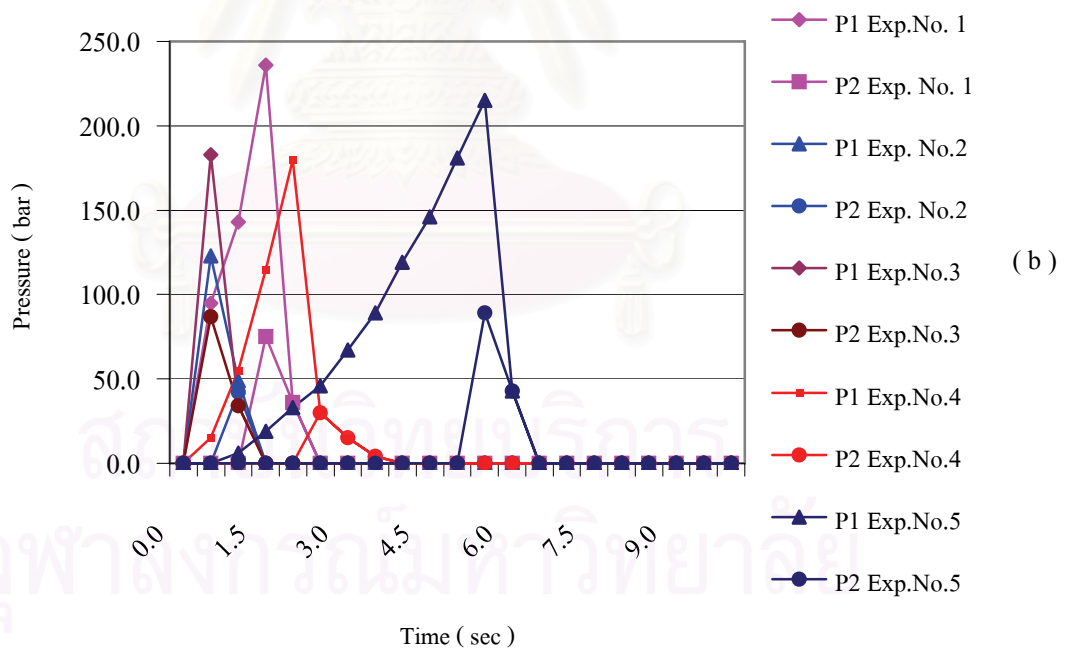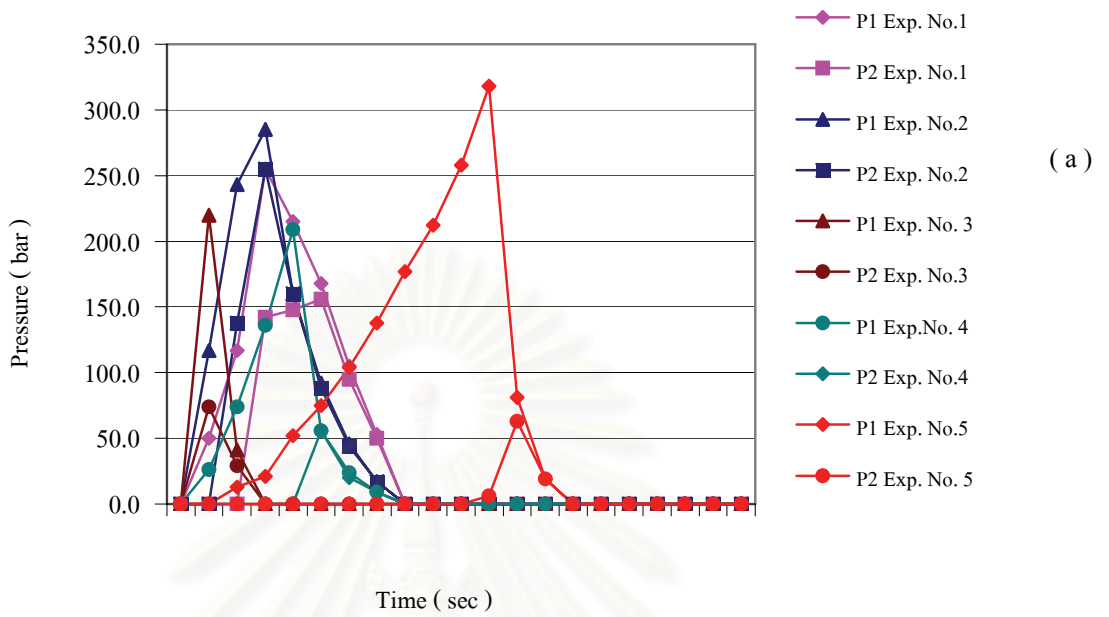
Figure 4.6   Pressure prediction as injection speed was varied

for   ABS Lustran 250.

(a) Moldflow standard database for inputs

(b) Personal database for inputs

4.2.2.2 Effect of Holding Pressure on Pressure Curve

Figure 4.7 (a) shows the pressure curve predicted by Moldflow ® at various holding pressure by Moldflow ® standard material information input. Figure 4.7 (b) also shows the pressure curve predicted by Moldflow® and the database was selected from a personal database.

From Fig. 4.7 (a) and (b) , the pressure curves (Exp. No. 1 , Exp. No. 7 , Exp. No. 8 and Exp. No. 11) had the same slope of pressure rising in the filling phase. As the holding pressure increased, the pressure curve did not change and the effective holding pressure time did not increase. However , for the low holding pressure (Exp. No. 11) , the pressure curve observed was low.

(a)
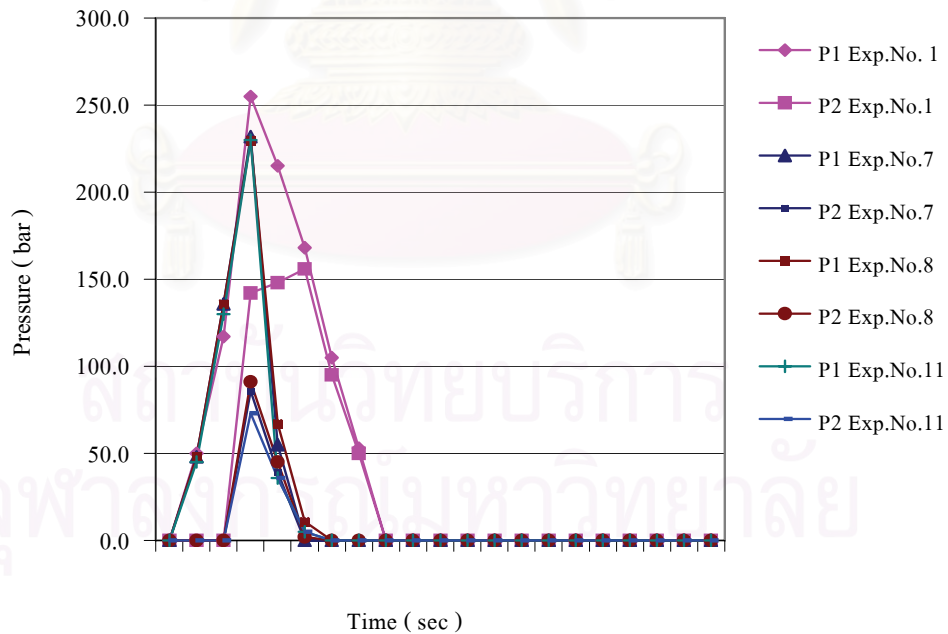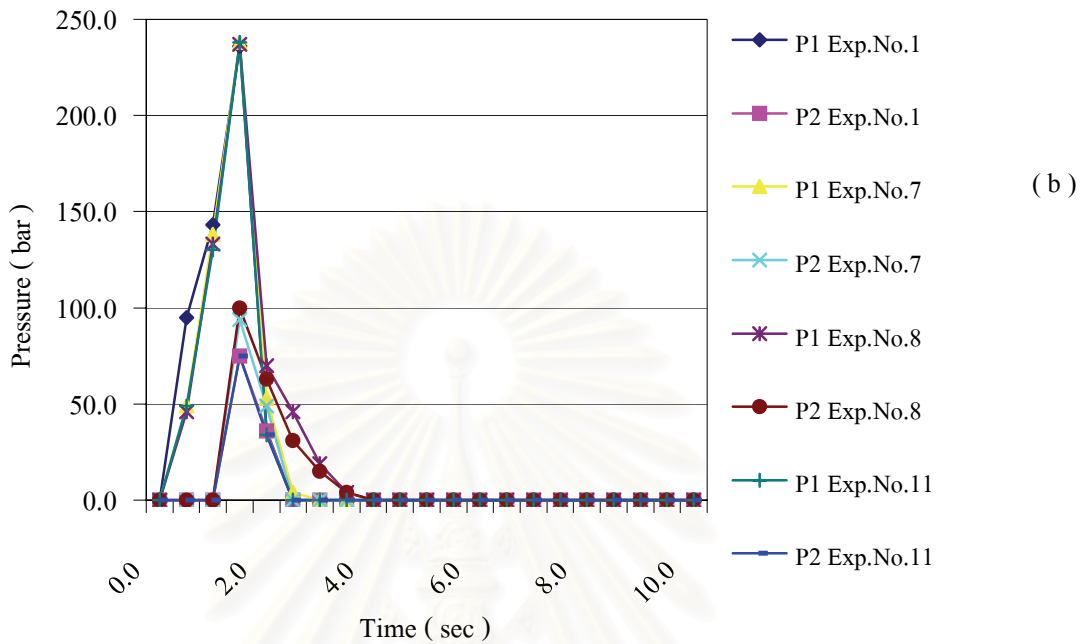
Figure 4.7 Pressure prediction as holding pressure was varied

for ABS Lustran 250.

(a) Moldflow standard database for inputs

(b) Personal database for inputs

4.2.2.3 Effect of Holding Time on Pressure Curve

Figure 4.8 (a) shows the pressure curve predicted by Moldflow ® at various holding time by Moldflow ® standard was database material information input. Figure 4.8 (b) also shows the pressure curves predicted by Moldflow® at various holding time but a personal database was selected.

From Fig. 4.8 (a) and (b) , the pressure curves predicted (Moldflow ® standard database and a personal database) at various holding time for Exp. No. 1 , Exp. No. 13 and Exp. No. 15 showed the same slope of

pressure rising in the filling phase. As well as , the longer holding time or
sh

(a)

(b)

Time (sec)
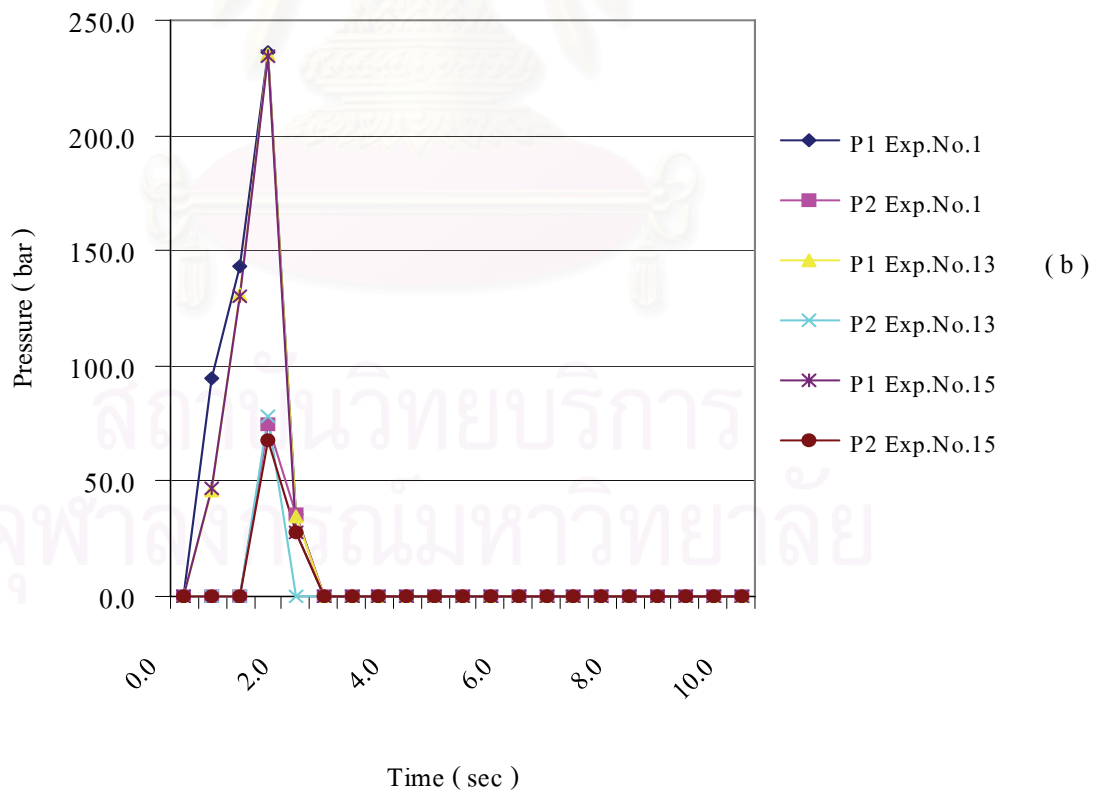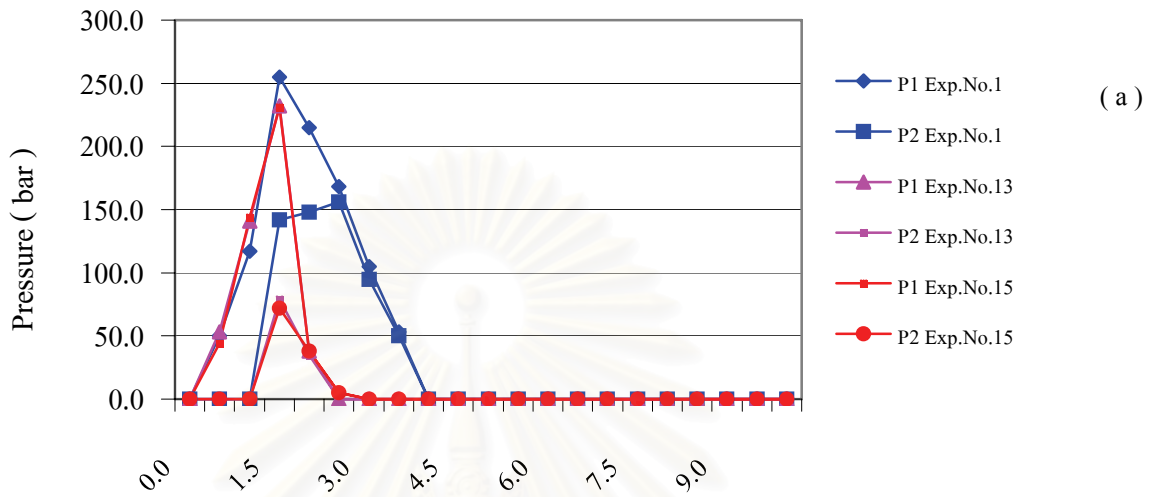
(a) Moldflow standard database for input

(b) Personal database for input

4.2.2.4 Effect of Melt Temperature on Pressure Curve

Figure 4.9 (a) shows the pressure curves predicted by Moldflow ® at various melt temperature (Moldflow ® standard database was selected for material information input). Figure 4.9 (b) also shows the pressure curves predicted by Moldflow® at various melt temperature but a personal database was selected .

Moldflow (Moldflow ® standard database and a personal database) gave the high pressure curves at low melt temperature conditions (Exp. No. 21 , Exp. No. 20). Pressure curves of Exp. No. 21 which was at lower melt temperature was higher than that of Exp. No. 20. The higher the melt temperature, the lower the pressure value (Exp. No. 18 and Exp. No. 19).

(a)
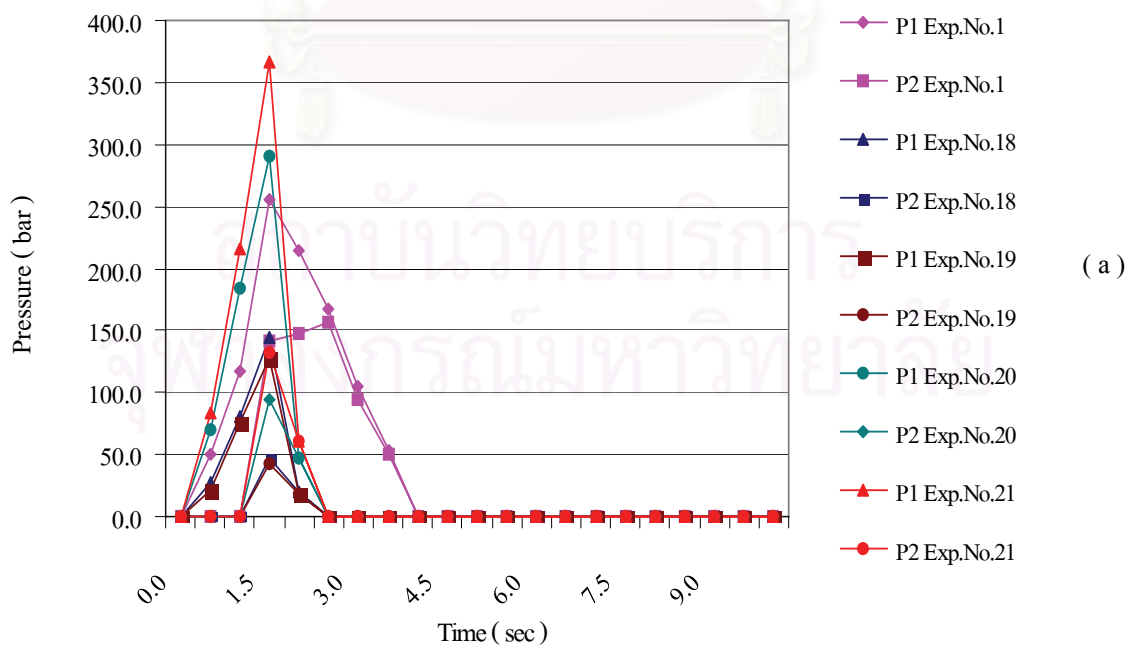
Figure 4.9 Pressure prediction as melt temperature was varied

(b)
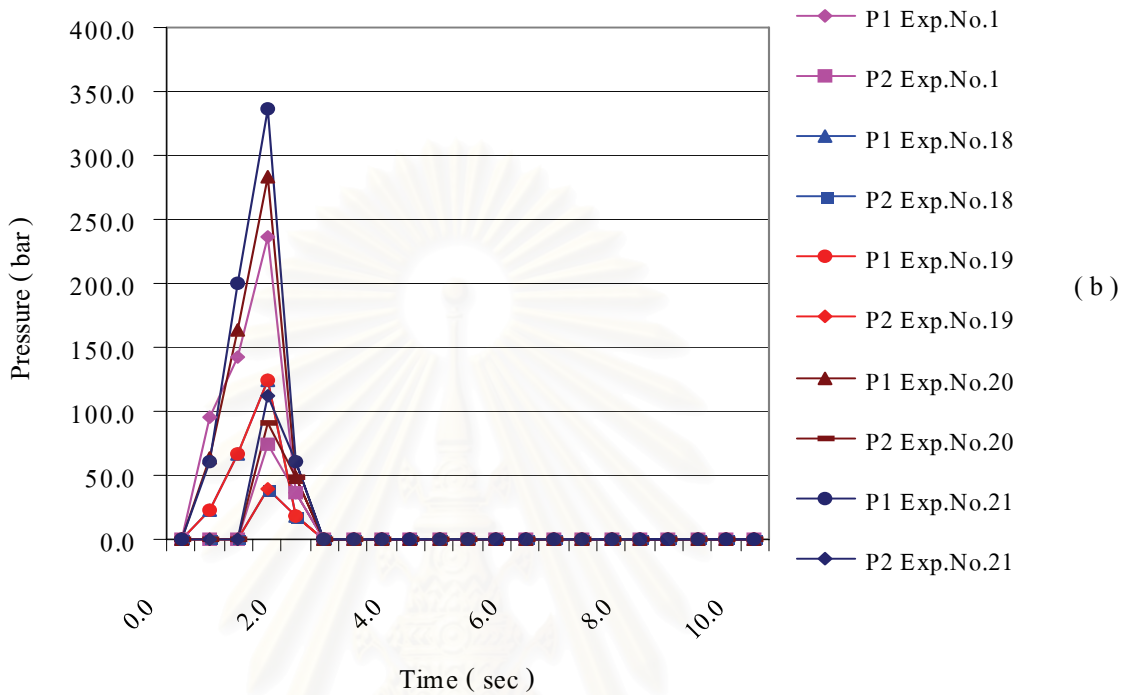
for ABS Lustran 250.

(a) Moldflow standard database for input

(b) Moldflow standard database for input

4.2.3 Comparison of Pressure curves

From comparison of pressure predicted by selection of the existing Moldflow standard database and a personal database for ABS 250 , the pressure curves were similar. Therefore, presentation of the pressure predicted in this section is done by Moldflow standard database for input.

The differences in pressure and fill time prediction were attributed to the simple mould. Possibly , Moldflow could simulate such a simple mould easily. Flowing of melt or heat transfer for cooling should be predicted as simple which was not correct to the actual situations. The sensitivity of the transducer measurement and by computer simulation and the larger dimension of a pressure transducer than a node could cause the errors.

4.2.3.1 Comparison between Reference Conditions

Figure 4.10 shows the pressure curve of ABS 250 (predicted by Moldflow) which compared to the pressure curve (measured by experiment) at reference condition. Maximum pressure value was approximately equal for the Moldflow prediction and the measurement. For the pressure value comparison, the simulation showed quantitative agreement to the measurement. However, for the fill time , the simulation showed a large difference to the measurement in quantitative. Moldflow predicted fill time as less than 2 seconds but measurement showed that of 10 seconds approximately.

4.2.3.2 Comparison as Injection Speed was Varied

Figure 4.11 shows comparison of the pressure curves by prediction and by measurement at various injection speeds. The comparison showed the differences in quantitative. Moldflow predicted the higher pressure at the higher injection speed but predicted the lower pressure again at very high injection speed. Measurement showed the higher pressure , the higher injection speed. For the low injection speed, Moldflow predicted the higher pressure , the lower injection speed but measurement showed the lower pressure , the lower injection speed. The pressure was predicted steeper when the injection speed was higher which agreed to the measured pressure.

4.2.3.3 Comparison as Holding Pressure was Varied

Figure 4.12 shows comparison of the pressure curves by prediction and by measurement at various holding pressure. For measurement , there was an increase in the cavity pressure and the effective holding pressure time as the holding pressure increased. Decreasing holding pressure did not affect the pressure curve. However , for prediction , there was no changes in the pressure value and the effective holding pressure time as holding pressure was varied.

4.2.3.4 Comparison as Holding Time was Varied

Figure 4.13 shows comparison of the pressure curves by prediction and by measurement at various holding time. Moldflow predicted the same slope of pressure rising in the filling phase as the holding time was varied. The pressure value was not changed at longer holding time or shorter holding time. For measurement, there was a drop-off in the pressure curve at short holding time. For long holding time , no further change occurred in the pressure curve.

4.2.3.5 Comparison as melt temperature was varied

Figure 4.14 shows comparison of the pressure curves by prediction and by measurement at various melt temperature. Moldflow predicted the higher the melt temperature, the lower the pressure value and the lower the melt temperature , the higher the pressure value. The measurement , showed that the higher the melt temperature , the higher the pressure value. The lower the melt temperature, the lower the pressure value. Therefore , the simulation showed the reversed agreement in qualitative.
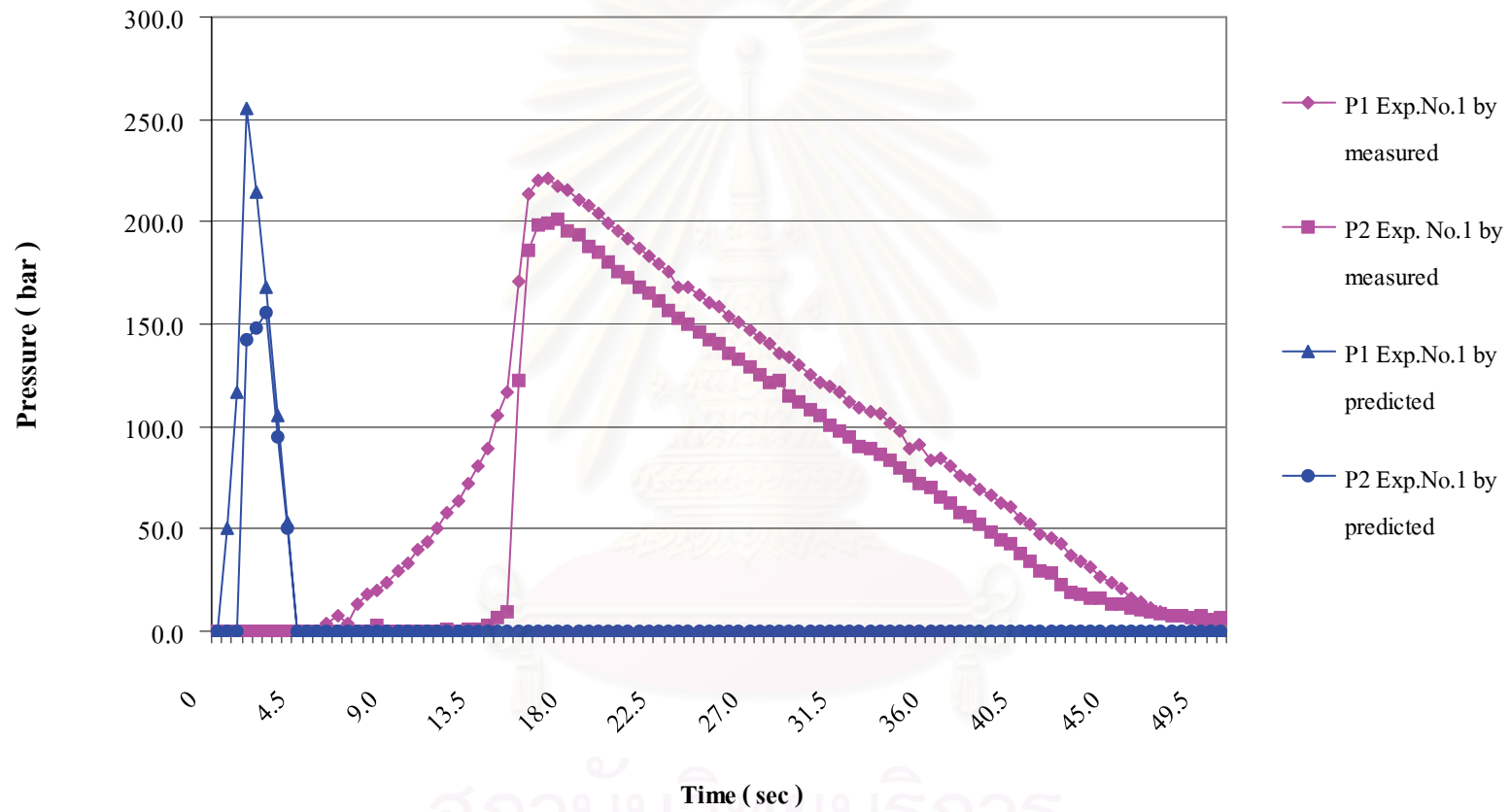
Figure 4.10 Comparison between reference conditions.
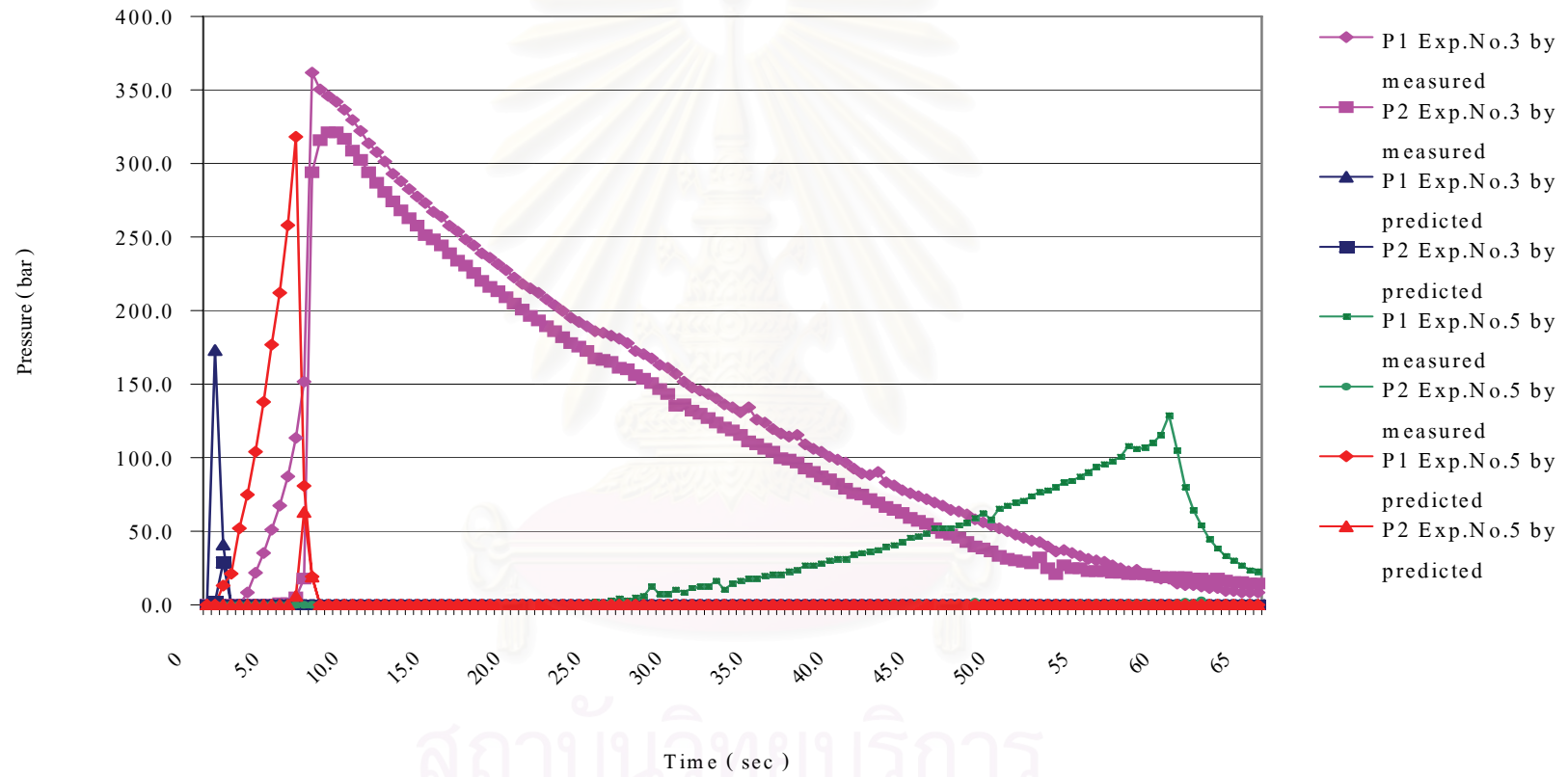
Figure 4.11 Comparison at various injection speeds .
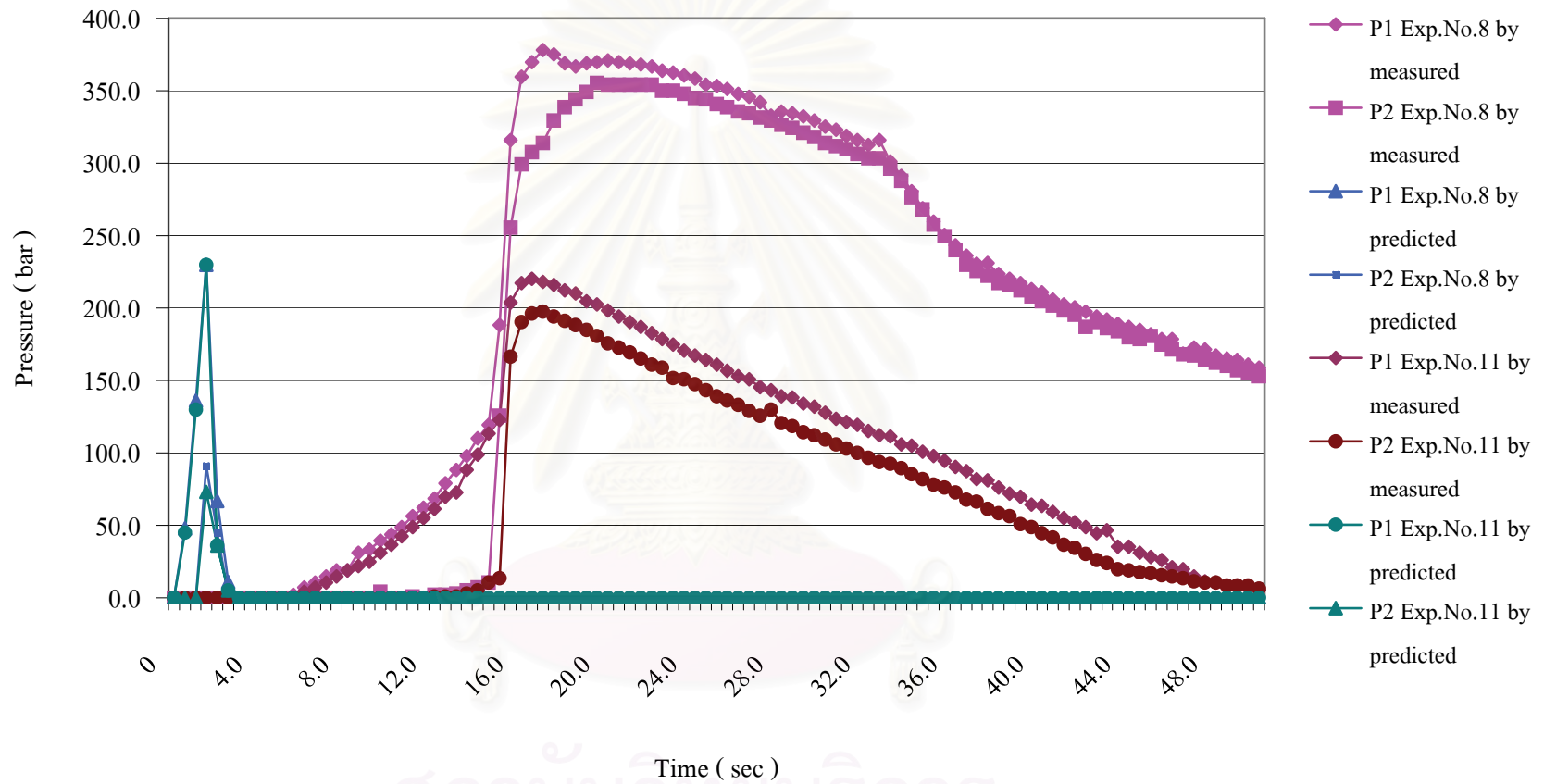
Figure 4.12 Comparison at various holding pressures .
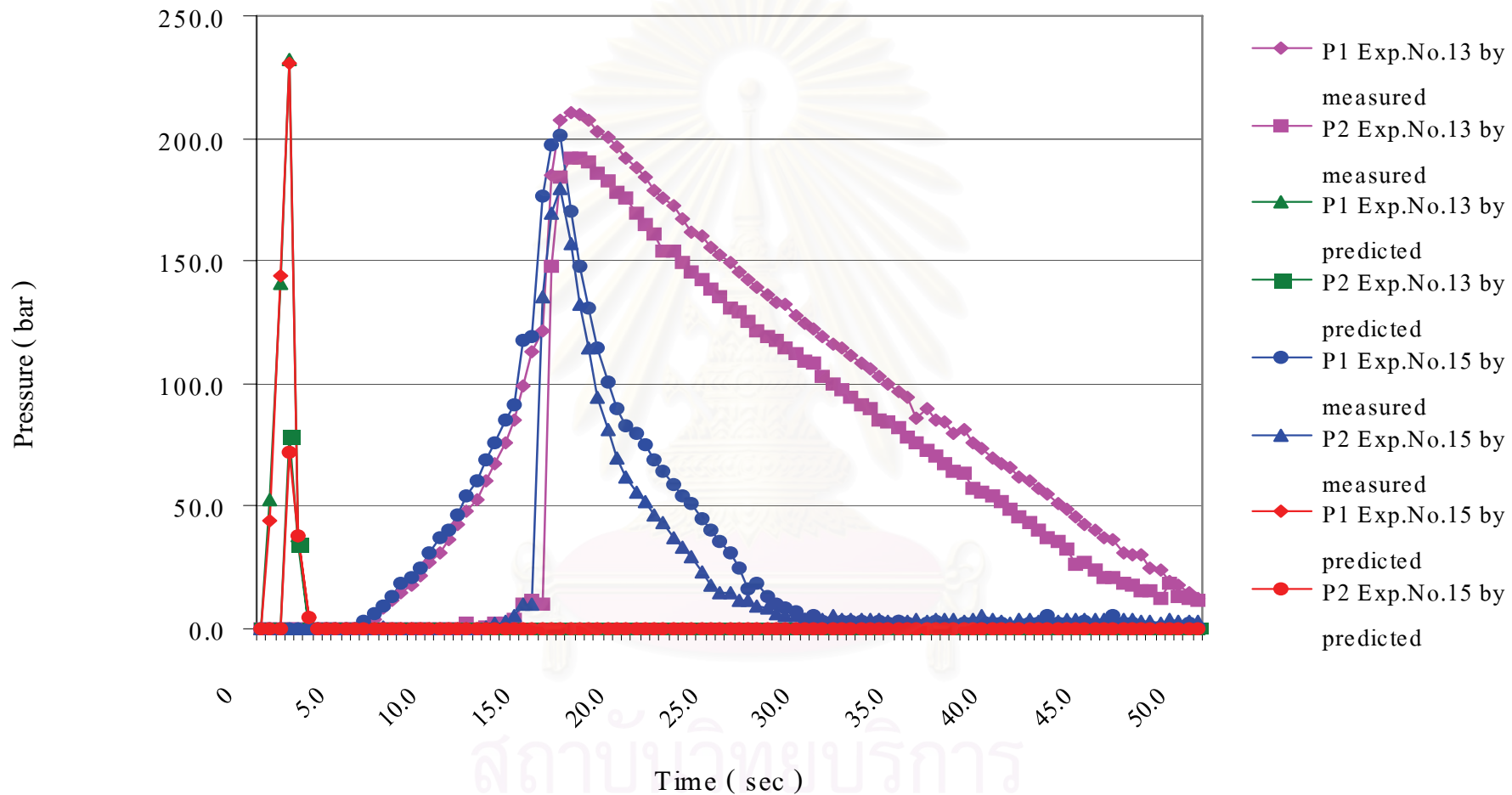
Figure 4.13 Comparison at various holding times .
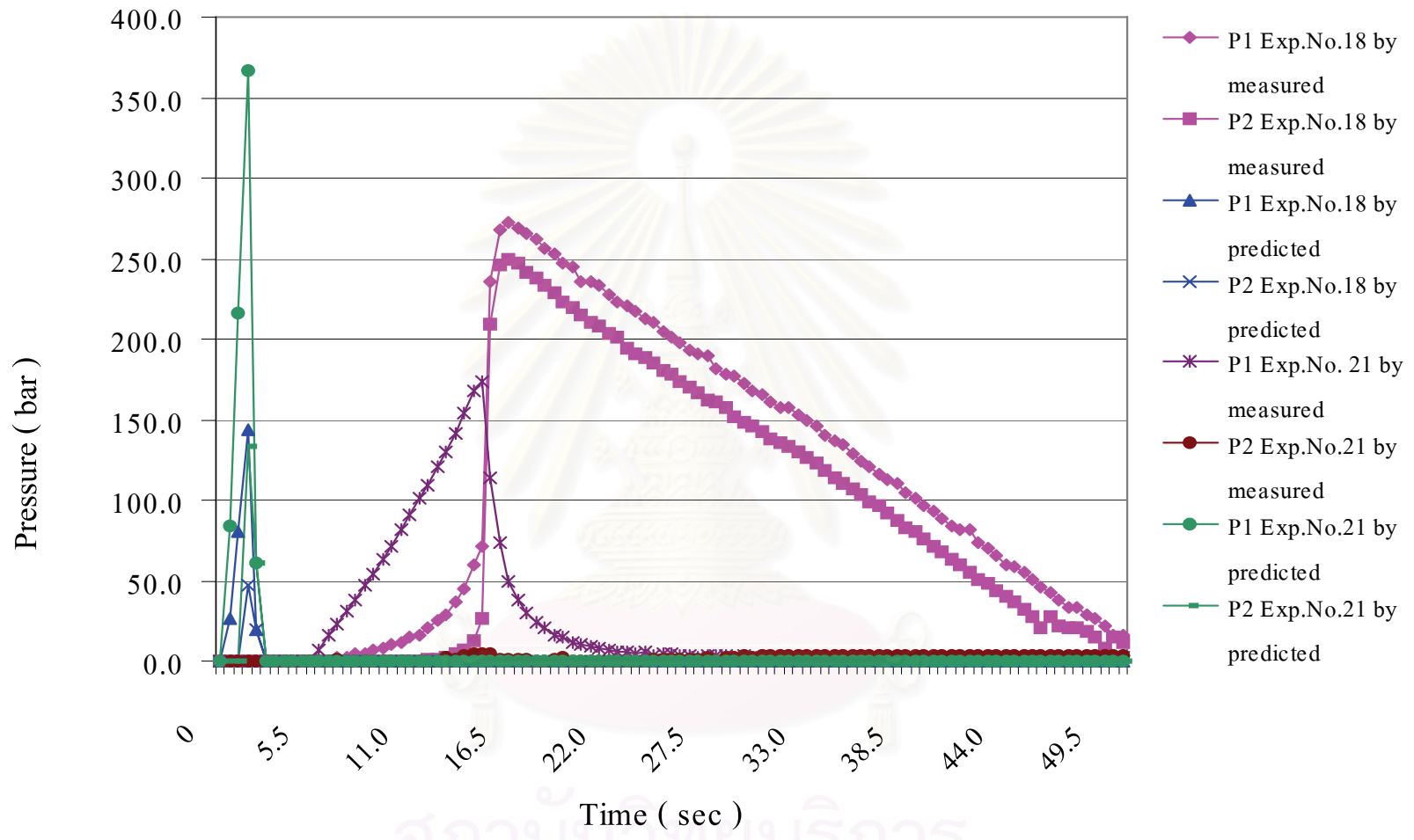
Figure 4.14 Comparison at various melt temperatures.

Legend:
- P1 Exp.No.18 by measured
- P2 Exp.No.18 by measured
- P1 Exp.No.18 by predicted
- P2 Exp.No.18 by predicted
- P1 Exp.No. 21 by measured
- P2 Exp.No.21 by measured
- P1 Exp.No.21 by predicted
- P2 Exp.No.21 by predicted

4.3 EFFECT OF INJECTION PARAMETERS ON IMPACT PROPERTY

The effect of injection moulding parameters on the impact property were investigated. The impact properties result of one experiment presented in this work was obtained by the average of the valid readings from 30 specimens.

4.3.1 Effect of Injection Speed on Impact Properties

Table 4.2 shows the impact properties results for ABS Lustran 250 , Lustran 440 and Lustran 640 as injection speed was varied from the reference conditions while the other parameters were kept constant as follows :

For ABS Lustran 250   : Holding Pressure   = 15 bar , Holding Time = 1.5 sec

                        Melt Temperature   = 230 $^{\circ}$ C

For ABS Lustran 440   : Holding Pressure   = 29 bar , Holding Time = 1.0 sec

                        Melt Temperature   = 230 $^{\circ}$ C

For ABS Lustran 640   : Holding Pressure   = 60 bar , Holding Time = 2.0 sec

                        Melt Temperature   = 230 $^{\circ}$ C

Table 4.2 Effect of injection speed on impact properties for ABS Lustran 250 , Lustran 440 and Lustran 640.

Injection Condition Description	Exp. No.			Injection Speed (mm/s)			Peak Energy (J/mm)			Break Energy (J/mm)			Displacement to Peak (mm)			Displacement to Break (mm)		
	L250	L440	L640	L250	L440	L640	L250	L440	L640	L250	L440	L640	L250	L440	L640	L250	L440	L640
Low Injection Speed	5	27	41	10	5	10	3.9	9.4	9.5	5	14	13	9.4	14	14	11	18	18
Reference Condition	1	22	38	40	38	30	4.4	9.6	9.9	5.3	15	14	9.7	14	14	11	19	18.1
High Injection Speed	3	25	39	100	100	100	4.7	10	9.9	5.9	15	14	10	14	14	12	18	18

The impact peak energy and break energy as a function of injection speed for ABS Lustran 250 were shown in Fig. 4.15 . There was approximately 20 % increase in both peak energy and break energy as the injection speed was increased. There was a slight increase in deflection to peak and deflection to break point with increasing injection speed. The energy absorbed was the area under the force-deflection curve, the energy depended upon the force and the deflection on the specimen. The impact energy and deflection values increased as increasing injection speed, this should be caused

by the molecular orientation. At high injection speeds , the relative maximum molecular orientation was more pronounced and closer to the wall. The velocity of the flow front strongly affected the molecular orientation [12] .

The impact peak energy and break energy as a function of injection speed for ABS Lustran 440 were shown in Fig. 4.15 (a) and (b). There was a slight increase in both peak energy and break energy as the injection speed was increased. There was an insignificant difference in deflection to peak and deflection to break point

From Fig. 4.15 (a) and (b) , there were no significant difference in impact energy at peak and at break for ABS Lustran 640 as the injection speed increased. The injection speed had no influence on impact displacement to peak and displacement to break as shown in Fig. 4.16 (a) and (b).

After leaving the runner channels , the melt flows into the cavity and is then subjected simultaneously to flow and cooling processes. Behind the flow front, a cross section from wall to wall has two distinct regions. A solidified or frozen layer is formed next to the cold mould wall, because of the cooling of the melt. No further flow is possible within this solidified layer. Inside there is a hot core that still contains fluid material. The highest velocity gradient (shear rate) is in the vicinity of the solidified layer, but because of the high melt viscosity in this area, it is not situated exactly at the edge of

the layer. In the area of the highest velocity gradient , the melt is subjected to especially strong shearing, which orients the molecules or embedded filler materials in the direction of flow. For this reason, maximum orientation is expected to be in the section immediately below the surface of the moulding. An important consequence of molecular orientation is anisotropy in the macroscopic physical properties of the material. Several quality-related properties are strongly influenced by the flow and cooling processes that take place in the filling phase [15,21-23]. A frozen layer form as hot melt cools at the cold wall of the mould. Because of the flow processes , this layer is oriented mainly in the direction of flow. The degree of orientation, that is, the alignment of macromolecules or embedded fillers caused by the flow is greater in this frozen layer than at any other point of the cross section. The mechanical properties of the moulding depends strongly on the amount and direction of the orientation. In the direction of orientation the mechanical properties are higher, and are lower in the perpendicular direction.

The comparison of impact properties for ABS Lustran 250, Lustran 440 and Lustran 640 shows that injection speed had a strong influence on the impact property of ABS Lustran 250 but it did not significantly affect on the impact properties of ABS Lustran 440 and Lustran 640. The reason was due to the difference of the viscosity. ABS Lustran 640 and Lustran 440 had higher viscosity than ABS Lustran 250 . Probably for the high viscosity grades, the injection speed slightly affected on the molecular orientation. Therefore , the impact properties of ABS Lustran 440 and Lustran 640 did not change so much as the injection speed was varied.
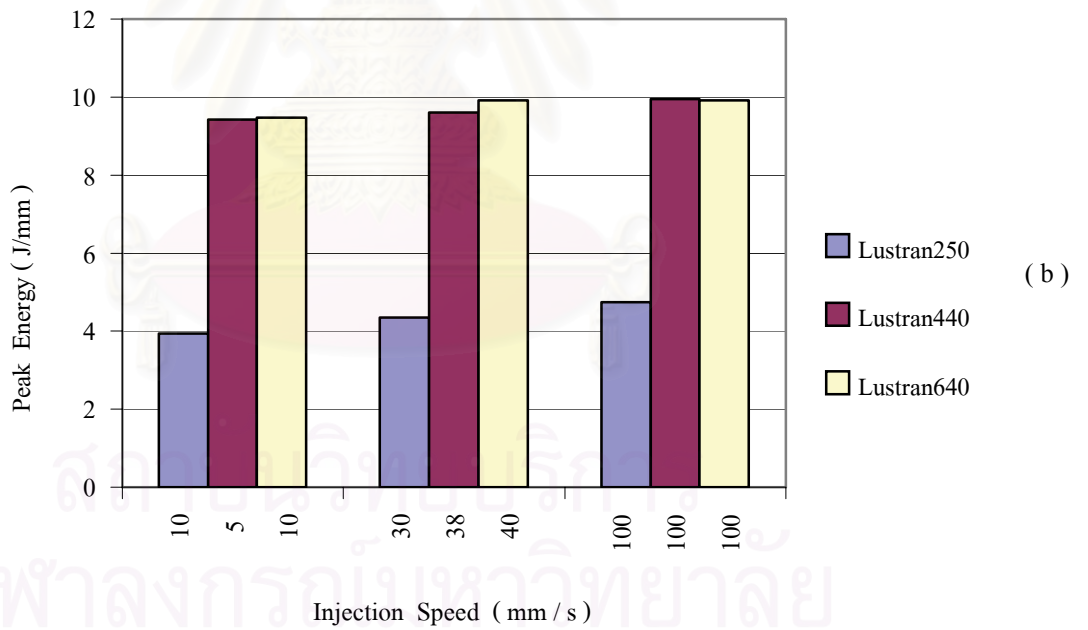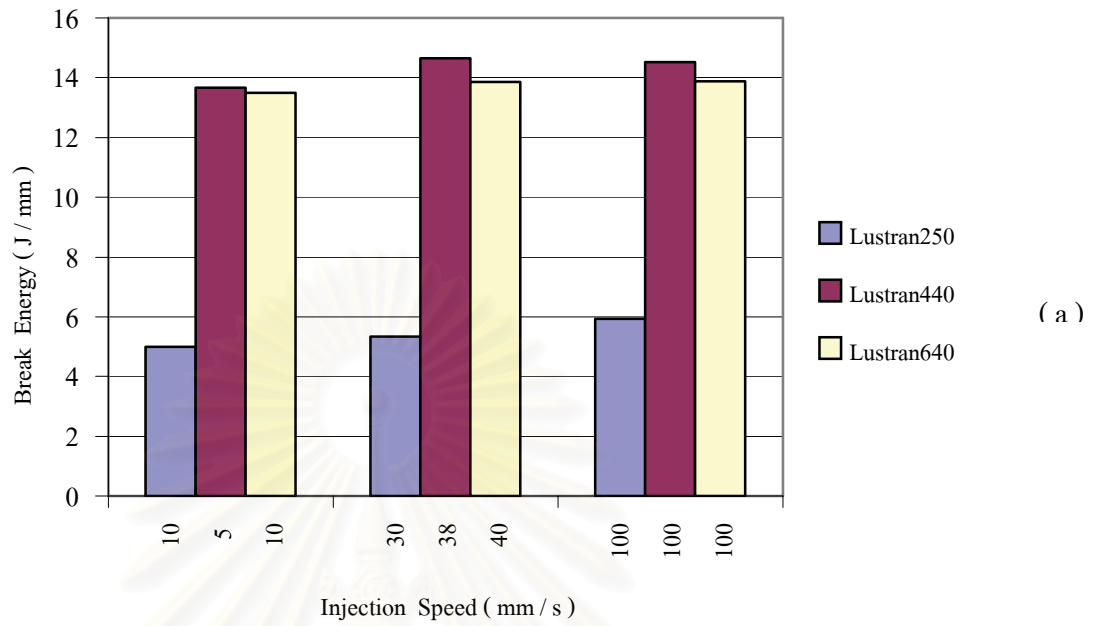
Figure 4.15 Effect of injection speed for ABS L250 , L440 and L640 on
(a) Impact peak energy (b) Impact break energy.
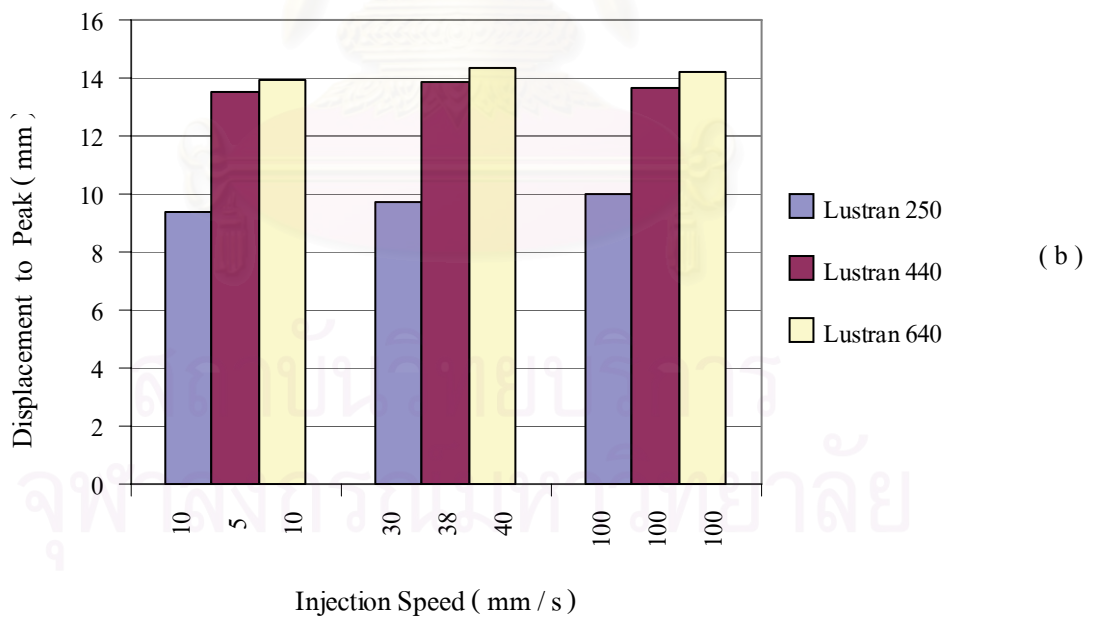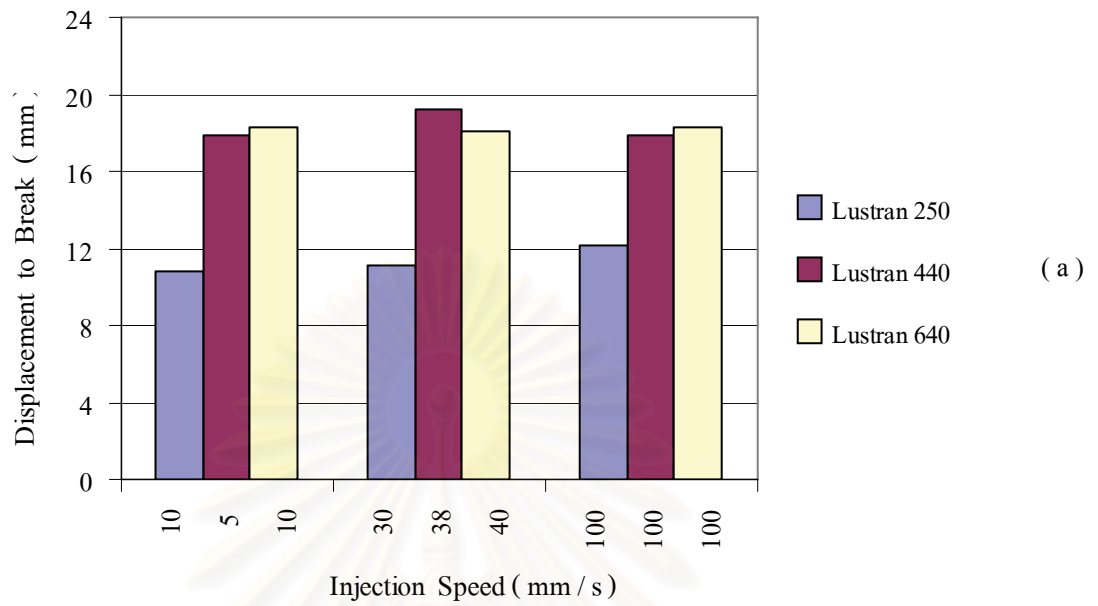
Figure 4.16 Effect of injection speed for ABS L250, L440 and L640 on (a) Impactdisplacementto peak (b) impact displacement to break .

4.3.2 Effect of Holding Pressure on Impact Properties

Table 4.3 shows the impact properties for ABS Lustran 250 , Lustran 440 and Lustran 640 as holding pressure was varied from the reference

conditions while the other parameters were kept constant as follows:

For ABS Lustran 250 : Injection Speed = 40 mm/s, Holding Time = 1.5 sec
Melt Temperature = 230 $^\circ$ C
For ABS Lustran 440 : Injection Speed = 38 mm/s, Holding Time = 1.0 sec
Melt Temperature = 230 $^\circ$ C
For ABS Lustran 640 : Injection Speed = 30 mm/s, Holding Time = 2.0 sec
Melt Temperature = 230 $^\circ$ C

Figure 4.17 illustrates the effect of holding pressure on impact peak energy and impact break energy for ABS Lustran 250 , Lustran 440 and Lustran 640. Figure 4.18 illustrates the effect of holding pressure on impact displacement to peak and impact displacement to break for ABS Lustran 250 , Lustran 440 and Lustran 640.

The peak energy , break energy, displacement to peak and displacement to break for ABS Lustran 250 did not change over the range of holding pressures (0, 15 and 100 bar) . During the holding phase , the effect of molecular orientation is negligible since the frozen layer is already built up when the unit is switched to holding pressure.

The peak energy, break energy, displacement to peak and displacement to break for ABS Lustran 440 had insignificant difference over the range of holding pressure (0,15 and 100 bar). However, the impact break energy was slightly decreased at high holding pressure.

There was significant increase approximately 10 % and 15 % in impact peak energy and break energy for ABS Lustran 640 as the holding

pressure increased. However , there was a slight significant difference in impact displacement   over the range of holding pressure.

The holding pressure had a weak influence on the impact properties for ABS Lustran 250 and Lustran 440. However, the impact peak energy and break energy of ABS Lustran 640   increased significantly with increasing holding pressure. The difference might be from the scattering data of impact property values.

Table 4.3   Effect   of   Holding   Pressure   on   Impact   Properties   for ABS Lustran 250 , Lustran 440 and Lustran 640.

Injection Condition Description	Exp. No.			Holding Pressure (bar)			Peak Energy (J/mm)			Break Energy (J/mm)			Displacement to Peak (mm)			Displacement to Break (mm)		
	L250	L440	L640	L250	L440	L640	L250	L440	L640	L250	L440	L640	L250	L440	L640	L250	L440	L640
Low Holding Pressure	11	32	45	0	0	0	4.3	10.3	9.1	5.3	14.9	12.4	9.7	14.1	13.7	10.8	13.4	18.2
Reference Condition	1	22	38	15	29	60	4.4	9.6	9.9	5.3	14.7	13.9	9.7	13.9	14.3	11.1	19.2	18.1
High Holding Pressure	8	29	42	100	100	80	4.4	9.6	10.1	5.4	13.8	14.2	9.4	13.5	14.4	10.8	17.6	18.9
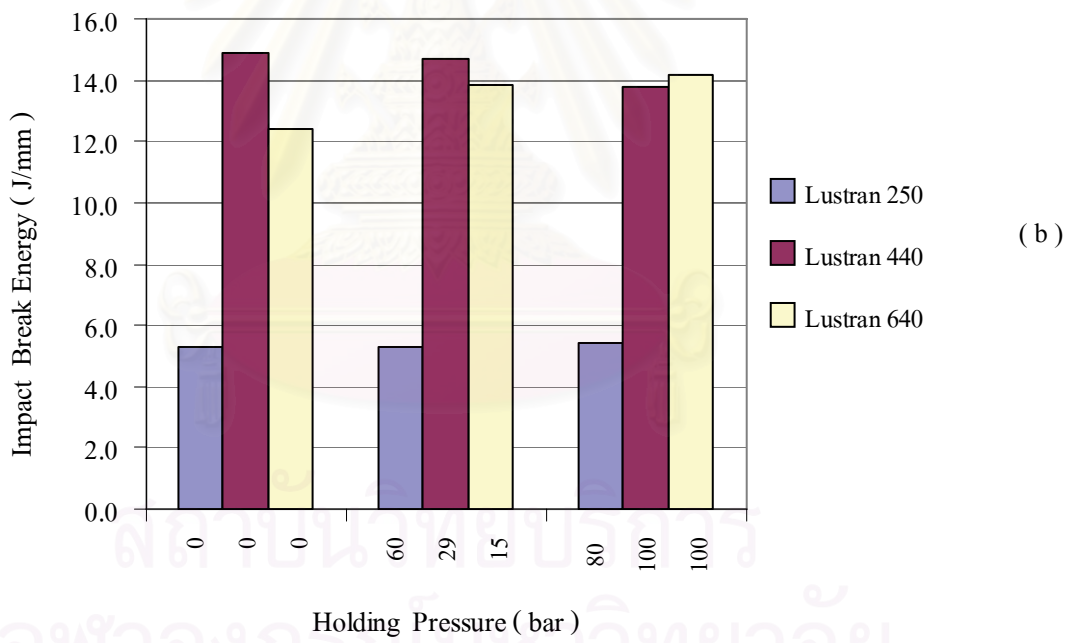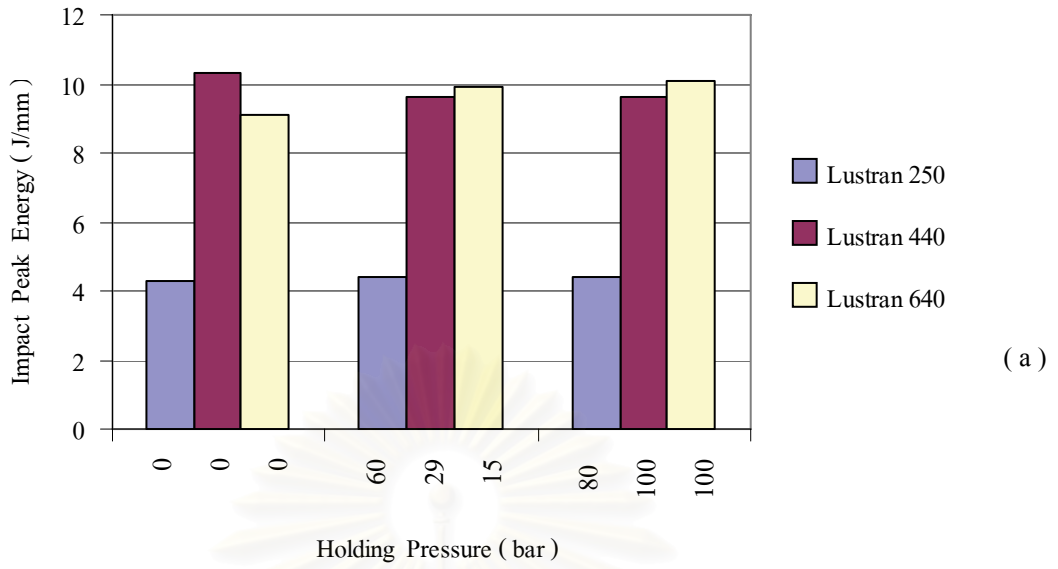
Figure 4.17 Effect of holding pressure for ABS L250, L440 and L640 on
(a) Impact peak energy (b) Impact break energy .
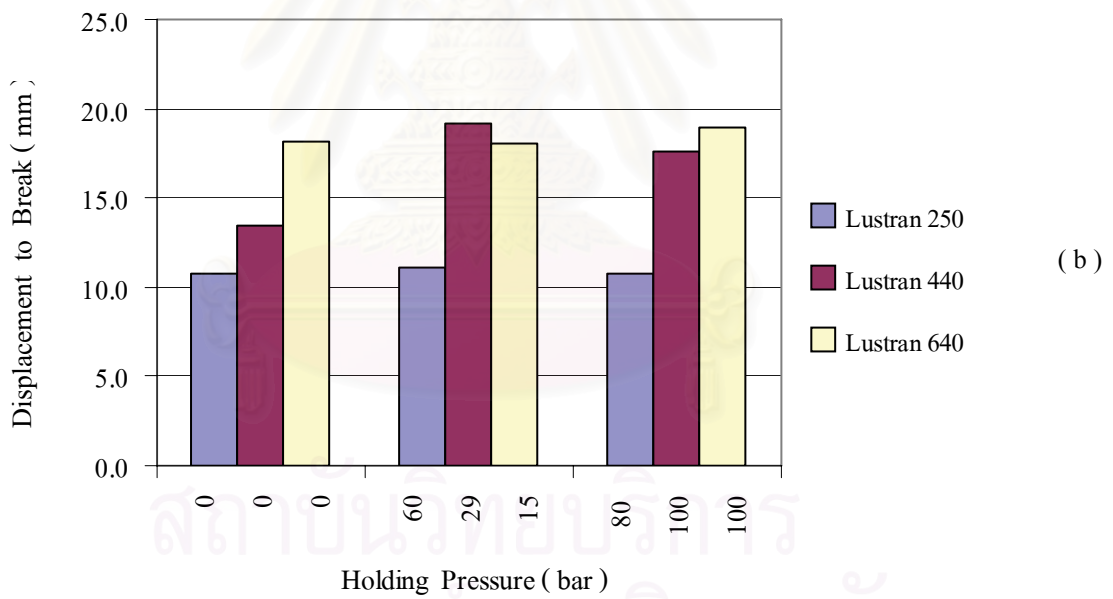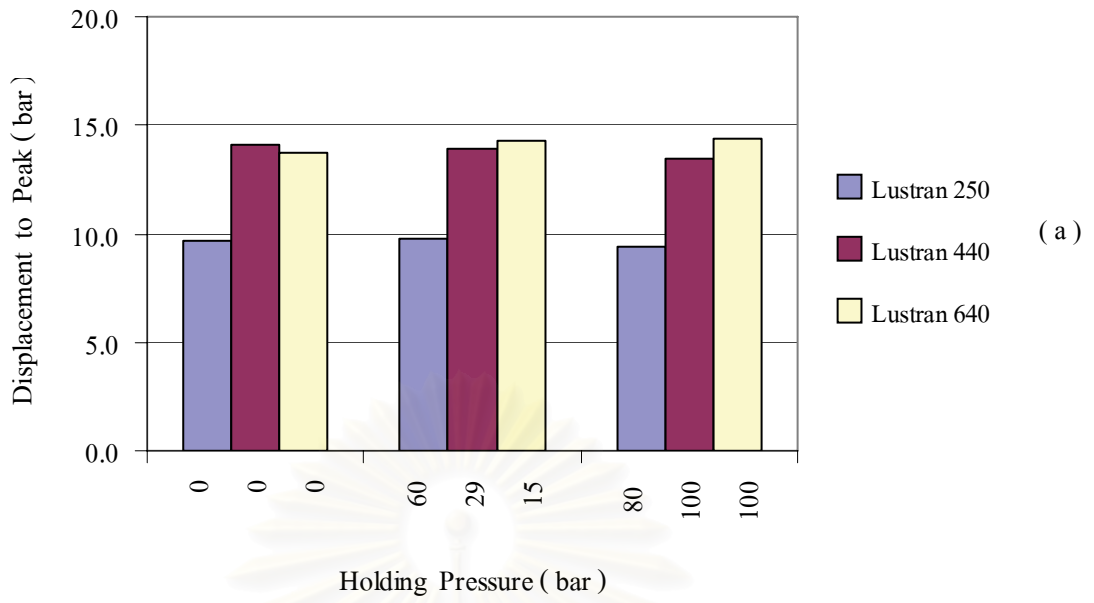
Figure 4.18 Effect of holding pressure for ABS L250, L440 and L640 on (a) Impact displacement to peak (b) Impact displacement to break.

4.3.3 Effect of Holding Time on Impact Properties

Table 4.4 shows the effect of holding time on impact properties. The parameters were kept constant as follows :

For ABS Lustran 250 : Injection Speed = 40 mm/s, Holding Pressure = 15 bar
Melt Temperature = 230 $^\circ$ C

For ABS Lustran 440 : Injection Speed = 38 mm/s, Holding Pressure = 29 bar
Melt Temperature = 230 $^\circ$ C

For ABS Lustran 640 : Injection Speed = 30 mm/s, Holding Pressure = 60 bar
Melt Temperature = 230 $^\circ$ C

Fig. 4.19 illustrates the effect of holding time on impact peak energy and impact break energy for ABS Lustran 250, Lustran 440 and Lustran 640. Figure 4.20 also illustrates the effect of holding time on impact displacement to peak and impact displacement to break for ABS Lustran 250 , Lustran 440 and Lustran 640.

There was essentially no change in the impact properties for ABS Lustran 250 as the holding time was increased . But at the very long holding time (20 sec), both impact energy and impact displacement were slightly decreased. From the result of glacial acetic acid immersion , the stress whitening occurred for the sample moulded at long holding time. The stress whitening indicated that more internal stress occurred at long holding time than the samples moulded at low holding time (0 sec) and the reference condition (1.5 sec).

For ABS Lustran 440, there was no change in the impact properties as the holding time increased. However, at the very long holding time (15 sec), there was also slightly decrease in both impact energy and impact displacement.

There was insignificant difference as the holding time was varied for ABS Lustran 640 . However, impact energy and impact displacement decreased slightly at very long holding time (20 sec).

The holding time did not affect the impact properties of ABS Lustran 250 , Lustran 440 and Lustran 640. There was slightly decrease in impact properties at the long holding time. The slightly drop of impact properties at high holding pressure or very long holding time occurred due to the higher internal stress.
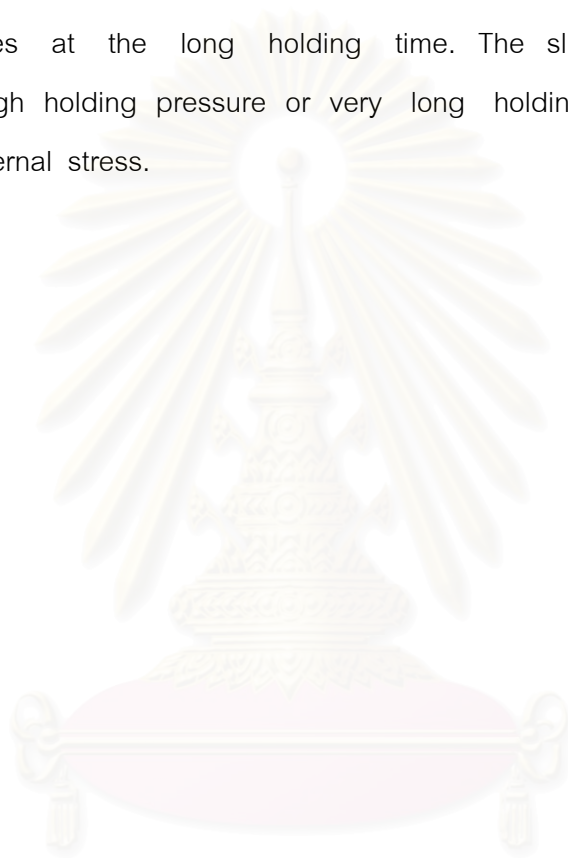
Table 4.4 The effect of Holding Time on Impact Properties for ABS Lustran 250 , Lustran 440 and Lustran 640.

Injection Condition Description	Exp. No.			Holding Time (sec)			Peak Energy (J/mm)			Break Energy (J/mm)			Displacement to Peak (mm)			Displacement to Break (mm)		
	L250	L440	L640	L250	L440	L640	L250	L440	L640	L250	L440	L640	L250	L440	L640	L250	L440	L640
Short Holding Time	15	34	46	0	0	0	4.45	10.0	9.3	5.5	14.2	12.7	11.2	19.9	14.1	11.3	17.8	18.1
Reference Condition	1	22	38	1.5	1	2	4.4	9.6	9.9	5.3	14.7	13.9	9.7	19.9	14.3	11.1	19.2	18.1
Long Holding Time	13	33	45	20	15	20	4.07	9.1	8.5	5.0	13.7	12.0	9.4	13.3	13.3	10.8	17.9	17.1
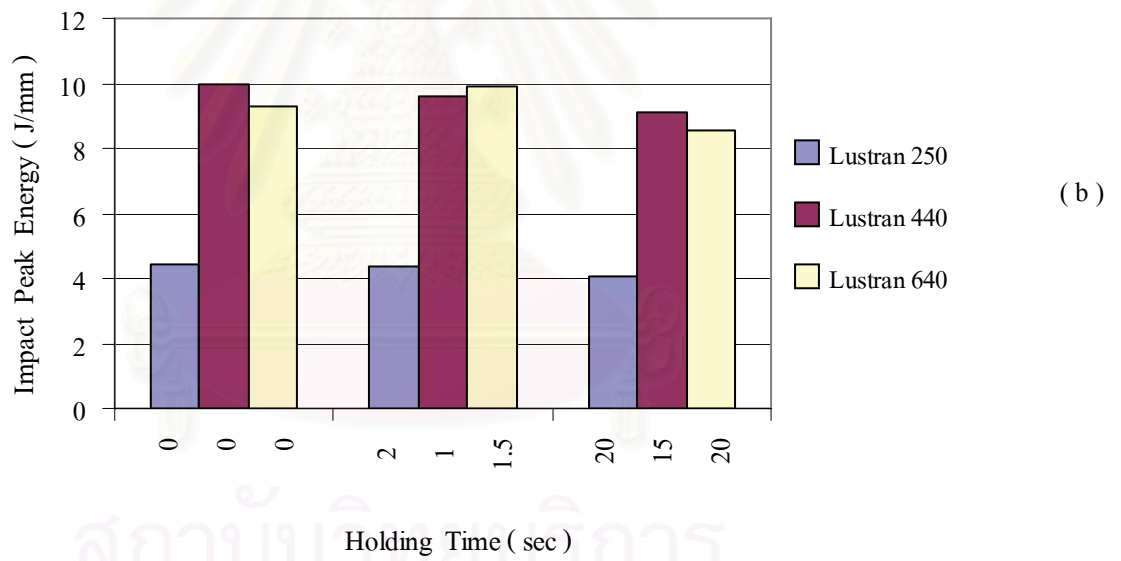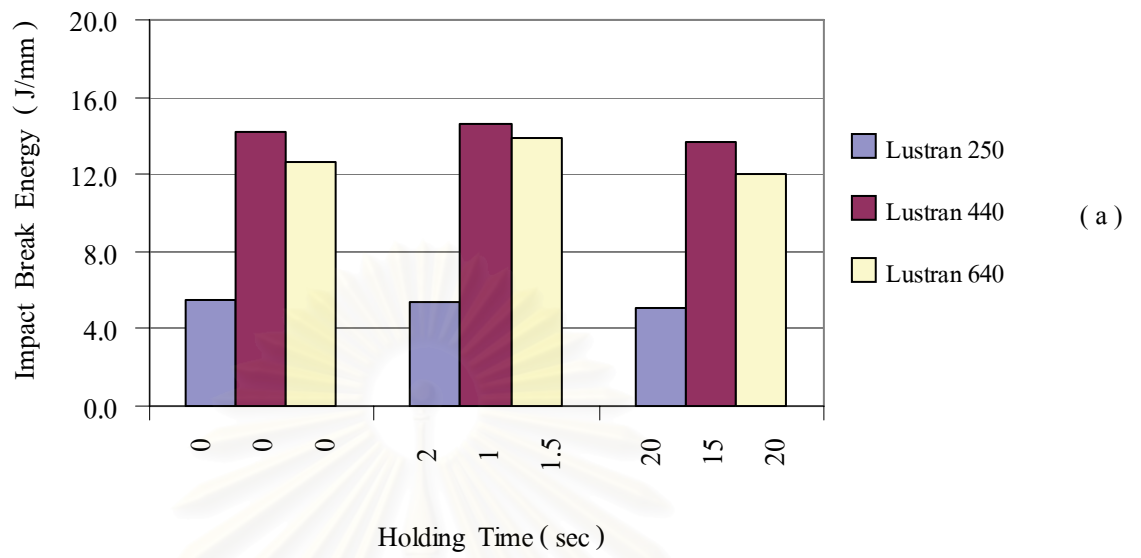
Figure 4.19 Effect of holding time for ABS L250, L440 and L640
on (a) impact peak energy (b) Impact break energy.
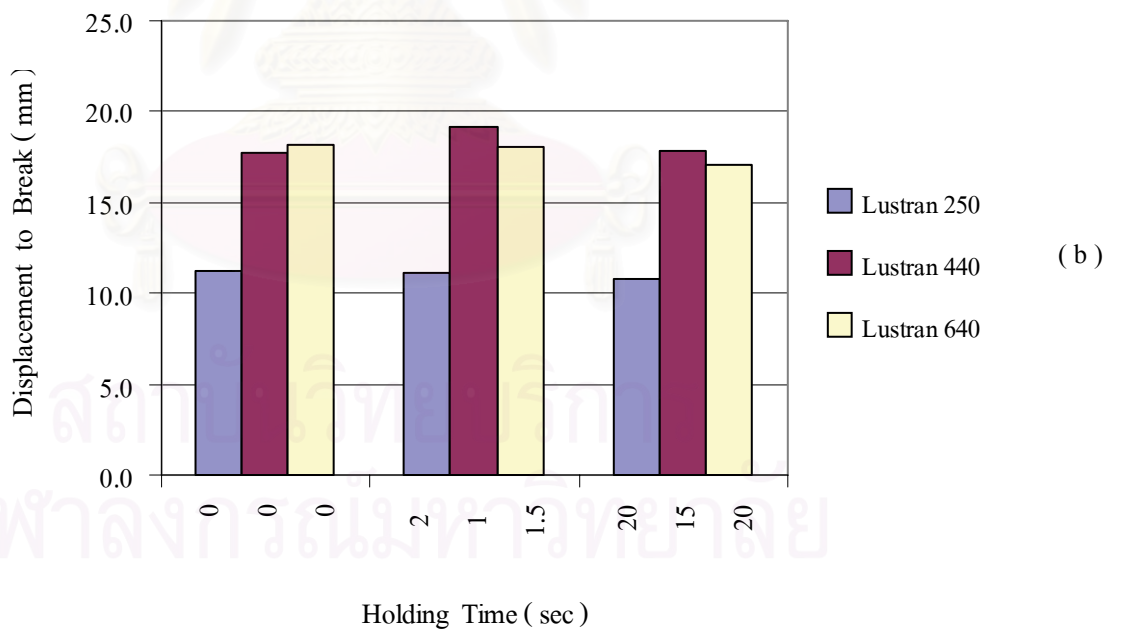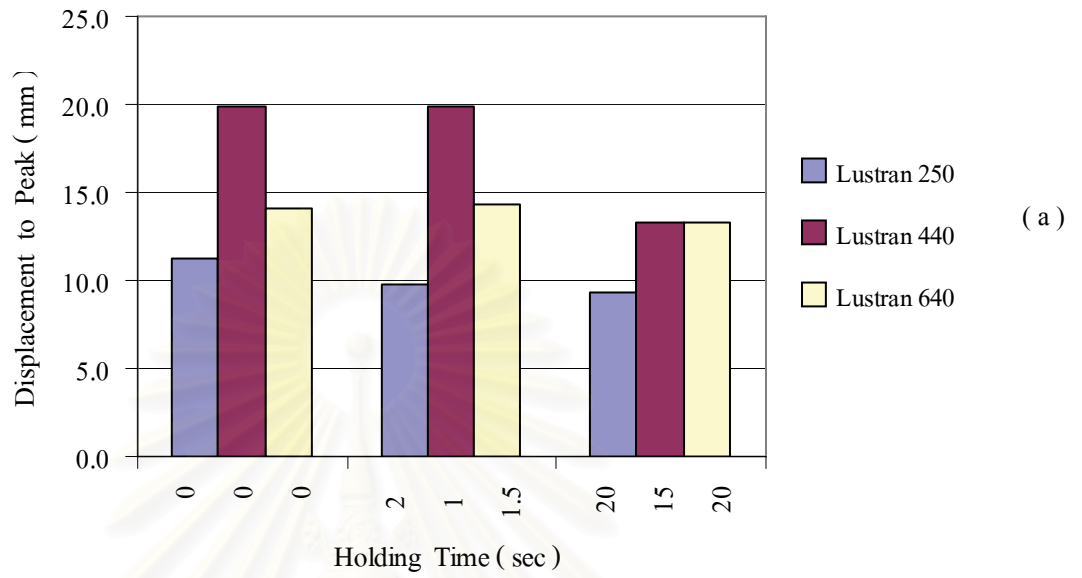
Figure 4.20 Effect of holding time for ABS L250, L440 and L640
on (a) impact displacement to peak (b) impact displacement to break .

4.3.4 Effect of Melt Temperature on Impact Properties

Table 4.5 shows the effect of melt temperature on impact properties for ABS Lustran 250 , Lustran 440 and Lustran 640. The parameters were kept constant as follows :

For ABS Lustran 250 : Injection Speed = 40 mm/s, Holding Pressure = 15 bar
Holding Time = 1.5 sec

For ABS Lustran 440 : Injection Speed = 38 mm/s, Holding Pressure = 29 bar
Holding Time = 1.0 sec

For ABS Lustran 640 : Injection Speed = 30 mm/s, Holding Pressure = 60 bar
Holding Time = 2.0 sec

Figure 4.21 illustrates the effect of melt temperature on impact peak energy and impact break energy for ABS Lustran 250, Lustran 440 and Lustran 640. Figure 4.22 illustrates the effect of melt temperature on impact displacement to peak and impact displacement to break for ABS Lustran 250 , Lustran 440 and Lustran 640.

The impact properties for ABS Lustran 250 showed a dependence on the melt temperature. There was a decrease of approximately 25 % of peak energy and 15 % of break energy for samples moulded at 280 $^\circ$C. However , there was unexpected increment of the impact displacement . The results showed insignificant difference of impact energy for samples moulded at melt temperature 190 $^\circ$C and 230 $^\circ$C but there was also an increase in the deflection to peak and deflection to break. Unsurprisingly, there was a large decrease in impact energy for very high melt temperature condition due to the effect of polymer degradation which caused a decrease in mechanical property. The result of MFI (Melt flow index) of the crushed moulded parts showed that MFI of part moulded at melt temperature of 280 $^\circ$C was 2 times higher than that moulded at 190 $^\circ$C and 230 $^\circ$C. However , there was an

increase in impact displacement for the high melt temperature. Possibly, the scattering data of impact values caused the inconsistent data and the unexpected increment in impact displacement for ABS Lustran 250.

The impact properties for ABS Lustran 440 had a strong dependence on the high melt temperature. The decrease of approximately 60 % of peak energy , 65 % of break energy were observed. The deflection to peak and deflection to break decreased approximately 30 % and 45 % respectively for the samples moulded at 280 $^\circ$C. There was insignificant difference of impact energy for the samples moulded at melt temperature of 190° C and 230 $^\circ$C but the trend was an increase in impact energy with increasing melt temperature. In addition , the impact displacement to peak and to break of the samples moulded at 230 $^\circ$C melt temperature was higher than that of the samples moulded at melt temperature of 190° C.

The impact properties for ABS Lustran 640 had a strong dependence on the high melt temperature. The decrease of approximately 20 % of peak energy and 25 % of break energy were observed , as well as the deflection to peak and deflection to break decreased significantly for the samples moulded at 280 $^\circ$ C. There was a slightly increase in impact energy and displacement values for the sample moulded at melt temperature of 230 $^\circ$C compared to the samples moulded at melt temperature of 190° C .

Reduction of the impact property of ABS 440 and ABS 640 was more than that of ABS 250 , moulded at the same low melt temperature. Possibly, this occurred because the melt frozen-in for higher viscosity grades of ABS 440 and ABS 640 was more than that of ABS 250. Therefore, higher internal stress for ABS 440 and ABS 640 caused slightly more impact property reduction.

The melt temperature had a strong influence on the impact properties for ABS Lustran 250 , Lustran 440 and Lustran 640. There was a large

decrease in impact energy at high melt temperature moulding. A reduction in impact displacement for ABS Lustran 440 and Lustran 640 were found but a slight increase for ABS Lustran 250 occurred. Possibly, the large scattering data in impact values caused the unexpected increment in the impact displacement for ABS Lustran 250.

Table 4.5 The effect of Melt Temperature on Impact Properties for ABS Lustran 250 , Lustran 440 and Lustran 640

Injection Condition Description	Exp. No.			Melt Temperature			Peak Energy (J/mm)			Break Energy (J/mm)			Displacement to Peak (mm)			Displacement to Break (mm)		
	L250	L440	L640	L250	L440	L640	L250	L440	L640	L250	L440	L640	L250	L440	L640	L250	L440	L640
Low Melt Temperature	21	37	53	190	190	190	4.4	9.3	9.3	5.1	13.0	13.0	8.5	13.3	13.9	9.4	17.2	17.8
Reference Condition	1	22	38	230	230	230	4.3	9.6	9.9	5.3	14.7	13.9	9.7	13.9	14.3	11.1	19.2	18.1
High Melt Temperature	19	35	51	280	280	280	3.2	3.6	7.5	4.4	4.5	9.6	10.7	9.2	12.9	14.4	10.9	15.4
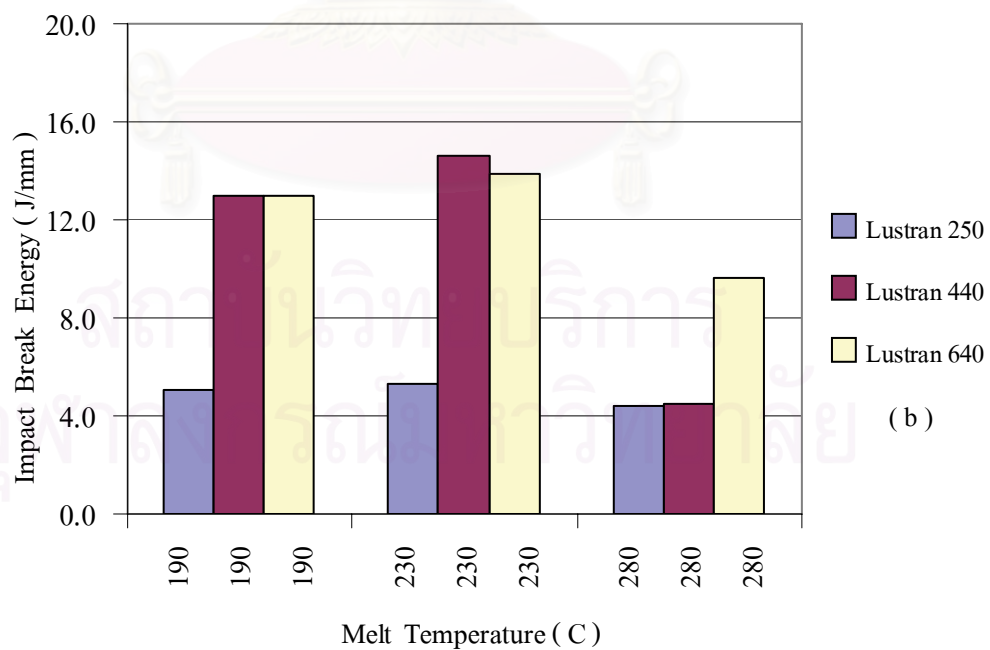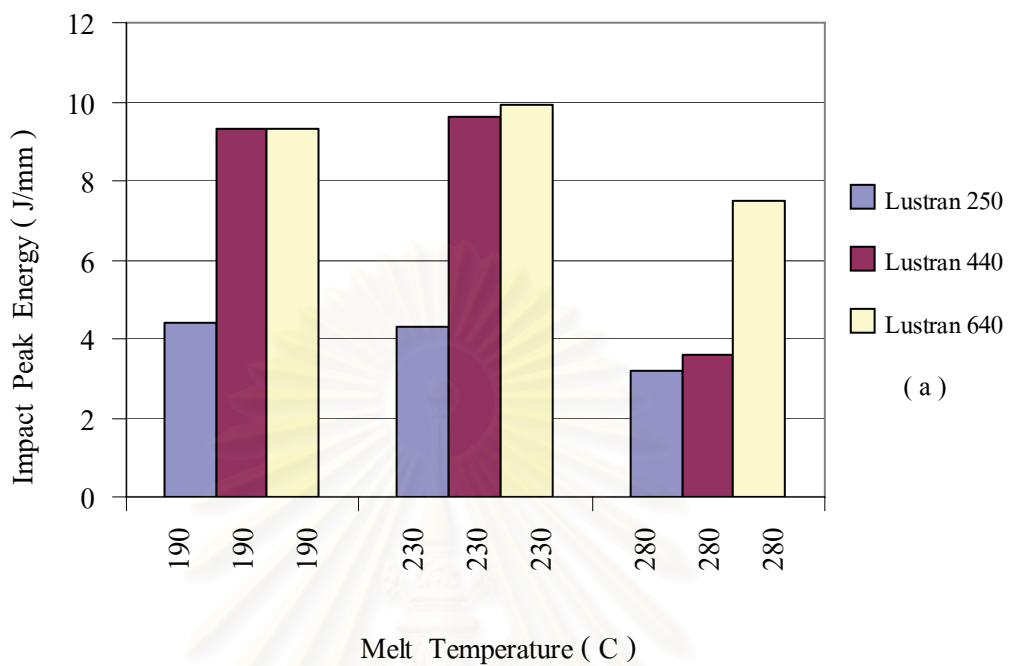
Figure 4.21 Effect of melt temperature for ABS L250,L440 and L640 on

(a) impact peak energy   (b) impact break energy.
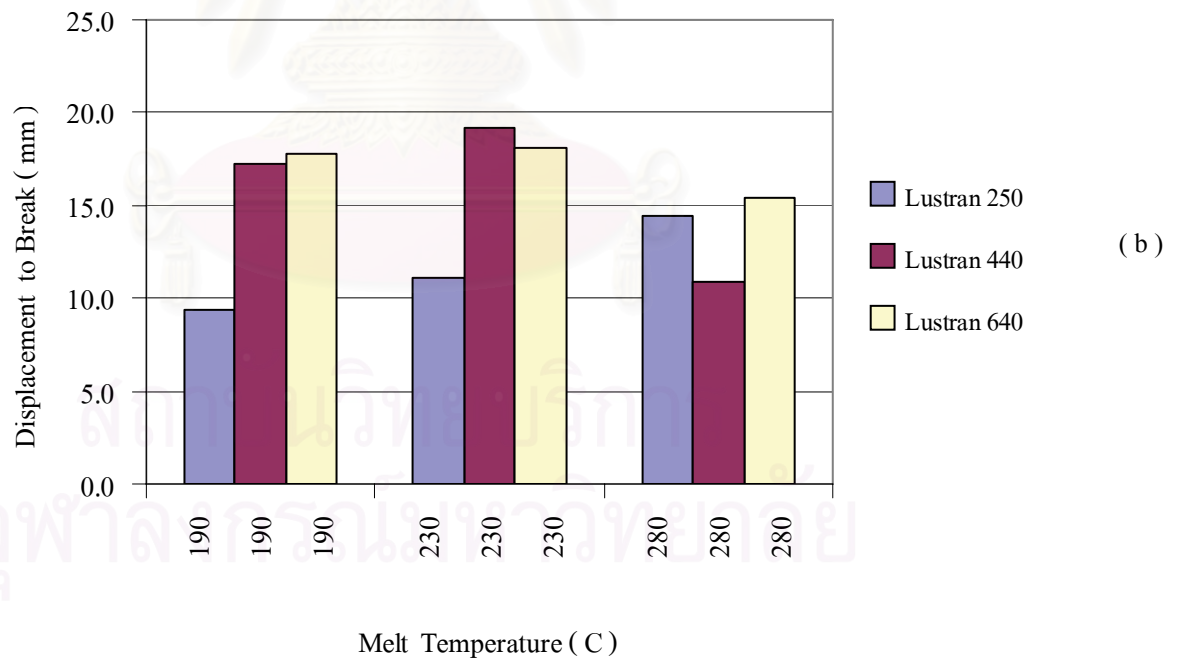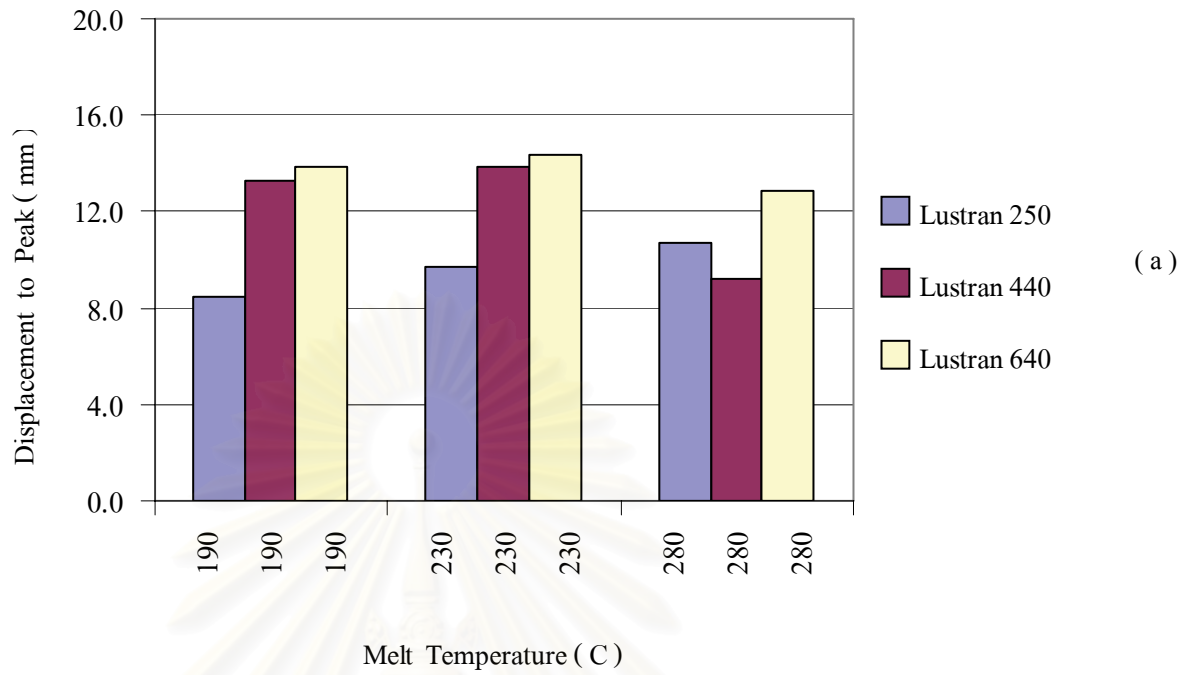
Figure 4.22 Effect   of   melt   temperature for   ABS L250 , L440 and   L640

on (a) Impact displacement to peak (b) Impact displacement to

break.

4.3.5 Analysis of Failure Mode and Force-Deflection Curve

The impact failure was related to the features of the force-deflection curves of specimens. The types of failure after impact test and the features of force-deflection curve for ABS Lustran 250 , Lustran 440 and Lustran 640 were identified by visual inspection.

4.3.5.1 ABS Lustran 250

The type of failure of specimen by visual inspection could identify the failure mode [19] . The major cracks form of ABS Lustran 250 specimens was ductile failure as shown in Fig. 4.23. The cracked specimen had a white spot developed around the puncture. There was a thin cap of deformed material flicked off by the striker penetration as same as the rack pattern of polypropylene copolymer. [24] There were the radial cracks hat should be visible at or after the first peak in the force-deflection curve. The release of energy on forming these cracks was responsible for the first peak. Then , the radial cracks extended slowly out towards the edge of the specimen. The circular cracks formed because the triangular segments formed by the radial cracks were being bent over an annular support. Consequently, further energy was required for propagation. The final fracture pattern and the total energy to failure depended on how quickly each of the cracks propagated. The corresponded force-deflection curve of ABS Lustran 250 was shown in Fig.4.24 .

The first peak in the force-deflection plot corresponded to the crack initiation. The force, the deflection and the energy absorbed at this point were the initiation properties. From Fig.4.24 , the deformation of ABS Lustran 250 developed gradually, no sharp peak , at this point it was indicated that the material was not brittle. The deformation was moderate (approximately 11 mm at the peak point and 13 mm at the break point). After the peak point, the cracks continued to open up and this was the second part

of the curve. The radial cracks then extended slowly out towards the edge of the specimen corresponding to the crack propagation from the initial failure to the edge of the specimen. The curve shows the non sharp drop of deformation from the peak to the break point. When the cracks reached the edge, the complete fracture occurred and the force fell to zero. The defection at this point and the total energy absorbed were the fracture properties. Sometimes, there was a small force recorded after failure due to the friction between the hole of a specimen and a striker then maintained superimposed on the ringing of the apparatus. Therefore, this portion had no utility for describing the impact fracture. The pattern of some cracks of ABS Lustran 250 as the breaking in 1 piece as shown in Fig.4.25. The corresponding force-deflection curve is shown in Fig.4.26 . There was a decrease load with increasing deformation followed by a further increase in load to the maximum load value; and the decrease in load could indicate the first crack in the specimens. Sometimes , the curve showed the low value of the force and deformation at peak or at break. It indicated the low toughness of the specimen.

In addition, the cracked specimen of ABS Lustran 250 moulded at melt temperature of 280 $^\circ$C exhibited brittle failure. The specimen was broken as shown in Fig. 4.27. The force-defection curve is shown as Fig.4.28 . From this figure there was no plastic flow and the crack propagated quickly from the peak point to the break point. The small deformation was occurred (approximately 10.4 mm at the peak point and 10.8 mm at the break point). The slope of the initial force-deflection curve was very sharp, therefore , it indicated the elastic response of the specimen.
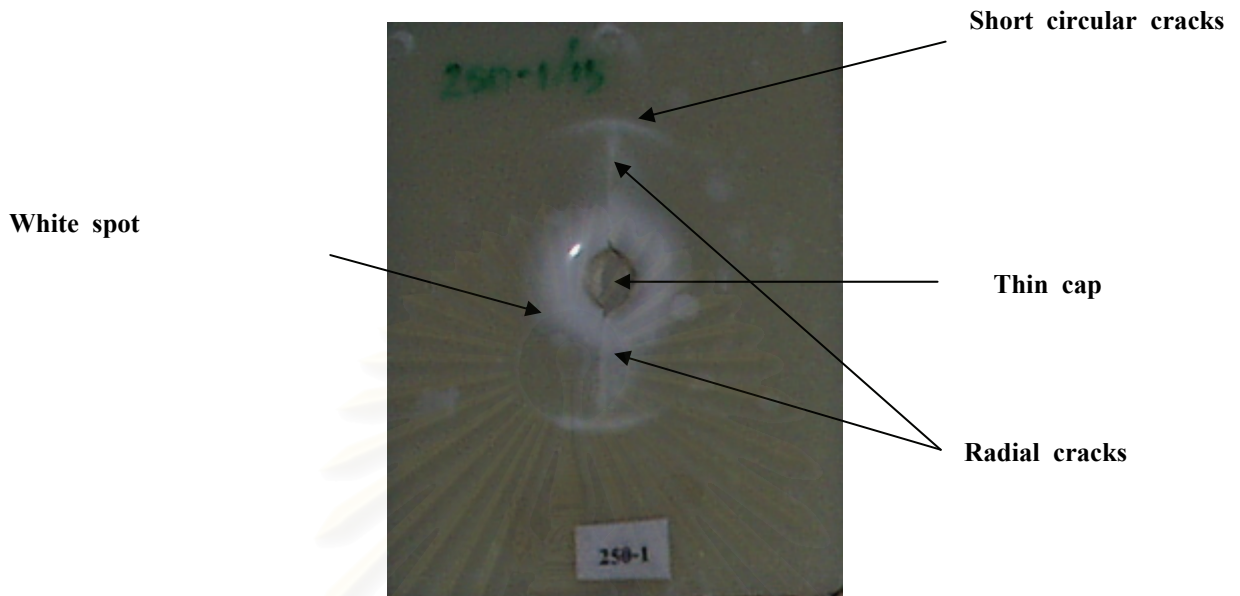
Figure 4.23   Cracks form of ABS Lustran 250.

Figure 4.24   Force-deflection curve of ABS Lustran 250.

Figure 4.25 Minor cracks form of ABS Lustran 250.

Figure 4.26 Minor force-defection curve of ABS Lustran 250.

Figure 4.27   Cracked specimens of ABS Lustran 250 moulded at   melt

temperature of 280   C.
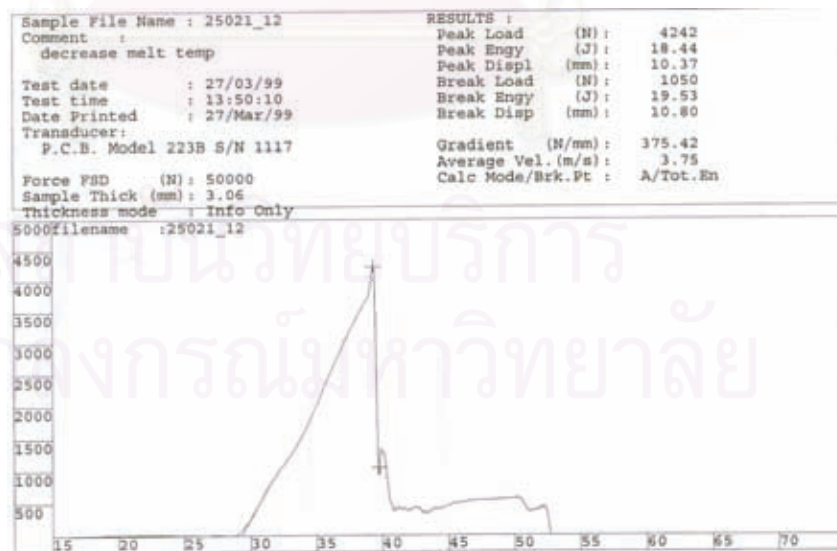
Figure 4.28 Force-deflection curve of ABS Lustran 250 moulded   melt

temperature of 280   C.

4.3.5.2 ABS Lustran 440 and Lustran 640

The type failure pattern of ABS Lustran 440 and Lustran 640 is shown in Fig. 4.29 . The cracked specimens exhibited the ductile failure and there was a thin cap of deformed material. It was a uniform extruded section after penetration of the striker. A white spot was developed around the hole circularly. Sometimes, there were only short radial cracks on some cracked specimens. The features of the corresponding force-deflection curve as shown in Fig. 4.30 .

From Fig. 4.30 , there was gradually increasing load with increasing deformation. A large amount of energy was absorbed to initiate and then propagated the cracks. A large deformation before failure approximately 14 mm at the peak point and 19 mm at the break point. It indicated the toughness of the specimen. The cracks pattern of ABS Lustran 440 and Lustran 640 moulded at melt temperature of 280 $^\circ$C indicated the ductile failure. The characteristics of the corresponding force-deflection curve was similar to Fig. 4.30. The value of force and deflection was lower as shown in Fig. 4.31. Therefore, there was a drop of the impact performance for the ABS Lustran 440 and Lustran 640 specimens moulded at high melt temperature. ABS Lustran 440 and Lustran 640 were the medium and high impact grades respectively , therefore, their impact performance was higher than ABS Lustran 250. In addition, the cracks pattern was ductile failure when the specimen was moulded at high melt temperature.
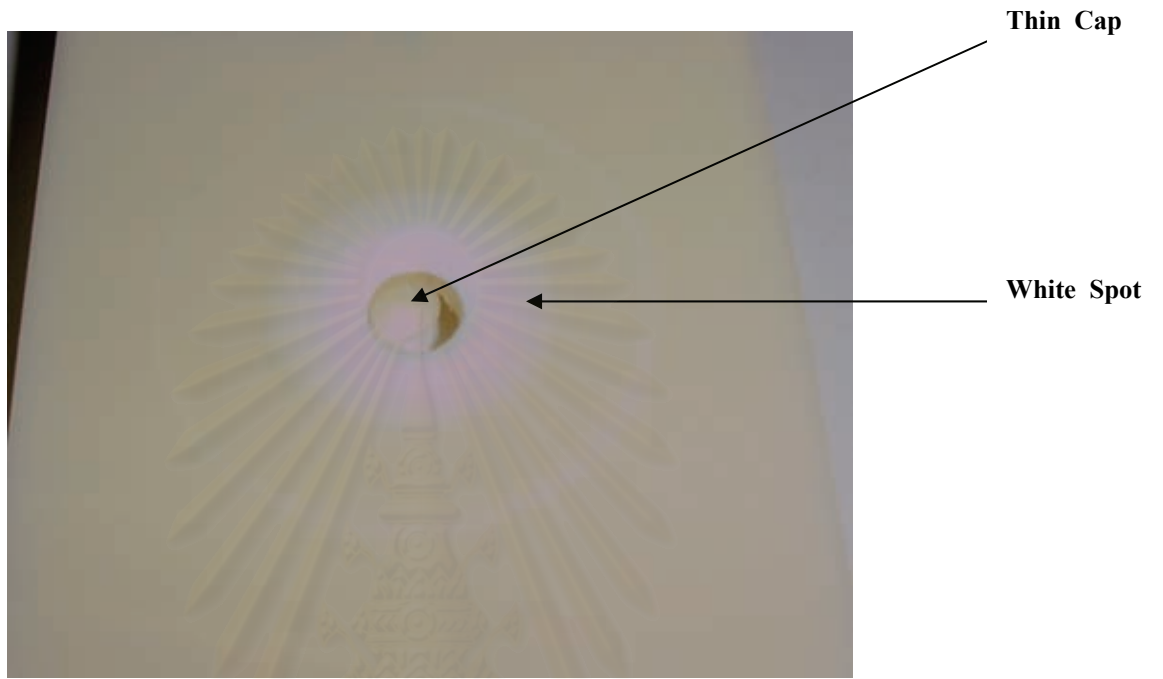
Figure 4.29   Cracks form of ABS Lustran 440 and Lustran 640.
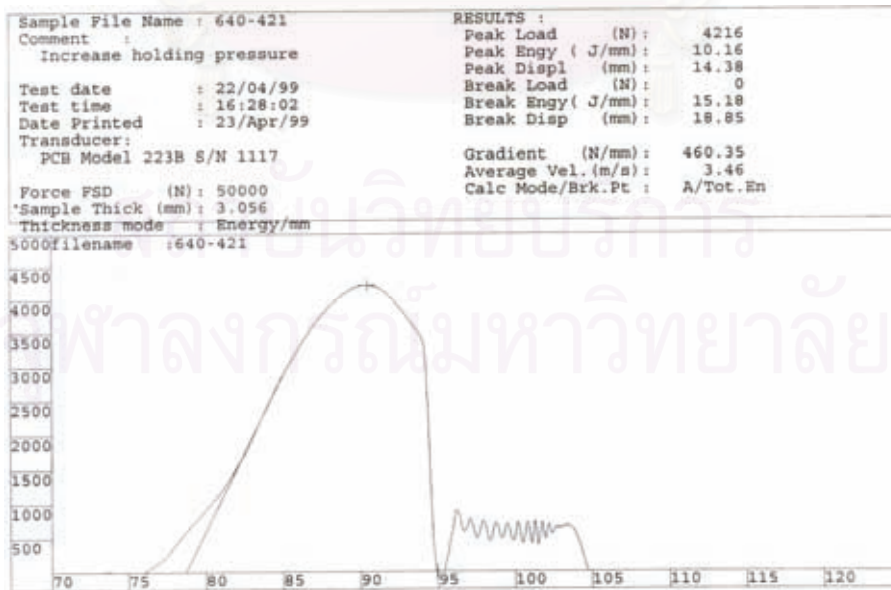
Figure 4.30   Force-deflection curve of ABS Lustran 440 and Lustran 640.

```
Sample File Name : 640-5116            RESULTS :
Comment     :                          Peak Load      (N):     3723
  Increase melt temp                   Peak Engy ( J/mm):      6.42
                                       Peak Displ    (mm):    11.71
Test date        : 22/04/99            Break Load     (N):     1317
Test time        : 18:59:34            Break Engy( J/mm):      7.51
Date Printed     : 23/Apr/99           Break Disp    (mm):    13.13
Transducer:
  PCB Model 223B S/N 1117              Gradient    (N/mm):   470.28
                                       Average Vel.(m/s):      3.52
Force FSD     (N): 50000               Calc Mode/Brk.Pt :   A/Tot.En
Sample Thick (mm): 3.032
Thickness mode  : Energy/mm
5000 filename    :640-5116
```
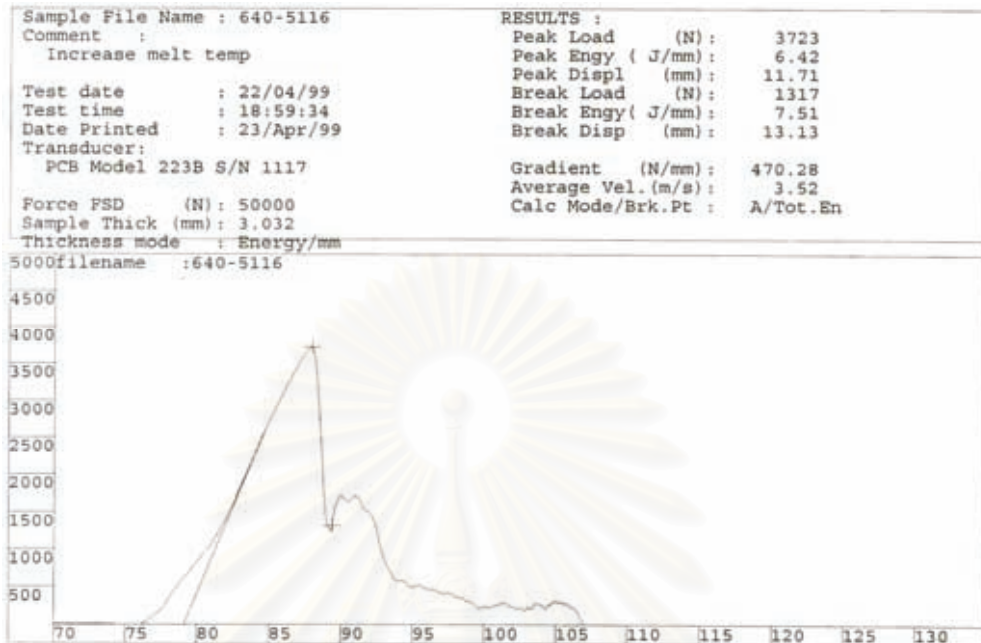

Figure 4.31   Force-deflection   curve   of   ABS   Lustran 440   and   Lustran 640
moulded   melt   temperature   of   280 $^\circ$ C.

4.4 EFFECT OF INJECTION PARAMETERS ON INTERNAL STRUCTURE

For the effect of injection parameters on the impact properties for ABS Lustran 250 , Lustran 440 and Lustran 640 , the results are presented in section 4.3 . The first parameter which had the significant effect on impact properties was the injection speed. Impact properties increased with increasing injection speed. Molecular orientation was expected higher for faster injection speed. The second parameter affected the impact properties significantly was the melt temperature. Too low and too high melt temperature decreased the impact properties. Internal stress was expected for the cause of impact reduction as the melt temperature was too low. However, molecular degradation was expected for the cause of a large impact properties drop for the parts moulded at high melt temperature. Investigation of the effect of injection parameters was done by testing molecular orientation, internal stress and molecular degradation for ABS Lustran 250 moulded parts.

4.4.1 Molecular Orientation

Molecular orientation has been reported to affect the mechanical properties of ABS mouldings [15,21-23]. Therefore, the influence of any molecular orientation in the moulded parts in this work must be investigated. It has been reported that molecular orientation frozen-in the injection moulded parts can be detected by the change in properties after annealing the ABS parts at a temperature of 80 °C. Table 4.6 shows tensile strength of ABS Lustran 250 moulded parts without annealing and after annealing results. Figures 4.32, 4.33, 4.34 , and 4.35 show the tensile strength of the parts without annealing and after annealing in graphs for each injection parameter varied.

The result of tensile strength of the moulded parts at injection speed of 100 mm/s showed that there was approximately 12 % increase in tensile strength after annealing. The Increase in tensile strength after annealing could support the molecular orientation for the high injection speed.

Table 4.6 Tensile Strength of ABS L250 parts without annealing and after annealing

Exp. No.	Injection Condition	Tensile Strength (MPa) without Annealing	Tensile Strength (MPa) after Annealing 80 C , 4 Hrs
5	Injection Speed 10 mm/s	39.78	43.14
1	Injection Speed 40 mm/s	39.16	41.82
3	Injection Speed 100 mm/s	39.1	43.87
11	Holding Pressure 0 bar	39.41	39.67
1	Holding Pressure 15 bar	39.16	41.82
8	Holding Pressure 100 bar	41.19	42.47
15	Holding Time 0 sec	41.43	41.75
1	Holding Time 1.5 sec	39.16	41.82
13	Holding Time 20 sec	41	41.76
21	Melt Temperature 180 C	41.83	42.56
1	Melt Temperature 230 C	39.16	41.82
19	Melt Temperature 280 C	39.35	40.21
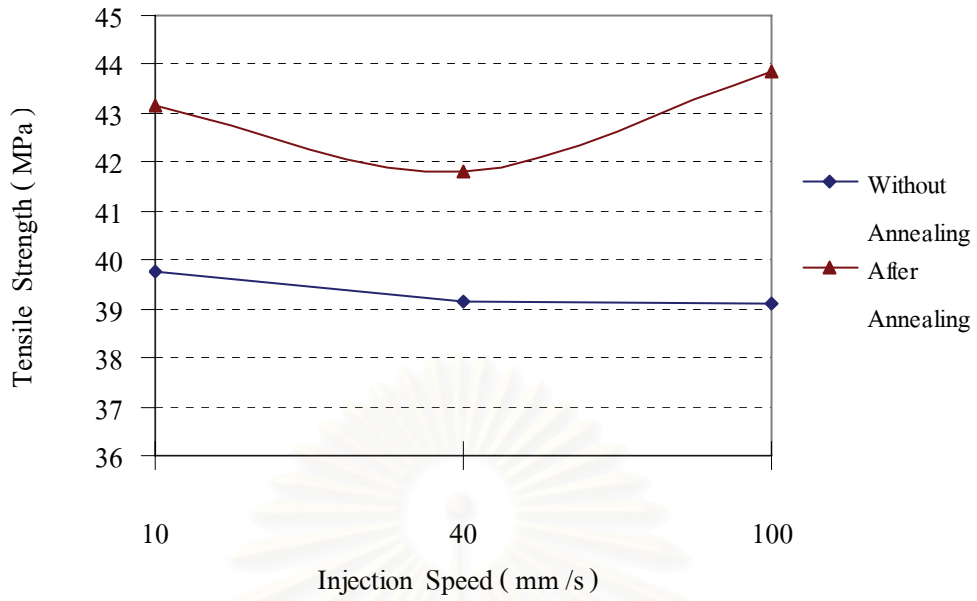
Figure 4.32 Effect of injection speed on tensile strength of ABS Lustran 250.
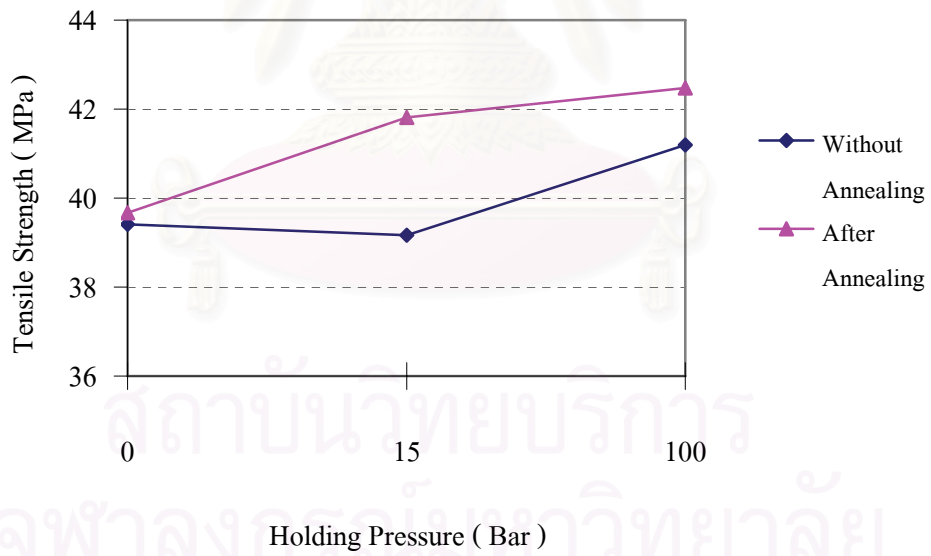
Figure 4.33 Effect of holding pressure on tensile strength of ABS Lustran 250.
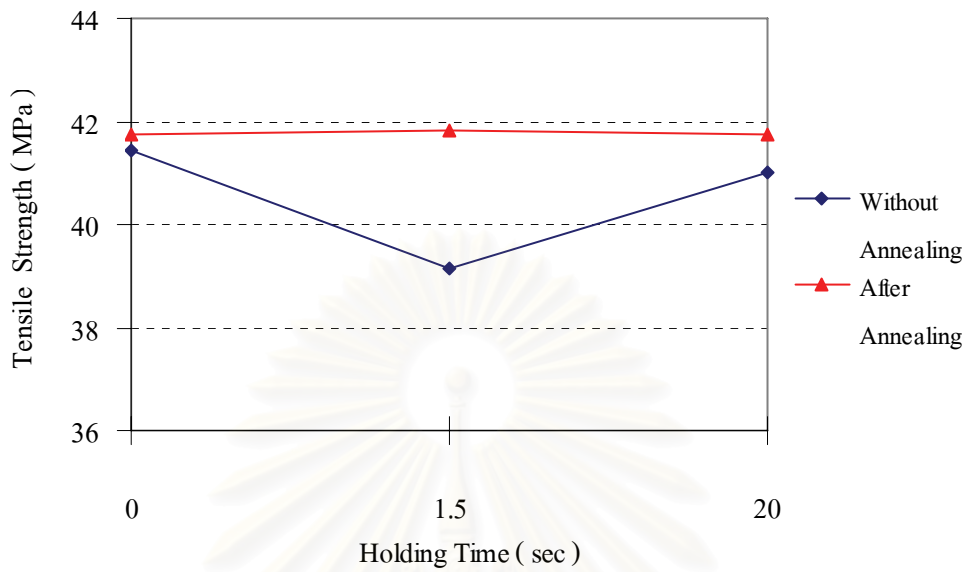
Figure 4.34 Effect of holding time on tensile strength of ABS Lustran 250.
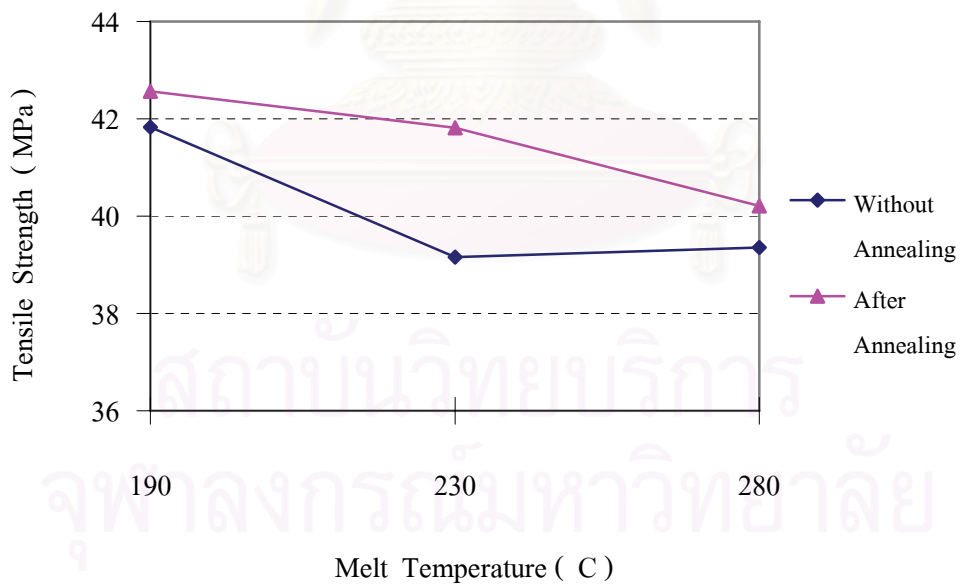
Figure 4.35 Effect of melt temperature on tensile Strength of ABS Lustran 250.

4.4.2 Internal stress

Frozen - in internal stress occurs from the rapid cooling in the injection moulding process. It has been reported that the internal stress can greatly influence the mechanical properties of ABS moulding [20,23]. The investigation of internal stress was conducted by immersion in a liquid which relaxed the stress and cause the stress whitening. Table 4.7 shows the result of stress whitening on ABS Lustran 250 moulded parts after immersion in the solvent. The photographs of the moulded parts with the stress whitening are shown in Fig. 4.36 .

Stress whitening occurred after immersion in acetic acid was high in the specimen moulded at melt temperature of 190 $^\circ$C (Exp. No. 21). There was more stress whitening at the end of flow for the high holding pressure condition (Exp. No. 8) and less stress whitening near the gate for high holding time condition (Exp.No.13).

The high internal stress of the part moulded at low melt temperature should be caused by the increase of viscosity and the excessive cooling. The higher pressure drop across the part the higher the part stress

differentially. The increment of internal stress could also be seen by examining the stress levels and pressure losses through the part calculated by the Moldflow computer program as a function of melt temperature. The stress level and pressure losses are presented in Table 4.8 . At the low melt temperature of 190°C, the maximum stress and the pressure losses increased. Thus , the amount of internal stress was expected to increase.

It has been reported that the internal stress can be greatly influenced by low melt temperature such as the previous study of M. Serrano [20] to reduce injection moulded part stress in plating grade ABS. It was shown that the part stress differential or pressure differential was

minimized by increasing the melt temperature. Siegmann, *et al*. found that the stresses in the surface region decreased with increasing melt temperature in zones far away from the gate. This was allowed more stress relaxation.

Table 4.7 Glacial Acetic Acid (AA) Immersion Test for Stress Visualization
of ABS Lustran 250.

Exp. No.	Injection Moulding Condition	Parts Appearance	Stress Whitening
1	Reference Condition	Good	Slightly
3	High Injection Speed	Flash	Slightly
5	Low Injection Speed	Short Shot	Slightly
8	High Holding Pressure	Flash	Large at the end of flow
11	Low Holding Pressure	A Little Sink Mark at the edge	Slightly
13	Long Holding Time	Good	Slightly near the gate area
15	Short Holding Time	Sink Mark at the end	Slightly
19	High Melt Temperature	Silver Streaks and Sink Marks Color changed	Slightly
21	Low Melt Temperature	Short Shot	Very Large
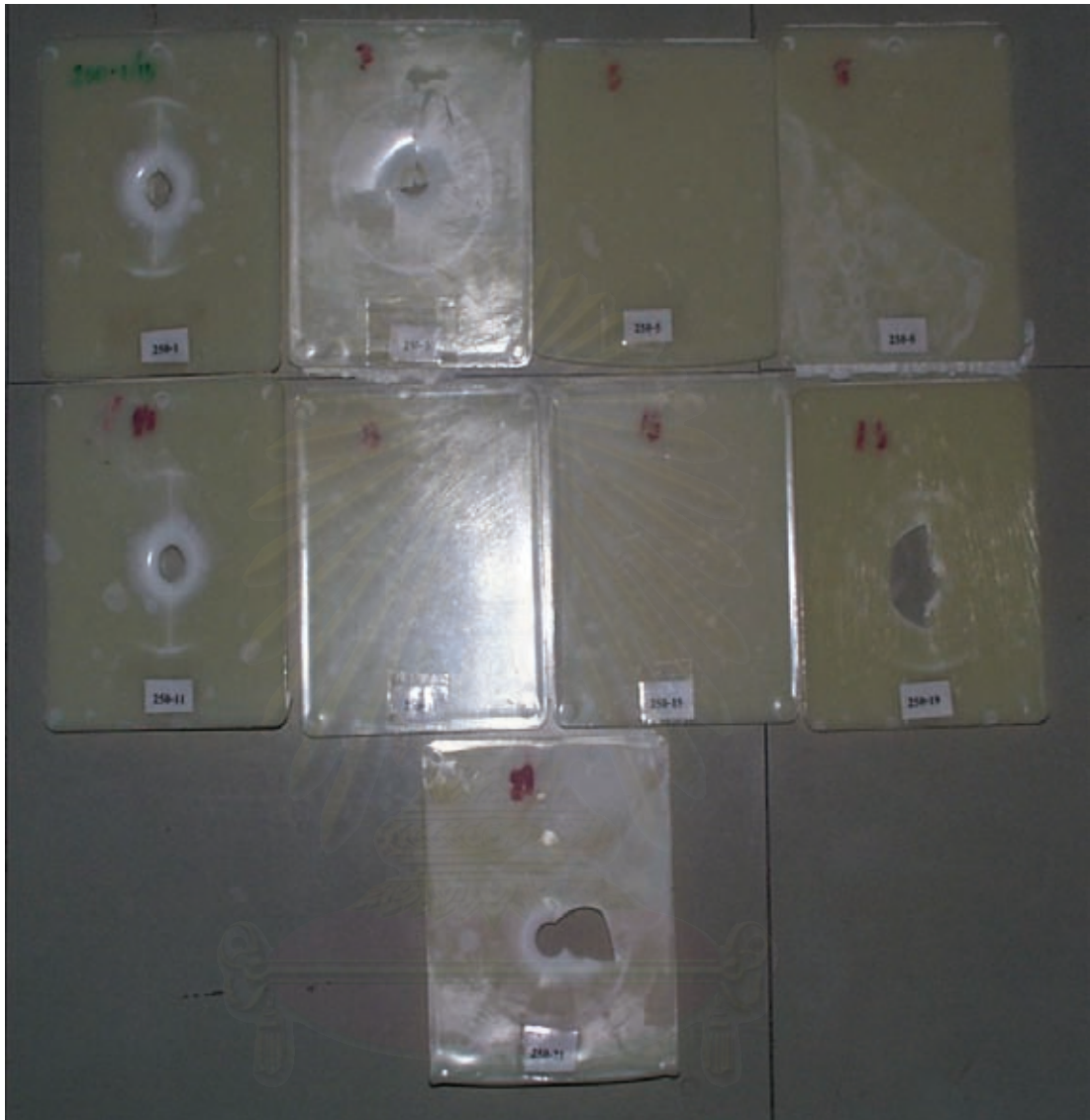
Remark : Some parts showed cracks or holes because the parts were tested the internal stress after impact test (no more spare parts for that Exp. No.) ; however , the visual whitening inspection was ignored the impact tested area.

Figure 4.36 ABS Lustran 250 moulded parts after the stress whitening test.

Table 4.8 Maximum stress and pressure losses predicted by Moldflow $\circledR$

Melt Temperature ($^\circ$C)	Max. Stress (MPa)	Pressure (MPa)
190	0.826	61.736
230	0.373	41.463
280	0.262	29.545

4.4.3 Molecular Degradation

At high melt temperatures the mechanical properties are affected by thermal degradation of polymer. To investigate if there was any polymer degradation occurred in the experiments, the moulding parts were crushed and the melt flow index was measured and compared to virgin ABS. An increase in MFI would confirm some molecular degradation. The higher the melt flow index , the higher degree of degradation.

From   Table 4.9 , the increase of   melt flow index of moulded parts at melt temperature of 280   C was approximately 2   times of virgin ABS. It was corresponded to a large drop of impact property. In addition, the color of the moulded parts by visual inspection was more yellow than the   parts of the other moulding conditions. It was indicated that there was some molecular degradation at high melt temperature condition.

From Table 4.9 , the melt   flow indexes for the parts moulded at   melt temperature of 190 $^\circ$C and 230   C are approximately the same. The melt flow indexes did not   increase significantly when compared to the value of   virgin ABS.

Table 4.9 Melt flow index   of   ABS Lustran 250   granule and after   moulded.

	Melt Flow Index (g / 10 min.) at 230°C , 2.16 Kg			
	Virgin granule	After moulding at melt temperature 190 ° C	After moulding at melt temperature 230 °C	After moulding at melt temperature 280 ° C
1	4.01	5.80	5.85	8.79
2	4.03	5.88	5.91	8.98
3	4.09	5.90	6.00	9.20
Average Value	4.04	5.86	5.92	8.99

CHAPTER V

CONCLUSIONS AND RECOMMENDATION

5.1 CONCLUSION

A comparison between the pressure predicted by the Moldflow®
simulation software and measured during the injection moulding experiments
was made to study the effects of injection moulding parameters on mechanical
property by testing impact performance. The simulation was investigated for the
Moldflow standard database and personal database which was prepared by
testing ABS properties. The cavity pressures of a rectangular plaque mould
were measured by two pressure transducers fitted near the gate and far from
the gate. The comparison was made using three grades of amorphous
thermoplastic ABS. The injection moulding conditions used for the simulation
were the same as those used for the experiments.

For the study of the effects of injection moulding parameters on impact
properties , two important influence parameters were injection speed and melt
temperature. Increasing injection speed increased impact properties due to high
molecular orientation. High melt temperature caused the decrease of impact
property due to molecular degradation. As well as, low melt temperature gave
slightly reduction in impact property because of higher internal stress.

Investigation of the effect of injection moulding parameters was also
supported by some tests such as the tensile test for molecular orientation, the
melt flow index test for molecular degradation and the glacial acetic acid
immersion for internal stress. There was an increase in tensile strength after

annealing the parts moulded at high injection speed. The molecular degradation test result showed that the increase of melt flow index of moulded parts at melt temperature of 280 C was approximately two times of virgin ABS. For internal stress test , there was stress whitening occurred on the moulded parts at low melt temperature.

For the simulation , selection of the material information input as Moldflow standard database or a personal database showed insignificant difference of the predicted pressure for ABS Lustran 250. For ABS Lustran 440 and Lustran 640 , the simulation predicted higher pressure values as a personal database was selected. The simulation was done by the selection of Moldflow standard database for ABS 250 to compare with the measurement. The simulation showed qualitative disagreement to the measurement. For Moldflow prediction , the higher the predicted pressure, the lower the injection speed. For the measurement , the lower the pressure , the lower the injection speed. From simulation , the cavity pressure increased with increasing injection speed and then decreased at very high injection speed. However, the pressure given by the measurement showed only the increase of pressure with increasing injection speed.

Moldflow predicted no changes in the pressure value and the effective holding pressure time of the pressure curves as each holding pressure and holding time was varied. For various holding pressures investigated, the pressure shown by measurement increased and the effective holding pressure time increased at high holding pressure time. For short holding time, the measurement showed that there was a drop-off in the pressure curve.

As melt temperature was varied, the simulation showed the reverse agreement in qualitative to the measurement. For Moldflow prediction , the higher the melt temperature , the lower the pressure value and the lower the melt temperature , the higher the pressure value . However , the measurement showed that the higher the melt temperature , the higher the pressure value and the lower the melt temperature , the lower the pressure value. In addition , the predicted fill time was different quantitatively when compared from the measurement.

The differences in the prediction were attributed to the over-estimation of the cooling rate of Moldflow. Moldflow is designed to simulate the industrial injection moulding practice with sophisticated mould design, including very efficient cooling systems for high output production. However, the experimental mould had very simple cooling system which possibly was inefficient in terms of Moldflow software design assumptions. Therefore, the cooling rates was over-estimated leading to the inaccurate prediction as melt temperature and injection speed were varied. Moldflow could over-estimate the shear-heating during the injection phase since the nozzle design , runners and gate system in the experimental mould were not complex. In addition , The differences of material properties existed in the standard database and the actual material properties used could lead to inaccurate prediction. The database in Moldflow was different from personal database developed for Lustran 440 and Lustran 640. This would indicate some limitations to the standard database applicability to all grades of ABS.

5.2 SUGGESTION FOR FUTURE WORK

For the additional work suggestions were shown as follows.

1. A sophisticated mould geometry should be used for the simulation.

2. For verification of the effect of cooling system , an experiment should be done with a new mould having very efficient cooling. The experimental results and the Moldflow predictions will be compared.

3. The material properties should be tested for every requirement items   for the database input.

REFERENCES

1. SIMCON Seminar, <u>Layout of Injection Moulds</u>, Simcon Kunststoff Tech Nische Software, pp.1, Korea Academy of Industrial Technology, 1990.

2. Weber, A., Plastics in Automotive Engineering :Use and Re-use, *Mat. & Design.*, **12**, 199, (1991).

3. Manzione, L.T., <u>Application of Computer- Aided Engineering in Injection Molding</u>, pp.2, 265, 138-172, New York, Hanser Publishers, 1987.

4. Halasz, L., Computer Aided Technology and Mould Design in Injection Moulding, *Int. Polym. Sci. Tech.*, **22**, T/50, (1995).

5. Kennedy, P., Flow Analysis Reference Manual, pp.1-4, Moldflow Pty.Ltd., Victoria, Australia, 1993.

6. Axtell, F.H., and Haworth, B., A Practical Verification of a Computer Simulation for Injection Molding Applied to Amorphous Thermoplastic Polyesters, *Polym.-Plast. Techol. Eng*, **30** (5&6), 441, (1991).

7. Kistler Seminar, <u>Cavity Pressure Measurement a Method to Increase Quality and Productivity in Injection Molding</u>, Kistler Instrument (Pty), Ltd.

8. Birley, W., Haworth, B., Batchelor, J., <u>Physics of Plastics : Processing, Properties and Materials Engineering</u>, pp.165-166, Hanser Publishers, 1991.

9. Crawford, R.I., <u>Plastics Engineering</u>, pp.187-188, Pergamon press, 2 nd-ed, 1987.

10. Brydson, J.A., <u>Handbook for Plastics Processors</u>, pp.76-77, Heinemann Newnes, 1990.

11. Axtell, F.H., A Study of the Flow Properties and Processability of Thermoplastic Polyesters, pp.183-187, Ph.D.Thesis, Loughborough University, 1987.

12. Kistler, <u>An Introduction Course of Process and Process Control in injection Molding</u>, Kistler Instrument (Pty), Ltd.

13. Greener, J., General Consequences of the Packing Phase in Injection Molding, *Polym. Eng. Sci.*, **26**, 886, (1986).

14. NSTDA, <u>Simulation Programs for the Injection Moulding Process Workshop</u>, National Science and Technology Development Agency, Thailand.

15. Cox, H.W. and Mentzer, C.C., Injection Molding : The Effect of Fill Time on Properties, *Polym. Eng. Sci*, **26**, 488, (1986).

16. Dairanich, I.S., Haufe, A., WOLF, H. J., and Mennig, G., Computer Simulation of Weld Lines in Injection Molded Poly(Methyl Methacrylate), *Polym. Eng. Sci*, **36**, 2050, (1996).

17. Seow, L.W., and Lam, Y.C., Optimization Flow in Plastic Injection Molding, *Mat. Proc. Tech.*, **72**, 333, (1997).

18. Gao, F., Patterson, W., and Kamal, M.R., Cavity Pressure Control during the Cooling Stage in Thermoplastic Injection Moulding, *Polym. Eng. Sci*, **36**, 2467, (1996).

19. ASTM D 3763, Standard Test Method for High Speed Puncture Properties of Plastics using Load and Displacement Sensors.

20. Serrano, M., Injection Molding for Parts Stress Reduction in Plating Grade ABS, *ANTEC' 94*, 601, (1994).

21. Dietz, W., White, J.L., Clark, E.S., Orientation Development and Relaxation in Injection Molding of Amorphous Polymers, *Polym. Eng. Sci*, **18**, 273, (1978).

22. Sanou, M., Chung, B., Cohen, C., Glass Fiber-Filled Thermoplastics : Cavity Filling and Fiber Orientation in Injection Molding, *Polym. Eng. Sci*, **25**, 1008, (1985).

23. Struik, L.C.E., Orientation Effects and Cooling Stresses in Amorphous Polymers, *Polym. Eng. Sci*, **18**, 799, (1978).

24. Jones, D.P., Leach, D.C., and Moor, D.R., The Application of Instrumented Falling Weight Impact Techniques to the Study of Toughness in Thermoplastics, *Plast. Rubb. Process. App.*, **6**, 67, (1986).

APPENDICES

Appendix A

Material Properties Data of the Existing Standard Moldflow Database and a Personal Database for ABS
Lustran 250 , Lustran 440 and Lustran 640

MATERIAL INFORMATION

Reading MOLDFLOW PVT001 from Standard database.

Material DATABASE type : MATDB <Standard>

SUPPLIER/file name   : MONEUR

GRADE code   : MON102

Material MODEL order : DEFAULT

Material description :

MON102 ABS   LUSTRAN 240   MONEUR   VI(240)227 MONEUR SEP95

Conductivity   0.150000 W/m/degC

Specific Heat   2100.000000 J/kg/degC

Melt Density   900.000000 kg/cu.m

Ejection Temperature   108.000000 deg.C

No Flow Temperature   130.000000 deg.C

Viscosity

Temperature	Shear Rate	Viscosity
deg.C	1/s	Pa.s
220.000	1000.000	308.799957
240.000	100.000	966.099976
240.000	1000.000	227.000000
240.000	10000.000	40.900002
260.000	100.000	667.799988
260.000	1000.000	171.699997

Generic PVT Specific Volume

Temperature	Pressure	PVT Specific Volume
deg.C	MPa	cu.cm/g
0.000	0.000	0.941092
0.000	160.000	0.911333
20.000	0.000	0.947145
20.000	160.000	0.914493
92.320	0.000	0.968832
129.552	160.000	0.932220
210.000	0.000	1.041063
210.000	160.000	0.957964
250.000	0.000	1.065615

250.000	160.000	0.970765

Processing Conditions:

Melt Temperature Minimum	220.000000 deg.C
Melt Temperature Maximum	260.000000 deg.C
Melt Temperature Suggested	240.000000 deg.C
Generic Mold Temperature Minimum	40.000000 deg.C
Generic Mold Temperature Maximum	80.000000 deg.C
Generic Mold Temperature Suggested	60.000000 deg.C
Melt Temperature Absolute Maximum	280.000000 deg.C
Generic Maximum Shear Stress	0.300000 MPa
Generic Maximum Shear Rate	50000.000000 1/s

MATERIAL INFORMATION

Reading MOLDFLOW PVT001 from Standard database.

Material DATABASE type : MATDB <Standard>

SUPPLIER/file name   : MONEUR

GRADE code   : MON105

Material MODEL order   : DEFAULT

Material description   :

MON105 ABS   LUSTRAN 440   MONEUR   VI(240)223 MONEUR   OCT93

Conductivity	0.150000 W/m/degC
Specific Heat	2100.000000 J/kg/degC
Melt Density	900.000000 kg/cu.m
Ejection Temperature	107.000000 deg.C
No Flow Temperature	130.000000 deg.C

Viscosity

Temperature	Shear Rate	Viscosity
deg.C	1/s	Pa.s
220.000	1000.000	312.399994
240.000	100.000	895.900024
240.000	1000.000	223.399994
240.000	10000.000	41.700001
260.000	100.000	615.599976
260.000	1000.000	169.699997

Generic PVT Specific Volume

Temperature	Pressure	PVT Specific Volume
deg.C	MPa	cu.cm/g
0.000	0.000	0.941092

0.000	160.000	0.911333
20.000	0.000	0.947145
20.000	160.000	0.914493
92.320	0.000	0.968832
129.552	160.000	0.932220
210.000	0.000	1.041063
210.000	160.000	0.957964
250.000	0.000	1.065615
250.000	160.000	0.970765

Processing Conditions:

Melt Temperature Minimum	220.000000 deg.C
Melt Temperature Maximum	260.000000 deg.C
Melt Temperature Suggested	240.000000 deg.C
Generic Mold Temperature Minimum	40.000000 deg.C
Generic Mold Temperature Maximum	80.000000 deg.C
Generic Mold Temperature Suggested	60.000000 deg.C
Melt Temperature Absolute Maximum	280.000000 deg.C
Generic Maximum Shear Stress	0.300000 MPa
Generic Maximum Shear Rate	50000.000000 1/s
Material Compressibility : PVT	
Extensional Viscosity Effects : OFF	
Determining Connectivities...	

MACHINE SETTINGS:

Maximum Injection Pressure : 100.00 MPa	
Maximum Clamp Tonnage : 10000.00 tonne	

MATERIAL INFORMATION

Reading MOLDFLOW PVT001 from Standard database.

Material DATABASE type : MATDB <Standard>

SUPPLIER/file name   : MONEUR

GRADE code   : MON106

Material MODEL order   : DEFAULT

Material description   :

MON106 ABS   LUSTRAN 640   MONEUR   VI(240)241 MONEUR   SEP95

Conductivity	0.150000 W/m/degC
Specific Heat	2100.000000 J/kg/degC
Melt Density	900.000000 kg/cu.m
Ejection Temperature	104.000000 deg.C

No Flow Temperature   130.000000 deg.C

Viscosity

Temperature	Shear Rate	Viscosity
deg.C	1/s	Pa.s
220.000	1000.000	326.600006
240.000	100.000	1020.599976
240.000	1000.000	241.500000
240.000	10000.000	46.599998
260.000	100.000	721.000000
260.000	1000.000	183.399994

Generic PVT Specific Volume

Temperature	Pressure	PVT Specific Volume
deg.C	MPa	cu.cm/g
0.000	0.000	0.941092
0.000	160.000	0.911333
20.000	0.000	0.947145
20.000	160.000	0.914493
92.320	0.000	0.968832
129.552	160.000	0.932220
210.000	0.000	1.041063
210.000	160.000	0.957964
250.000	0.000	1.065615
250.000	160.000	0.970765

Processing Conditions:

Melt Temperature Minimum	220.000000 deg.C
Melt Temperature Maximum	260.000000 deg.C
Melt Temperature Suggested	240.000000 deg.C
Generic Mold Temperature Minimum	40.000000 deg.C
Generic Mold Temperature Maximum	80.000000 deg.C
Generic Mold Temperature Suggested	60.000000 deg.C
Melt Temperature Absolute Maximum	280.000000 deg.C
Generic Maximum Shear Stress	0.300000 MPa
Generic Maximum Shear Rate	50000.000000 1/s

Material Compressibility   : PVT

Extensional Viscosity Effects : OFF

Determining Connectivities...

MACHINE SETTINGS:

Maximum Injection Pressure   :   100.00   MPa

Maximum Clamp Tonnage   : 10000.00   tonne

MATERIAL INFORMATION

Reading MOLDFLOW PVT001 from Standard database.

Material DATABASE type : MATDB <Local>

SUPPLIER/file name   : BAYERRY

GRADE code   : L250

Material MODEL order   : DEFAULT

Material description   :

L250 ABS   LUSTRAN 250   BAYERRY   VI(240)227 BUSARIN   FEB99

Conductivity   0.176700 W/m/degC

Specific Heat   2100.000000 J/kg/degC

Melt Density   900.000000 kg/cu.m

Ejection Temperature   108.000000 deg.C

No Flow Temperature   130.000000 deg.C

Viscosity

Temperature	Shear Rate	Viscosity
deg.C	1/s	Pa.s
220.000	1000.000	354.970001
240.000	100.000	792.789978
240.000	1000.000	258.059998
240.000	10000.000	49.980000
260.000	100.000	545.169983
260.000	1000.000	181.910004

Generic PVT Specific Volume

Temperature	Pressure	PVT Specific Volume
deg.C	MPa	cu.cm/g
0.000	0.000	0.941092
0.000	160.000	0.911333
20.000	0.000	0.947145
20.000	160.000	0.914493
92.320	0.000	0.968832
129.552	160.000	0.932220
210.000	0.000	1.041063

210.000	160.000	0.957964
250.000	0.000	1.065615
250.000	160.000	0.970765

Processing Conditions:

Melt Temperature Minimum	220.000000 deg.C
Melt Temperature Maximum	260.000000 deg.C
Melt Temperature Suggested	240.000000 deg.C
Generic Mold Temperature Minimum	40.000000 deg.C
Generic Mold Temperature Maximum	80.000000 deg.C
Generic Mold Temperature Suggested	60.000000 deg.C
Melt Temperature Absolute Maximum	280.000000 deg.C
Generic Maximum Shear Stress	0.300000 MPa
Generic Maximum Shear Rate	50000.000000 1/s

Material Compressibility   : PVT

Extensional Viscosity Effects : OFF

Determining Connectivities...

MACHINE SETTINGS:

Maximum Injection Pressure   :   100.00   MPa

Maximum Clamp Tonnage   : 10000.00   tonne

MATERIAL INFORMATION

 Reading MOLDFLOW PVT001 from Standard database.

 Material DATABASE type : MATDB <Local>

SUPPLIER/file name   : BAYERRY

GRADE code   : L440

Material MODEL order   : DEFAULT

Material description   :

L440 ABS   LUSTRAN 440   BAYERRY   VI(240)223 BUSARIN   FEB99

Conductivity	0.184100 W/m/degC
Specific Heat	2100.000000 J/kg/degC
Melt Density	900.000000 kg/cu.m

Ejection Temperature   107.000000 deg.C

No Flow Temperature   130.000000 deg.C

Viscosity

Temperature	Shear Rate	Viscosity
deg.C	1/s	Pa.s
220.000	1000.000	421.700012
240.000	100.000	1276.680054
240.000	1000.000	302.950012
240.000	10000.000	55.400002
260.000	100.000	805.489990
260.000	1000.000	211.619995

Generic PVT Specific Volume

Temperature	Pressure	PVT Specific Volume
deg.C	MPa	cu.cm/g
0.000	0.000	0.941092
0.000	160.000	0.911333
20.000	0.000	0.947145
20.000	160.000	0.914493
92.320	0.000	0.968832
129.552	160.000	0.932220
210.000	0.000	1.041063
210.000	160.000	0.957964
250.000	0.000	1.065615
250.000	160.000	0.970765

Processing Conditions:

Melt Temperature Minimum	220.000000 deg.C
Melt Temperature Maximum	260.000000 deg.C
Melt Temperature Suggested	240.000000 deg.C
Generic Mold Temperature Minimum	40.000000 deg.C
Generic Mold Temperature Maximum	80.000000 deg.C
Generic Mold Temperature Suggested	60.000000 deg.C
Melt Temperature Absolute Maximum	280.000000 deg.C
Generic Maximum Shear Stress	0.300000 MPa
Generic Maximum Shear Rate	50000.000000 1/s

Extensional Viscosity Effects : OFF

Determining Connectivities...

MACHINE SETTINGS:

Maximum Injection Pressure   :   100.00   MPa

Maximum Clamp Tonnage   : 10000.00   tonne

MATERIAL INFORMATION

 Reading MOLDFLOW PVT001 from Standard database.

 Material DATABASE type : MATDB <Local>

SUPPLIER/file name   : BAYERRY

GRADE code   : L250

Material MODEL order   : DEFAULT

Material description   :

L250 ABS   LUSTRAN 250   BAYERRY   VI(240)227 BUSARIN   FEB99

Conductivity	0.176700 W/m/degC
Specific Heat	2100.000000 J/kg/degC
Melt Density	900.000000 kg/cu.m
Ejection Temperature	108.000000 deg.C
No Flow Temperature	130.000000 deg.C

 Viscosity

Temperature	Shear Rate	Viscosity
deg.C	1/s	Pa.s
220.000	1000.000	354.970001
240.000	100.000	792.789978
240.000	1000.000	258.059998
240.000	10000.000	49.980000
260.000	100.000	545.169983
260.000	1000.000	181.910004

Generic PVT Specific Volume

Temperature	Pressure	PVT Specific Volume
deg.C	MPa	cu.cm/g
0.000	0.000	0.941092
0.000	160.000	0.911333
20.000	0.000	0.947145
20.000	160.000	0.914493

92.320	0.000	0.968832
129.552	160.000	0.932220
210.000	0.000	1.041063
210.000	160.000	0.957964
250.000	0.000	1.065615
250.000	160.000	0.970765

Processing Conditions:

Melt Temperature Minimum	220.000000 deg.C
Melt Temperature Maximum	260.000000 deg.C
Melt Temperature Suggested	240.000000 deg.C
Generic Mold Temperature Minimum	40.000000 deg.C
Generic Mold Temperature Maximum	80.000000 deg.C
Generic Mold Temperature Suggested	60.000000 deg.C
Melt Temperature Absolute Maximum	280.000000 deg.C
Generic Maximum Shear Stress	0.300000 MPa
Generic Maximum Shear Rate	50000.000000 1/s

Material Compressibility   : PVT

Extensional Viscosity Effects : OFF

Determining Connectivities...

MACHINE SETTINGS:

Maximum Injection Pressure   :   100.00   MPa

Maximum Clamp Tonnage   : 10000.00   tonne

APPENDIX B

IMPACT PROPERTIES RAW DATA

Exp. No.	Thickness (mm)	Impact Property for ABS Lustran 250 Condition : Standard condition					
		Load at Peak (N)	Peak Energy (J / mm)	Displ. to Peak (mm)	Load at Break (N)	Break Energy (J / mm)	Displ. to Break (mm)
1 / 1	3.06	3648	5.77	10.95	950	6.77	12.44
1 / 2	3.06	3659	5.65	10.76	879	6.91	12.67
1 / 3	3.056	2268	2.44	8.32	1357	3.2	9.62
1 / 4	-						
1 / 5	-						
1 / 6	-						
1 / 7	3.072	2629	3.00	8.33	1161	3.79	9.62
1 / 8	3.072	3375	4.49	9.88	1196	5.5	11.15
1 / 9	3.066	1977	1.96	7.70	1228	2.66	9.03
1 / 10	3.068	3646	5.36	10.53	1056	6.37	11.79
1 / 11	3.06	3861	5.97	11.09	1109	7.34	12.92
1 / 12	3.056	3445	4.81	10.04	1104	5.78	11.31
1 / 13	3.052	3716	5.5	11.27	1164	6.86	13.16
1 / 14	3.056	3801	5.96	11.36	1056	6.99	12.62
1 / 15	-						
1 / 16	-						
1 / 17	3.056	3899	6.2	11.27	1169	7.30	12.54
1 / 18	3.052	3037	3.72	9.07	1214	4.68	10.36
1 / 19	3.054	2741	3.19	8.72	1349	4.08	10.03
1 / 20	3.056	3579	5.15	10.43	1146	6.19	11.71
1 / 21	-						
1 / 22	3.066	2750	3.14	8.35	1240	4.02	9.67
1 / 23	-						
1 / 24	3.06	3162	4.08	10.01	1209	5.06	11.32
1 / 25	-						
1 / 26	3.056	3149	4.06	9.44	1151	4.98	10.70
1 / 27	3.064	2913	3.46	8.79	1317	4.38	10.07
1 / 28	3.064	2679	3.03	8.41	1265	3.88	9.70
1 / 29	-						
1 / 30	-						
Average	3.0603	3196.7	4.347	9.736	1166	5.337	11.1215
Standard dev.	0.006131026	556.55672	1.3106812	1.1979034	120.94496	1.4613984	1.3122591
Varience	0.00004	309755.38	1.7178853	1.4349726	14627.684	2.1356853	1.7220239
Maximum	3.072	3899	6.2	11.36	1357	7.34	13.16
Minimum	3.052	1977	1.96	7.7	879	2.66	9.03

Exp. No.	Thickness (mm)	Impact Property for ABS Lustran 250 Condition : Increase Injection Speed					
		Load at Peak (N)	Peak Energy (J/mm)	Displ. to Peak (mm)	Load at Break (N)	Break Energy (J/mm)	Displ. to Break (mm)
3 / 1	-						
3 / 2	3.168	3498	4.51	9.73	1355	5.54	11.01
3 / 3	3.168	3586	4.79	9.99	1302	5.80	11.27
3 / 4	-						
3 / 5	-						
3 / 6	3.156	2806	3.03	8.14	1230	3.80	9.29
3 / 7	-						
3 / 8	3.17	3206	3.92	9.02	1354	4.73	10.32
3 / 9	-						
3 / 10	3.178	3998	5.90	10.84	1295	7.38	12.80
3 / 11	3.156	4273	7.08	11.67	0	8.27	14.53
3 / 12	3.198	2320	5.43	13.09	200	8.29	22.97
3 / 13	3.182	2888	3.19	8.46	1323	4.12	9.83
3 / 14	-						
3 / 15	-						
3 / 16	-						
3 / 17	3.184	3328	4.12	9.32	1408	5.16	10.68
3 / 18	3.188	4256	6.81	11.61	1115	8.29	13.58
3 / 19	-						
3 / 20	3.168	3606	4.89	10.02	1199	5.92	11.34
3 / 21	-						
3 / 22	3.162	2877	3.18	8.38	1262	4.09	9.73
3 / 23	-						
3 / 24	-						
3 / 25							
3 / 26	3.168	2708	2.94	8.14	1436	3.9	9.59
3 / 27	-						
3 / 28	-						
3 / 29	-						
3 / 30	3.17	4143	6.54	11.28	1061	7.85	13.06
Average	3.172571429	3392.3571	4.7378571	9.9778571	1110	5.9385714	12.142857
Standard dev.	0.01206211	624.31065	1.4400063	1.53617	441.94935	1.7524526	3.5109005
Varience	0.00015	389763.79	2.0736181	2.3598181	195319.23	3.0710901	12.326422
Maximum	3.198	4273	7.08	13.09	1436	8.29	22.97
Minimum	3.156	2320	2.94	8.14	0	3.8	9.29

Exp. No.	Thickness (mm)	Impact Property for ABS Lustran 250 Condition : Decrease Injection Speed					
		Load at Peak (N)	Peak Energy (J / mm)	Displ. to Peak (mm)	Load at Break (N)	Break Energy (J / mm)	Displ. to Break (mm)
5 / 1	-						
5 / 2	-						
5 / 3	3.056	3153	4.01	9.24	809	5.23	11.22
5 / 4	3.062	3166	4.03	9.55	1293	5.07	10.87
5 / 5	-						
5 / 6	3.08	2779	3.24	8.55	1312	4.17	9.91
5 / 7	3.054	2374	2.53	7.74	1289	3.39	9.12
5 / 8	3.074	3781	5.88	10.96	1226	7.01	12.28
5 / 9	3.08	3001	3.76	9.11	1375	4.74	10.46
5 / 10	-						
5 / 11	3.08	2662	3.03	8.32	1510	3.97	9.69
5 / 12	3.066	2600	2.92	8.17	1248	3.80	9.55
5 / 13	-						
5 / 14	3.084	3498	4.86	10.23	1272	6.24	12.24
5 / 15	-						
5 / 16	3.058	3502	4.97	11.16	938	6.26	13.13
5 / 17	-						
5 / 18	3.07	3412	4.68	10.05	1417	5.77	11.36
5 / 19	-						
5 / 20	3.07	2287	2.47	7.64	1296	3.27	9.02
5 / 21	3.07	3269	4.29	10.00	1262	5.34	11.33
5 / 22	3.08	4187	7.70	13.18	1076	9.22	15.09
5 / 23	3.074	2846	3.32	8.71	1312	4.29	10.06
5 / 24	-						
5 / 25	-						
5 / 26	3.078	2666	3.06	8.88	1261	3.95	10.25
5 / 27	3.082	2551	2.89	8.19	1285	3.75	9.58
5 / 28	3.072	2796	3.36	8.76	1369	4.29	10.13
5 / 29	-						
5 / 30	-						
Average	3.071666667	3029.4444	3.9444444	9.3577778	1252.7778	4.9866667	10.849444
Standard dev.	0.009286296	508.64424	1.3201792	1.3988716	165.02497	1.5000471	1.5588324
Varience	0.00009	258718.97	1.7428732	1.9568418	27233.242	2.2501412	2.4299585
Maximum	3.084	4187	7.7	13.18	1510	9.22	15.09
Minimum	3.054	2287	2.47	7.64	809	3.27	9.02

Exp. No.	Thickness (mm)	Impact Property for ABS Lustran 250 Condition : Increase Holding Pressure					
		Load at Peak (N)	Peak Energy (J / mm)	Displ. to Peak (mm)	Load at Break (N)	Break Energy (J / mm)	Displ. to Break (mm)
8 / 1	3.28	3719	4.90	9.97	1548	6.01	11.28
8 / 2	-						
8 / 3	-						
8 / 4	-						
8 / 5	-						
8 / 6	-						
8 / 7	3.258	2629	2.82	7.97	1451	3.67	9.35
8 / 8	-						
8 / 9	3.266	1984	1.82	6.60	1591	2.57	7.99
8 / 10	-						
8 / 11	-						
8 / 12	3.296	4090	5.92	10.73	1411	7.07	12.05
8 / 13	-						
8 / 14	3.27	4285	6.62	12.18	1245	8.09	14.16
8 / 15	-						
8 / 16	3.272	4162	6.08	10.91	1272	7.52	12.83
8 / 17	3.264	3757	4.86	9.84	1506	5.98	11.14
8 / 18	-						
8 / 19	3.266	4139	6.14	10.90	1407	7.28	12.19
8 / 20	3.268	3088	3.44	8.54	1604	4.43	9.88
8 / 21	-						
8 / 22	3.258	2961	3.30	8.33	1399	4.20	9.68
8 / 23	3.286	2698	2.77	7.82	1485	3.67	9.19
8 / 24	3.27	2831	3.08	8.1	1520	3.98	9.48
8 / 25	3.256	3701	4.87	9.91	1506	5.99	11.24
8 / 26	-						
8 / 27	-						
8 / 28	-						
8 / 29	-						
8 / 30	-						
Average	3.27	3388	4.3553846	9.3692308	1457.3077	5.42	10.804615
Standard dev.	0.011518102	730.87596	1.5660226	1.6007678	109.76671	1.767701	1.7291212
Varience	0.00013	534179.67	2.4524269	2.5624577	12048.731	3.1247667	2.9898603
Maximum	3.296	4285	6.62	12.18	1604	8.09	14.16
Minimum	3.256	1984	1.82	6.6	1245	2.57	7.99

Exp. No.	Thickness (mm)	Impact Property for ABS Lustran 250 Condition : Decrease Holding Pressure					
		Load at Peak (N)	Peak Energy (J / mm)	Displ. to Peak (mm)	Load at Break (N)	Break Energy (J / mm)	Displ. to Break (mm)
11 / 1	3.08	3125	4.07	9.96	1203	5.03	11.31
11 / 2	3.054	3001	3.71	9.05	1174	4.66	10.39
11 / 3	-						
11 / 4	3.064	3267	4.36	10.14	1234	5.36	11.47
11 / 5	3.064	2576	2.92	8.28	1267	3.78	9.66
11 / 6	-						
11 / 7	3.066	2790	3.24	8.71	1209	4.16	10.08
11 / 8	-						
11 / 9	3.064	2965	3.58	9.00	1230	4.55	10.36
11 / 10	-						
11 / 11	3.064	4261	7.85	12.50	926	9.19	14.44
11 / 12	3.06	3218	4.20	9.57	1333	5.21	10.88
11 / 13	3.068	3918	6.28	11.24	1064	7.68	13.15
11 / 14	-						
11 / 15	-						
11 / 16	-						
11 / 17	-						
11 / 18	3.058	4181	7.35	12.08	1037	8.82	14.14
11 / 19	-						
11 / 20	3.06	2765	3.18	9.35	1169	3.97	10.55
11 / 21	3.056	3510	4.99	10.15	1158	6.00	11.4
11 / 22	3.062	3066	3.89	9.28	1188	4.79	10.55
11 / 23	3.054	2627	3.00	8.27	1161	3.79	9.55
11 / 24	3.062	2204	2.24	7.37	1217	2.97	8.65
11 / 25							
11 / 26	-						
11 / 27	-						
11 / 28	3.06	3251	4.26	9.53	1197	5.25	10.82
11/ 29	3.058	3479	4.86	10.46	1216	6.16	12.38
11 / 30	3.066	2917	3.48	8.81	1178	4.39	10.11
Average	3.062222222	3173.3889	4.3033333	9.6527778	1175.6111	5.32	11.105
Standard dev.	0.006015231	544.36992	1.5069642	1.3149986	90.703874	1.7088799	1.5490272
Varience	0.00004	296338.6	2.2709412	1.7292212	8227.1928	2.9202706	2.3994853
Maximum	3.08	4261	7.85	12.5	1333	9.19	14.44
Minimum	3.054	2204	2.24	7.37	926	2.97	8.65

Exp. No.	Thickness (mm)	Impact Property for ABS Lustran 250 Condition : Increase Holding Time					
		Load at Peak (N)	Peak Energy (J / mm)	Displ. to Peak (mm)	Load at Break (N)	Break Energy (J / mm)	Displ. to Break (mm)
13 / 1	3.054	3432	4.96	10.26	1299	6.02	11.53
13 / 2	3.058	3930	6.62	11.69	1160	8.01	13.53
13 / 3	-						
13 / 4	-						
13 / 5	3.062	2651	2.98	8.28	1194	3.68	9.37
13 / 6	3.064	2621	2.91	9.02	1195	3.73	10.30
13 / 7	3.058	3462	4.80	10.06	1273	5.86	11.32
13 / 8	3.062	3428	4.79	10.06	1169	5.77	11.32
13 / 9	3.058	3119	4.03	9.42	1223	4.95	10.70
13 / 10	3.06	3198	4.09	9.31	1183	5.07	10.59
13 / 11	3.06	2556	2.80	8.04	1261	3.62	9.33
13 / 12	3.062	3156	4.12	9.36	1219	5.06	10.64
13 / 13	3.058	2385	2.60	7.82	1389	3.39	9.11
13 / 14	-						
13 / 15	3.058	3067	3.89	9.22	1287	4.74	10.37
13 / 16	3.064	4176	7.56	12.20	378	9.86	17.20
13 / 17	3.066	3349	4.49	9.73	1374	5.55	11.02
13 / 18	-						
13 / 19	3.06	2851	3.39	8.78	1214	4.26	10.05
13 / 20	3.056	2797	3.31	8.53	1323	4.19	9.81
13 / 21	-						
13 / 22	3.06	2541	2.84	7.94	1281	3.50	8.99
13 / 23	3.06	3476	4.94	10.02	1275	5.78	11.05
13 / 24	3.06	2960	3.54	8.89	1236	4.31	9.94
13 / 25	3.064	3031	3.72	9.11	1185	4.47	10.16
13 / 26	3.066	3160	4.02	10.1	1214	4.98	11.38
13 / 27	3.06	2731	3.16	8.31	1189	3.99	9.59
13 / 28	-						
13/ 29	-						
13 / 30	-						
Average	3.060454545	3094.4091	4.0709091	9.3704545	1205.5	5.0359091	10.786364
Standard dev.	0.003081856	451.50665	1.2265046	1.1180658	195.25143	1.5290322	1.7584938
Varience	0.00001	203858.25	1.5043134	1.2500712	38123.119	2.3379396	3.0923004
Maximum	3.066	4176	7.56	12.2	1389	9.86	17.2
Minimum	3.054	2385	2.6	7.82	378	3.39	8.99

Exp. No.	Thickness (mm)	Impact Property for ABS Lustran 250 Condition : Increase Holding Time					
		Load at Peak (N)	Peak Energy (J / mm)	Displ. to Peak (mm)	Load at Break (N)	Break Energy (J / mm)	Displ. to Break (mm)
15 / 1	3.06	3887	7.11	13.17	1278	8.57	14.97
15 / 2	3.062	3147	4.11	9.52	1299	5.08	10.77
15 / 3	3.064	3976	6.85	11.90	1034	8.22	13.71
15 / 4	3.064	3436	4.91	10.79	1115	5.89	12.03
15 / 5	3.06	3431	4.91	10.20	1154	5.88	11.44
15 / 6	-	-	-	-	-	-	-
15 / 7	3.068	4433	8.95	13.29	603	10.27	15.00
15 / 8	3.066	2109	2.18	7.34	952	2.79	8.57
15 / 9	3.066	3232	4.24	10.19	1230	5.17	11.41
15 / 10	3.068	3332	4.45	9.97	1286	5.44	11.19
15 / 11	-	-	-	-	-	-	-
15 / 12	3.07	2246	2.34	7.51	1228	3.04	8.74
15 / 13	-	-	-	-	-	-	-
15 / 14	3.066	2060	2.14	7.18	1242	2.79	8.42
15 / 15	3.068	2991	3.78	9.17	1185	4.64	10.41
15 / 16	-	-	-	-	-	-	-
15 / 17	3.064	1580	1.85	6.82	1265	2.51	8.12
15 / 18	3.058	2732	3.14	8.53	1298	4.05	9.83
15 / 19	-	-	-	-	-	-	-
15 / 20	3.062	2646	3.07	8.49	1224	3.89	9.78
15 / 21	3.058	4034	7.70	12.43	0	9.24	16.39
15 / 22	3.06	3037	3.78	9.13	1290	4.76	10.42
15 / 23	-	-	-	-	-	-	-
15 / 24	-	-	-	-	-	-	-
15 / 25	3.064	2131	2.18	7.22	1224	2.91	8.52
15 / 26	3.068	4024	7.3	12.38	1096	8.70	14.25
15 / 27	3.072	2978	3.69	9.18	1391	4.66	10.48
15 / 28	3.068	2910	3.71	9.20	1149	4.59	10.51
15/ 29	3.058	3571	5.55	10.89	1177	6.88	12.8
15 / 30	-	-	-	-	-	-	-
Average	3.064272727	3087.4091	4.4518182	9.75	1123.6364	5.4531818	11.261818
Stand dev.	0.004107853	751.34056	2.0243862	1.9840915	298.16751	2.2902368	2.3717497
Varience	0.00002	564512.63	4.0981394	3.936619	88903.861	5.2451846	5.6251965
Maximum	3.072	4433	8.95	13.29	1391	10.27	16.39
Minimum	3.058	1580	1.85	6.82	0	2.51	8.12

Exp. No.	Thickness (mm)	Impact Property for ABS Lustran 250 Condition : Increase Melt Temperature					
		Load at Peak (N)	Peak Energy (J/mm)	Displ. to Peak (mm)	Load at Break (N)	Break Energy (J/mm)	Displ. to Break (mm)
19 / 1	-	-	-	-	-	-	-
19 / 2	3.072	1442	2.18	8.52	946	3.19	11.16
19 / 3	3.054	1563	2.61	9.57	1331	3.24	10.89
19 / 4	3.058	1515	2.26	8.78	1348	2.87	10.1
19 / 5	-	-	-	-	-	-	-
19 / 6	3.056	1382	3.71	13.19	898	4.72	15.73
19 / 7	3.07	1922	4.75	13.26	173	6.96	22.81
19 / 8	3.064	1864	3.55	11.95	437	4.66	15.77
19 / 9	-	-	-	-	-	-	-
19 / 10	3.074	1718	2.81	9.47	1466	3.47	10.75
19 / 11	3.098	1254	1.78	7.82	961	2.48	9.74
19 / 12	3.104	1441	2.30	10.53	488	3.81	13.74
19 / 13	3.114	2054	4.95	13.18	262	5.93	16.34
19 / 14	3.136	1467	3.81	12.23	94	5.39	17.37
19 / 15	3.116	1467	3.09	10.81	954	3.81	12.73
19 / 16	3.096	1220	1.88	8.00	969	2.33	9.29
19 / 17	3.176	1428	3.34	11.50	82	5.58	19.22
19 / 18	3.104	1964	5.19	13.79	0	6.41	16.98
19 / 19	-	-	-	-	-	-	-
19 / 20	3.11	1464	2.06	8.17	986	2.80	10.12
19 / 21	3.104	1442	1.95	7.91	1216	2.50	9.2
19 / 22	3.082	1934	4.10	11.66	57	5.33	18.77
19 / 23	3.07	1503	2.21	8.55	1270	2.79	9.85
19 / 24	3.07	1839	3.68	11.29	38	6.02	17.79
19 / 25	3.086	1961	3.82	11.56	186	6.18	18.67
19 / 26	3.078	1860	3.60	10.90	420	4.63	14.13
19 / 27	3.068	1451	3.55	11.46	26	6.08	20.52
19 / 28	-	-	-	-	-	-	-
19/ 29	3.144	1835	4.15	12.19	0	5.69	16.85
19 / 30	3.088	1827	3.53	11.04	1286	4.09	12.14
Average	3.09168	1632.68	3.2344	10.6932	635.76	4.4384	14.4264
Stand dev.	0.029819904	248.58595	0.9944809	1.866576	523.77351	1.4459503	4.0105713
Varience	0.00089	61794.977	0.9889923	3.484106	274338.69	2.0907723	16.084682
Maximum	3.176	2054	5.19	13.79	1466	6.96	22.81
Minimum	3.054	1220	1.78	7.82	0	2.33	9.2

Exp. No.	Thickness (mm)	Impact Property for ABS Lustran 250 Condition : Decrease Melt Temperature					
		Load at Peak (N)	Peak Energy (J / mm)	Displ. to Peak (mm)	Load at Break (N)	Break Energy (J / mm)	Displ. to Break (mm)
21 / 1	3.06	3225	4.23	9.42	1121	5.17	10.67
21 / 2	-	-	-	-	-	-	-
21 / 3	3.058	3668	5.44	10.55	1574	6.50	11.69
21 / 4	3.066	3121	3.93	9.17	1099	4.84	10.42
21 / 5	-	-	-	-	-	-	-
21 / 6	3.066	2828	3.36	8.55	1225	4.21	9.81
21 / 7	3.068	4610	10.27	14.03	0	13.02	16.40
21 / 8	-	-	-	-	-	-	-
21 / 9	-	-	-	-	-	-	-
21 / 10	3.07	2137	2.16	6.49	1196	2.84	7.79
21 / 11	3.062	2860	2.82	7.07	1155	3.57	8.16
21 / 12	3.06	4242	6.03	10.37	1050	6.38	10.8
21 / 13	-	-	-	-	-	-	-
21/ 14	3.064	4491	6.18	10.41	904	6.66	10.74
21 / 15	3.062	4235	4.68	9.28	558	4.80	9.42
21 / 16	3.058	4588	3.38	5.07	598	3.75	5.39
21 / 17	3.064	4584	2.84	5.85	868	2.99	5.99
21 / 18	3.058	2479	0.76	2.68	1180	0.86	2.84
21 / 19	3.062	2677	1.17	3.59	1144	1.45	4.01
21 / 20	3.064	3333	1.76	4.53	1124	2.09	4.96
21 / 21	3.066	4140	2.99	4.83	0	3.50	5.58
21 / 22	-	-	-	-	-	-	-
21 / 23	-	-	-	-	-	-	-
21 / 24	3.046	3962	6.61	11.44	900	7.52	12.51
21 / 25	3.054	3613	5.13	10.23	1010	6.24	11.88
21 / 26	-	-	-	-	-	-	-
21 / 27	3.06	4085	7.43	12.02	1254	8.75	13.58
21 / 28	3.06	3107	3.92	9.65	1010	4.73	10.82
21/ 29	3.076	2994	3.75	9.10	1424	4.61	10.27
21 / 30	3.066	4111	7.32	11.95	772	8.44	13.53
Average	3.062272727	3595	4.3709091	8.4672727	962.09091	5.1327273	9.4209091
Stand dev.	0.005993503	754.07357	2.2903564	3.0355484	390.14428	2.7459393	3.4652464
Varience	0.00004	568626.95	5.2457325	9.2145541	152212.56	7.5401827	12.007932
Maximum	3.076	4610	10.27	14.03	1574	13.02	16.4
Minimum	3.046	2137	0.76	2.68	0	0.86	2.84

Exp. No.	Thickness (mm)	Impact Property for ABS Lustran 440 Condition : Standard condition					
		Load at Peak (N)	Peak Energy (J / mm)	Displ. to Peak (mm)	Load at Break (N)	Break Energy (J / mm)	Displ. to Break (mm)
22 / 1	3.076	3992	7.10	11.97	322	12.23	20.88
22 / 2	3.076	2130	4.05	10.09	0	6.27	15.85
22 / 3	3.068	4508	10.88	15.35	0	16.81	20.35
22 / 4	3.068	4522	10.91	14.12	0	15.91	18.47
22 / 5	3.072	4528	10.83	14.22	54	16.18	18.76
22 / 6	3.064	4154	7.79	12.94	602	13.89	23.75
22 / 7	3.07	4519	10.63	14.99	0	15.98	19.48
22 / 8	3.072	4527	10.74	15.1	0	17.26	20.49
22 / 9	3.072	4547	10.61	14.69	304	14.9	18.31
22 / 10	3.066	4571	10.61	14.97	0	17.49	20.25
22 / 11	3.066	4502	10.57	14.13	0	17.87	20.22
22 / 12	-	-	-	-	-	-	-
22 / 13	3.068	3827	6.49	11.43	583	12.14	20.48
22/ 14	-	-	-	-	-	-	-
22 / 15	3.068	4507	10.73	14.39	0	16.41	19.18
22 / 16	3.06	4549	10.89	14.35	38	15.03	18.01
22 / 17	3.062	4569	10.8	14.30	0	16.59	19.06
22 / 18	3.066	3678	5.63	12.25	1547	6.93	13.84
22 / 19	-	-	-	-	-	-	-
22 / 20	3.064	4564	10.74	14.42	100	15.26	18.55
22 / 21	3.074	4555	10.83	14.30	0	16.84	19.28
22 / 22	3.07	4533	10.72	14.35	150	15.95	18.81
22 / 23	3.07	4041	6.99	11.67	481	12.72	21.93
22 / 24	3.074	4482	10.16	14.00	293	13.26	17.11
22 / 25	3.068	4508	10.78	15.27	0	16.23	19.93
22 / 26	-	-	-	-	-	-	-
22 / 27	-	-	-	-	-	-	-
22 / 28	3.072	4499	10.43	14.89	504	14.24	18.34
22/ 29	3.076	4470	10.68	15.07	0	15.22	19.08
22 / 30	-	-	-	-	-	-	-
Average	3.06925	4303.4167	9.6079167	13.885833	207.41667	14.650417	19.18375
Stand dev.	0.004406024	528.85766	2.0301038	1.4007573	353.07148	2.9542798	1.9444521
Varience	0.00002	279690.43	4.1213216	1.962121	124659.47	8.7277694	3.780894
Maximum	3.076	4571	10.91	15.35	1547	17.87	23.75
Minimum	3.06	2130	4.05	10.09	0	6.27	13.84

Exp. No.	Thickness (mm)	Impact Property for ABS Lustran 440 Condition : Increase Injection Speed					
		Load at Peak (N)	Peak Energy (J / mm)	Displ. to Peak (mm)	Load at Break (N)	Break Energy (J / mm)	Displ. to Break (mm)
25 / 1	3.208	4851	10.07	13.51	1244	14.01	17.10
25 / 2	3.244	4799	10.92	14.31	0	17.55	19.97
25 / 3	-	-	-	-	-	-	-
25 / 4	3.214	4897	11.04	14.82	162	16.90	19.66
25 / 5	3.244	4953	11.01	14.15	222	15.74	18.00
25 / 6	-	-	-	-	-	-	-
25 / 7	-	-	-	-	-	-	-
25 / 8	3.234	4860	10.50	13.92	765	19.85	19.88
25 / 9	-	-	-	-	-	-	-
25 / 10	3.216	4127	6.42	11.10	1382	7.74	12.67
25 / 11	-	-	-	-	-	-	-
25 / 12	3.212	4851	10.93	14.14	414	15.46	18.12
25 / 13	3.214	48.4	10.30	13.69	645	14.28	19.79
25/ 14	3.216	4506	8.02	12.34	1055	12.49	16.94
25 / 15	3.222	4869	10.67	14.00	232	15.20	18.06
25 / 16	-	-	-	-	-	-	-
25 / 17	3.212	4756	10.27	13.64	502	14.27	16.97
25 / 18	3.226	4806	10.27	13.75	754	13.46	18.37
25 / 19	3.226	4848	10.94	13.98	0	16.06	18.07
25 / 20	3.218	4918	10.99	14.28	0	16.97	18.97
25 / 21	3.23	4872	10.28	13.51	0	13.99	16.79
25 / 22	3.228	4914	11.00	14.16	0	16.65	18.65
25 / 23	3.232	4874	10.84	14.39	119	15.55	18.31
25 / 24	3.234	4916	11.07	14.27	23	15.96	18.44
25 / 25	3.234	4911	11.01	14.28	0	17.24	19.26
25 / 26	3.236	4038	6.00	12.57	1690	7.26	14.09
25 / 27	3.224	4911	10.96	14.19	777	15.71	18.43
25 / 28	3.224	4624	9.12	12.9	277	13.28	22.22
25/ 29	3.23	4855	10.93	15.10	512	16.48	19.64
25 / 30	3.22	3674	5.15	10.01	1758	6.40	11.60
Average	3.224916667	4528.2667	9.94625	13.625417	522.20833	14.520833	17.916667
Stand dev.	0.010025692	1007.6617	1.7360145	1.1461162	553.72737	3.2760248	2.3443487
Varience	0.00010	1015382.1	3.0137462	1.3135824	306614	10.732338	5.495971
Maximum	3.244	4953	11.07	15.1	1758	19.85	22.22
Minimum	3.208	48.4	5.15	10.01	0	6.4	11.6

Exp. No.	Thickness (mm)	Impact Property for ABS Lustran 440 Condition : Decrease Injection Speed					
		Load at Peak (N)	Peak Energy (J / mm)	Displ. to Peak (mm)	Load at Break (N)	Break Energy (J / mm)	Displ. to Break (mm)
27 / 1	3.082	4584	10.82	14.50	0	15.91	18.71
27 / 2	3.064	4549	10.60	14.06	1053	16.20	19.18
27 / 3	3.068	3912	6.32	12.08	1194	10.82	16.80
27 / 4	3.064	4478	9.97	13.90	1104	13.08	16.85
27 / 5	3.076	4555	10.62	14.25	1218	14.57	14.46
27 / 6	3.062	4559	10.77	14.30	268	15.31	18.27
27 / 7	3.07	4525	10.75	14.41	48	16.14	18.83
27 / 8	3.064	4430	9.75	14.61	626	13.54	19.98
27 / 9	-	-	-	-	-	-	-
27 / 10	3.062	4523	10.82	14.07	578	14.72	17.45
27 / 11	3.066	2779	3.17	8.49	1524	4.01	9.62
27 / 12	3.072	4535	10.87	14.84	325	15.17	18.51
27 / 13	3.076	4474	10.04	13.98	937	13.36	16.79
27/ 14	3.068	4104	7.42	12.13	493	13.38	22.80
27 / 15	3.074	4509	10.59	14.26	0	16.33	18.99
27 / 16	3.078	3452	4.72	11.16	1272	5.58	12.23
27 / 17	3.084	4469	9.85	13.60	898	12.23	15.73
27 / 18	-	-	-	-	-	-	-
27 / 19	3.076	4525	10.26	14.09	749	14.49	19.86
27 / 20	3.07	4418	9.44	13.30	1044	12.09	15.89
27 / 21	3.064	4531	10.29	14.66	445	14.80	23.26
27 / 22	3.068	4550	10.71	14.89	1145	17.27	20.14
27 / 23	-	-	-	-	-	-	-
27 / 24	-	-	-	-	-	-	-
27 / 25	3.064	4521	10.53	14.08	937	15.25	18.03
27 / 26	3.07	4418	8.72	12.86	547	13.91	21.21
27 / 27	3.07	4545	10.53	14.13	0	16.61	19.07
27 / 28	3.056	3968	6.82	11.67	971	11.01	16.62
27/ 29	3.064	4444	10.29	13.88	943	13.96	17.28
27 / 30	3.06	4453	10.61	14.19	237	15.53	18.34
Average	3.068923077	4338.8462	9.4338462	13.553462	713.69231	13.664231	17.880769
Stand dev.	0.006840603	410.91524	2.0451662	1.4261499	446.88386	3.0995086	2.9008094
Varience	0.00005	168851.34	4.1827046	2.0339035	199705.18	9.6069534	8.4146954
Maximum	3.084	4584	10.87	14.89	1524	17.27	23.26
Minimum	3.056	2779	3.17	8.49	0	4.01	9.62

Exp. No.	Thickness (mm)	Impact Property for ABS Lustran 440 Condition : Increase Holding Pressure					
		Load at Peak (N)	Peak Energy (J / mm)	Displ. to Peak (mm)	Load at Break (N)	Break Energy (J / mm)	Displ. to Break (mm)
29 / 1	3.22	4702	10.66	14.34	153	16.49	19.26
29 / 2	3.222	4874	10.99	15.24	0	17.05	20.13
29 / 3	3.218	48.34	10.72	14.55	924	15.09	18.45
29 / 4	-	-	-	-	-	-	-
29 / 5	3.224	3448	4.80	9.77	18.26	5.71	10.83
29 / 6	3.22	4937	11.04	14.08	347	14.77	17.34
29 / 7	3.22	4923	11.23	14.15	0	17.10	18.81
29 / 8	3.216	4612	8.57	12.54	603	14.42	20.91
29 / 9	-	-	-	-	-	-	-
29 / 10	3.22	4939	11.16	14.30	0	16.06	18.14
29 / 11	3.224	4920	11.29	14.36	0	15.32	17.80
29 / 12	3.228	4962	11.36	14.19	0	17.69	19.10
29 / 13	3.226	4836	10.84	15.89	524	14.97	19.27
29/ 14	3.23	4932	11.20	14.26	0	16.9	18.73
29 / 15	3.222	3612	4.68	10.08	1933	5.66	11.17
29 / 16	-	-	-	-	-	-	-
29 / 17	3.248	4776	9.57	13.24	718	12.83	17.03
29 / 18	3.222	4647	9.17	12.94	442	13.71	19.34
29 / 19	3.232	4824	10.60	13.77	929	16.07	18.81
29 / 20	3.232	4498	8.35	12.50	1688	9.75	13.91
29 / 21	3.222	4846	10.51	14.64	833	15.06	18.66
29 / 22	-	-	-	-	-	-	-
29 / 23	3.234	2549	5.26	11.72	0	7.57	18.60
29 / 24	3.236	4889	10.68	14.50	816	14.49	17.87
29 / 25	3.226	4624	8.88	12.83	1117	11.63	15.42
29 / 26	-	-	-	-	-	-	-
29 / 27	3.22	4919	11.46	14.44	0	16.79	18.77
29 / 28	3.228	3968	6.82	11.67	971	11.01	16.62
29/ 29	3.064	4444	10.29	13.88	943	13.96	17.28
29 / 30	3.06	4453	10.61	14.19	237	15.53	18.34
Average	3.21256	4367.2936	9.6296	13.5228	527.8504	13.8252	17.6236
Standard dev.	0.045845829	1069.9877	2.1074461	1.478765	552.49119	3.4443881	2.4540695
Varience	0.00210	1144873.6	4.441329	2.186746	305246.51	11.863809	6.0224573
Maximum	3.248	4962	11.46	15.89	1933	17.69	20.91
Minimum	3.06	48.34	4.68	9.77	0	5.66	10.83

Exp. No.	Thickness (mm)	Impact Property for ABS Lustran 440 Condition : Decrease Holding Pressure					
		Load at Peak (N)	Peak Energy (J / mm)	Displ. to Peak (mm)	Load at Break (N)	Break Energy (J / mm)	Displ. to Break (mm)
32 / 1	-	-	-	-	-	-	-
32 / 2	3.066	4602	10.78	14.99	0	17.03	19.96
32 / 3	3.066	4566	10.72	14.32	377	16.93	19.39
32 / 4	3.058	4551	11.12	14.50	0	16.95	19.32
32 / 5	-	-	-	-	-	-	-
32 / 6	3.054	4535	10.78	14.20	204	16.03	18.79
32 / 7	-	-	-	-	-	-	-
32 / 8	3.066	4597	10.96	14.30	0	16.53	18.82
32 / 9	3.058	4610	11.05	14.29	41	15.80	18.41
32 / 10	3.056	4200	7.91	12.28	256	10.94	17.00
32 / 11	3.068	4590	10.98	14.35	0	16.31	18.71
32 / 12	3.064	4606	11.15	14.38	198	14.85	17.67
32 / 13	-	-	-	-	-	-	-
32 / 14	3.068	4623	10.84	14.24	72	14.56	17.59
32 / 15	3.068	4205	7.76	12.32	482	13.25	21.22
32 / 16	3.06	4537	11.06	14.40	277	15.43	18.36
32 / 17	3.066	4566	10.26	13.73	884	14.68	17.91
32 / 18	3.074	3646	5.35	11.47	1481	6.56	13.03
32 / 19	-	-	-	-	-	-	-
32 / 20	3.084	4574	11.03	14.46	0	16.01	18.59
32 / 21	3.07	4590	10.75	13.90	0	16.31	18.47
32 / 22	-	-	-	-	-	-	-
32 / 23	-	-	-	-	-	-	-
32 / 24	3.062	4585	10.44	14.06	293	15.17	18.31
32 / 25	-	-	-	-	-	-	-
32 / 26	3.06	4534	10.92	15.05	325	15.88	19.14
32 / 27	3.064	4545	10.70	14.66	422	14.27	17.96
32 / 28	-	-	-	-	-	-	-
32/ 29	3.06	4557	10.35	15.21	639	14.71	18.92
32 / 30	-	-	-	-	-	-	-
Average	3.0646	4490.95	10.2455	14.0555	297.55	14.91	18.3785
Standard dev.	0.006808663	230.81309	1.4915921	0.9583839	368.9515	2.4353083	1.5545562
Varience	0.00005	53274.682	2.2248471	0.9184997	136125.21	5.9307263	2.416645
Maximum	3.084	4623	11.15	15.21	1481	17.03	21.22
Minimum	3.054	3646	5.35	11.47	0	6.56	13.03

Exp. No.	Thickness (mm)	Impact Property for ABS Lustran 440 Condition : Increase Holding Time					
		Load at Peak (N)	Peak Energy (J / mm)	Displ. to Peak (mm)	Load at Break (N)	Break Energy (J / mm)	Displ. to Break (mm)
33 / 1	3.06	2419	2.74	7.74	1561	3.49	8.89
33 / 2	3.062	4484	10.92	14.36	0	17.01	19.49
33 / 3	3.058	4506	9.81	13.42	842	13.87	17.66
33 / 4	3.06	4609	11.11	14.29	0	17.21	19.17
33 / 5	-	-	-	-	-	-	-
33 / 6	3.062	4614	11.22	14.49	0	16.90	19.02
33 / 7	-	-	-	-	-	-	-
33 / 8	3.06	3990	6.54	13.12	1546	7.9	14.60
33 / 9	3.062	4597	11.18	14.46	238	16.70	19.21
33 / 10	3.062	4611	11.28	14.52	0	17.52	19.59
33 / 11	3.064	4591	10.19	14.83	15	15.48	19.62
33 / 12	3.056	4612	10.78	14.34	0	15.23	18.05
33 / 13	3.06	2783	3.25	9.74	1813	4.12	10.88
33 / 14	3.06	4609	10.32	14.79	0	17.54	20.58
33 / 15	3.064	4613	10.83	15.06	0	17.11	20.05
33 / 16	3.06	4135	7.74	12.15	297	9.79	16.14
33 / 17	-	-	-	-	-	-	-
33 / 18	-	-	-	-	-	-	-
33 / 19	3.06	4008	6.91	11.70	505	13.12	20.55
33 / 20	3.062	4574	10.91	14.30	819	14.56	17.23
33 / 21	3.06	4470	9.63	13.31	457	14.62	20.33
33 / 22	3.06	4551	9.88	13.27	603	13.99	18.51
33 / 23	3.06	4617	11.08	14.42	0	16.45	18.68
33 / 24	3.058	3621	5.82	10.66	425	11.60	21.02
33 / 25	-	-	-	-	-	-	-
33 / 26	3.058	3980	6.49	11.06	1883	9.17	13.90
33 / 27	3.054	4591	11.12	15.67	0	16.99	20.41
33 / 28	-	-	-	-	-	-	-
33/ 29	-	-	-	-	-	-	-
33 / 30	-	-	-	-	-	-	-
Average	3.060090909	4253.8636	9.0795455	13.259091	500.18182	13.653182	17.89
Stand dev.	0.002348436	607.39775	2.6504312	1.9812596	643.22126	4.2496211	3.2045221
Varience	0.00001	368932.03	7.0247855	3.9253896	413733.58	18.05928	10.268962
Maximum	3.064	4617	11.28	15.67	1883	17.54	21.02
Minimum	3.054	2419	2.74	7.74	0	3.49	8.89

Exp. No.	Thickness (mm)	Impact Property for ABS Lustran 440 Condition : Decrease Holding Time					
		Load at Peak (N)	Peak Energy (J / mm)	Displ. to Peak (mm)	Load at Break (N)	Break Energy (J / mm)	Displ. to Break (mm)
34 / 1	-	-	-	-	-	-	-
34 / 2	3.068	4316	8.49	12.86	414	13.19	22.19
34 / 3	3.068	4613	11.06	14.31	0	17.51	19.46
34 / 4	-	-	-	-	-	-	-
34 / 5	3.058	4662	10.93	14.13	0	15.04	17.56
34 / 6	3.058	3995	6.43	11.10	1329	7.70	12.54
34 / 7	3.068	4640	11.10	14.29	0	16.16	18.34
34 / 8	3.064	3505	5.16	10.64	1453	6.32	12.16
34 / 9	-	-	-	-	-	-	-
34 / 10	3.058	4626	10.49	14.39	372	13.91	17.42
34 / 11	3.054	3688	5.66	11.14	1607	6.89	12.65
34 / 12	-	-	-	-	-	-	-
34 / 13	3.056	4586	10.89	14.25	612	15.26	18.19
34 / 14	-	-	-	-	-	-	-
34 / 15	-	-	-	-	-	-	-
34 / 16	-	-	-	-	-	-	-
34 / 17	3.058	4639	11.19	16.15	0	16.58	20.46
34 / 18	3.052	4610	11.23	14.56	0	16.88	19.05
34 / 19	3.062	4607	11.03	14.37	0	16.61	18.93
34 / 20	3.064	4582	11.08	15.03	0	15.93	18.99
34 / 21	-	-	-	-	-	-	-
34 / 22	3.068	4552	10.65	15.00	0	15.22	18.79
34 / 23	3.072	4567	10.50	13.92	0	13.33	16.62
34 / 24	-	-	-	-	-	-	-
34 / 25	3.068	4538	10.89	14.67	0	16.83	19.51
34 / 26	3.072	4605	10.83	14.23	0	16.33	18.63
34 / 27	-	-	-	-	-	-	-
34 / 28	3.07	4608	10.88	14.44	0	15.71	18.32
34/ 29	-	-	-	-	-	-	-
34 / 30	3.07	4600	10.92	14.84	408	14.32	17.81
Average	3.063578947	4449.4211	9.9689474	13.911579	326.05263	14.195789	17.769474
Stand dev.	0.006379793	338.49738	1.9780627	1.4526461	542.15573	3.4375756	2.648296
Varience	0.00004	114580.48	3.9127322	2.1101807	293932.83	11.816926	7.0134719
Maximum	3.072	4662	11.23	16.15	1607	17.51	22.19
Minimum	3.052	3505	5.16	10.64	0	6.32	12.16

Exp. No.	Thickness (mm)	Impact Property for ABS Lustran 440 Condition : Increase Melt Temperature					
		Load at Peak (N)	Peak Energy (J / mm)	Displ. to Peak (mm)	Load at Break (N)	Break Energy (J / mm)	Displ. to Break (mm)
35 / 1	3.034	3466	4.79	9.60	1334	5.65	10.66
35 / 2	3.038	2644	3.00	8.30	1486	3.76	9.43
35 / 3	3.034	3224	4.15	10.39	1559	5.05	11.47
35 / 4	3.03	2158	5.47	12.61	46	6.95	16.96
35 / 5	-	-	-	-	-	-	-
35 / 6	-	-	-	-	-	-	-
35 / 7	3.028	2597	2.90	8.02	1574	3.70	9.16
35 / 8	-	-	-	-	-	-	-
35 / 9	-	-	-	-	-	-	-
35 / 10	-	-	-	-	-	-	-
35 / 11	3.028	2318	2.37	7.67	1565	3.14	8.85
35 / 12	-	-	-	-	-	-	-
35 / 13	3.034	2144	5.39	12.70	0	7.00	16.59
35 / 14	-	-	-	-	-	-	-
35 / 15	-	-	-	-	-	-	-
35 / 16	3.032	2128	2.12	7.09	1304	2.77	8.24
35 / 17	-	-	-	-	-	-	-
35 / 18	3.032	2720	3.09	8.46	1483	3.86	9.57
35 / 19	-	-	-	-	-	-	-
35 / 20	3.036	2964	3.57	9.01	1590	4.41	10.09
35 / 21	-	-	-	-	-	-	-
35 / 22	3.038	2270	2.35	7.57	1630	3.08	8.72
35 / 23	-	-	-	-	-	-	-
35 / 24	-	-	-	-	-	-	-
35 / 25	-	-	-	-	-	-	-
35 / 26	-	-	-	-	-	-	-
35 / 27	-	-	-	-	-	-	-
35 / 28	3.04	1942	3.35	9.46	1598	3.98	10.56
35/ 29	-	-	-	-	-	-	-
35 / 30	-	-	-	-	-	-	-
Average	3.033666667	2547.9167	3.5458333	9.24	1264.0833	4.4458333	10.858333
Stand dev.	0.003892495	477.0261	1.1608653	1.852237	588.56365	1.4326356	2.9111223
Varience	0.00002	227553.9	1.3476083	3.4307818	346407.17	2.0524447	8.4746333
Maximum	3.04	3466	5.47	12.7	1630	7	16.96
Minimum	3.028	1942	2.12	7.09	0	2.77	8.24

Exp. No.	Thickness (mm)	Impact Property for ABS Lustran 440 Condition : Decrease Melt Temperature					
		Load at Peak (N)	Peak Energy (J / mm)	Displ. to Peak (mm)	Load at Break (N)	Break Energy (J / mm)	Displ. to Break (mm)
37 / 1	3.056	4556	10.52	14.29	873	14.14	17.35
37 / 2	3.064	4375	8.40	13.38	954	11.13	16.44
37 / 3	3.072	4610	10.53	13.91	0	15.41	18.16
37 / 4	-	-	-	-	-	-	-
37 / 5	-	-	-	-	-	-	-
37 / 6	3.066	4475	10.08	13.70	279	14.31	17.44
37 / 7	3.082	4442	9.40	13.32	496	14.00	20.04
37 / 8	-	-	-	-	-	-	-
37 / 9	3.086	3857	5.74	10.56	1297	6.86	12.05
37 / 10	3.088	4540	10.59	14.53	839	15.36	18.70
37 / 11	3.074	4556	10.28	13.85	619	15.17	19.92
37 / 12	3.07	3376	4.39	9.48	1301	5.23	10.54
37 / 13	3.08	4625	10.71	14.02	54	14.96	17.92
37 / 14	3.074	4646	10.54	14.19	0	11.80	15.60
37 / 15	3.076	4343	7.76	12.10	454	12.74	19.65
37 / 16	3.076	4629	10.79	13.95	536	14.99	17.56
37 / 17	-	-	-	-	-	-	-
37 / 18	3.07	4667	10.73	13.82	124	16.09	18.33
37 / 19	3.066	4658	10.58	13.92	760	14.33	18.12
37 / 20	3.064	4674	10.79	14.13	0	15.27	18.11
37 / 21	3.06	3496	4.80	10.34	2015	6.14	11.92
37 / 22	3.07	4649	10.44	15.61	408	13.90	19.12
37 / 23	3.068	4658	10.68	14.27	110	15.29	18.33
37 / 24	3.072	4672	10.94	14.63	0	15.68	18.57
37 / 25	3.068	4613	10.89	15.47	181	15.28	19.20
37 / 26	-	-	-	-	-	-	-
37 / 27	3.068	4190	7.60	12.08	408	12.99	21.34
37 / 28	3.06	4627	10.76	14.53	302	14.67	18.08
37/ 29	3.07	4643	10.73	14.05	55	14.81	17.74
37 / 30	3.086	3012	3.52	8.76	1278	4.28	9.82
Average	3.07144	4383.56	9.2876	13.3156	533.72	12.9932	17.202
Stand dev.	0.008296987	455.66664	2.3003574	1.775256	524.06262	3.506231	2.9841372
Varience	0.00007	207632.09	5.291644	3.151534	274641.63	12.293656	8.905075
Maximum	3.088	4674	10.94	15.61	2015	16.09	21.34
Minimum	3.056	3012	3.52	8.76	0	4.28	9.82

Exp. No.	Thickness (mm)	Impact Property for ABS Lustran 640 Condition : Standard condition					
		Load at Peak (N)	Peak Energy (J / mm)	Displ. to Peak (mm)	Load at Break (N)	Break Energy (J / mm)	Displ. to Break (mm)
38 / 1	3.058	4399	10.45	14.48	0	14.52	17.87
38 / 2	3.058	4315	10.53	14.67	0	15.85	19.16
38 / 3	3.06	4218	10.27	14.63	0	15.36	19.05
38 / 4	-	-	-	-	-	-	-
38 / 5	3.06	4329	10.56	14.73	0	14.31	18.20
38 / 6	-	-	-	-	-	-	-
38 / 7	-	-	-	-	-	-	-
38 / 8	3.062	4365	10.56	14.87	0	15.58	19.08
38 / 9	-	-	-	-	-	-	-
38 / 10	-	-	-	-	-	-	-
38 / 11	3.064	4299	10.48	14.62	169	15.48	19.15
38 / 12	3.066	4317	9.77	14.40	0	12.39	17.29
38 / 13	3.066	4351	10.32	14.27	0	13.46	17.33
38 / 14	3.058	4311	10.52	14.6	0	14.37	18.15
38 / 15	3.062	4348	10.60	14.62	0	13.73	17.58
38 / 16	-	-	-	-	-	-	-
38 / 17	-	-	-	-	-	-	-
38 / 18	3.062	4368	10.78	15.54	0	15.71	19.65
38 / 19	3.064	4162	10.15	14.90	0	14.87	19.15
38 / 20	-	-	-	-	-	-	-
38 / 21	3.062	4240	10.01	14.32	729	13.14	17.39
38 / 22	-	-	-	-	-	-	-
38 / 23	3.062	4240	10.01	14.32	729	13.14	17.39
38 / 24	-	-	-	-	-	-	-
38 / 25	3.06	4196	10.07	15.31	97	14.63	19.54
38 / 26	3.064	4313	10.56	14.79	0	14.93	18.62
38 / 27	-	-	-	-	-	-	-
38 / 28	3.062	2518	3.07	8.75	1957	3.88	9.85
38/ 29	-	-	-	-	-	-	-
38 / 30	3.066	4196	9.74	14.19	569	13.88	21.41
Average	3.062	4193.6111	9.9138889	14.333889	236.11111	13.846111	18.103333
Stand dev.	0.002656845	423.68067	1.7338876	1.4358074	500.05822	2.677174	2.320616
Varience	0.00001	179505.31	3.0063663	2.0615428	250058.22	7.1672605	5.3852588
Maximum	3.066	4399	10.78	15.54	1957	15.85	21.41
Minimum	3.058	2518	3.07	8.75	0	3.88	9.85

Exp. No.	Thickness (mm)	Impact Property for ABS Lustran 640 Condition : Increase Injection Speed					
		Load at Peak (N)	Peak Energy (J / mm)	Displ. to Peak (mm)	Load at Break (N)	Break Energy (J / mm)	Displ. to Break (mm)
39 / 1	3.066	3957	7.47	12.42	201	11.09	22.37
39 / 2	3.07	4406	10.48	14.38	12	14.20	17.75
39 / 3	-	-	-	-	-	-	-
39 / 4	3.086	4240	10.20	14.30	225	15.08	18.99
39 / 5	-	-	-	-	-	-	-
39 / 6	3.082	3850	6.88	11.87	1707	8.19	13.32
39 / 7	-	-	-	-	-	-	-
39 / 8	3.08	4444	10.77	14.56	76	14.24	17.60
39 / 9	3.076	4426	10.64	15.56	0	15.59	19.72
39 / 10	3.076	4010	7.61	12.46	377	12.15	21.96
39 / 11	3.084	4354	9.94	14.09	252	12.57	16.59
39 / 12	3.076	4410	10.71	14.65	0	15.53	18.76
39 / 13	3.076	4426	10.83	14.64	0	14.31	17.80
39 / 14	-	-	-	-	-	-	-
39 / 15	3.072	4382	10.39	14.33	152	13.71	17.28
39 / 16	3.068	4405	10.57	15.06	0	15.34	19.07
39 / 17	3.074	4378	10.06	14.08	644	13.03	17.08
39 / 18	3.07	4405	10.55	14.49	0	15.74	18.84
39 / 19	3.07	4319	10.29	14.46	0	15.91	19.32
39 / 20	3.07	4379	10.37	14.48	0	14.67	18.22
39 / 21	3.068	4383	10.47	14.43	796	13.92	17.36
39 / 22	3.078	4404	10.49	14.46	0	15.20	18.45
39 / 23	-	-	-	-	-	-	-
39 / 24	3.072	4336	10.18	14.18	800	13.75	17.84
39 / 25	-	-	-	-	-	-	-
39 / 26	3.072	4109	7.91	12.69	1303	9.19	14.05
39 / 27	-	-	-	-	-	-	-
39 / 28	3.068	4286	10.27	14.47	0	15.20	18.72
39/ 29	3.068	4286	10.27	14.47	0	15.20	18.72
39 / 30	3.076	4372	10.61	15.50	0	15.67	19.83
Average	3.073826087	4302.913	9.9113043	14.175217	284.56522	13.890435	18.245217
Stand dev.	0.00549092	163.61149	1.177815	0.9361035	465.30604	2.0659985	1.996549
Varience	0.00003	26768.719	1.3872482	0.8762897	216509.71	4.2683498	3.9862079
Maximum	3.086	4444	10.83	15.56	1707	15.91	22.37
Minimum	3.066	3850	6.88	11.87	0	8.19	13.32

Exp. No.	Thickness (mm)	Impact Property for ABS Lustran 640 Condition : Decrease Injection Speed					
		Load at Peak (N)	Peak Energy (J / mm)	Displ. to Peak (mm)	Load at Break (N)	Break Energy (J / mm)	Displ. to Break (mm)
41 / 1	-	-	-	-	-	-	-
41 / 2	3.056	4305	10.54	14.67	0	15.03	18.59
41 / 3	3.064	3963	8.05	12.82	108	10.49	16.82
41 / 4	-	-	-	-	-	-	-
41 / 5	3.068	4277	10.14	14.41	338	12.96	17.24
41 / 6	3.068	4235	9.70	14.11	420	14.57	24.04
41 / 7	-	-	-	-	-	-	-
41 / 8	-	-	-	-	-	-	-
41 / 9	-	-	-	-	-	-	-
41 / 10	-	-	-	-	-	-	-
41 / 11	3.062	4319	10.59	14.62	251	14.41	18.11
41 / 12	3.066	3310	4.95	10.61	1654	6.12	12.13
41 / 13	3.066	4267	10.34	14.44	0	15.45	18.88
41 / 14	3.07	4300	10.49	14.64	0	14.81	18.39
41 / 15	3.068	4311	10.37	14.46	0	15.70	19.06
41 / 16	3.064	4271	10.06	14.27	791	13.12	17.68
41 / 17	-	-	-	-	-	-	-
41 / 18	3.062	3468	5.82	11.10	1809	8.73	14.41
41 / 19	3.056	4283	10.35	14.44	0	14.68	18.16
41 / 20	-	-	-	-	-	-	-
41 / 21	3.068	4212	10.15	14.56	0	15.25	19.06
41 / 22	3.064	4120	10.12	14.56	942	13.86	17.98
41 / 23	3.056	4212	10.33	14.63	0	15.26	19.03
41 / 24	3.056	4210	10.34	14.49	136	14.03	17.93
41 / 25	3.066	4324	10.58	14.69	0	14.41	18.13
41 / 26	3.062	4257	10.01	14.85	237	13.09	18.05
41 / 27	3.06	4346	10.60	14.74	0	14.79	18.52
41 / 28	3.072	4330	10.62	14.72	0	15.87	19.21
41/ 29	3.064	3271	4.94	10.45	558	10.64	22.51
41 / 30	-	-	-	-	-	-	-
Average	3.063714286	4123.381	9.4804762	13.918095	344.95238	13.489048	18.282381
Stand dev.	0.004786887	336.04784	1.8631062	1.4032057	537.29624	2.5080189	2.3552514
Varience	0.00002	112928.15	3.4711648	1.9689862	288687.25	6.290159	5.547209
Maximum	3.072	4346	10.62	14.85	1809	15.87	24.04
Minimum	3.056	3271	4.94	10.45	0	6.12	12.13

Exp. No.	Thickness (mm)	Impact Property for ABS Lustran 640 Condition : Increase Holding Pressure					
		Load at Peak (N)	Peak Energy (J / mm)	Displ. to Peak (mm)	Load at Break (N)	Break Energy (J / mm)	Displ. to Break (mm)
42 / 1	3.056	4216	10.16	14.38	0	15.18	18.85
42 / 2	-	-	-	-	-	-	-
42 / 3	3.056	4336	10.46	15.73	0	13.96	18.90
42 / 4	3.054	4296	10.02	14.25	552	14.17	21.00
42 / 5	3.062	4329	10.19	14.34	496	14.38	21.89
42 / 6	3.058	4350	10.53	15.16	0	14.92	18.87
42 / 7	-	-	-	-	-	-	-
42 / 8	-	-	-	-	-	-	-
42 / 9	3.058	4351	10.63	14.69	0	14.75	18.19
42 / 10	3.058	4373	10.57	14.88	82	15.46	19.13
42 / 11	3.056	3554	6.05	11.32	429	11.43	21.80
42 / 12	3.06	4266	9.69	13.95	437	13.63	20.79
42 / 13	3.064	4255	10.05	14.28	403	13.02	16.99
42 / 14	3.06	4341	10.52	14.62	0	14.87	18.36
42 / 15	-	-	-	-	-	-	-
42 / 16	3.06	4370	10.62	14.84	0	15.52	18.93
42 / 17	-	-	-	-	-	-	-
42 / 18	-	-	-	-	-	-	-
42 / 19	3.056	4333	10.51	14.77	0	15.23	18.79
42 / 20	3.06	4401	10.74	14.60	13	13.92	17.60
42 / 21	-	-	-	-	-	-	-
42 / 22	-	-	-	-	-	-	-
42 / 23	3.06	4311	10.31	14.40	415	13.59	17.46
42 / 24	3.058	4314	10.23	14.40	262	13.44	17.52
42 / 25	3.056	4336	10.34	14.41	360	13.43	17.18
42 / 26	3.056	4285	10.49	14.60	0	14.82	18.43
42 / 27	-	-	-	-	-	-	-
42 / 28	3.054	4331	10.58	14.57	0	15.15	18.50
42/ 29	-	-	-	-	-	-	-
42 / 30	3.046	4201	10.02	14.39	771	13.37	17.61
Average	3.0574	4277.45	10.1355	14.429	211	14.212	18.8395
Stand dev.	0.003733208	177.65089	0.9977421	0.8227675	248.10036	1.0181542	1.458974
Varience	0.00001	31559.839	0.9954892	0.6769463	61553.789	1.0366379	2.128605
Maximum	3.064	4401	10.74	15.73	771	15.52	21.89
Minimum	3.046	3554	6.05	11.32	0	11.43	16.99

Exp. No.	Thickness (mm)	Impact Property for ABS Lustran 640 Condition : Decrease Holding Pressure					
		Load at Peak (N)	Peak Energy (J / mm)	Displ. to Peak (mm)	Load at Break (N)	Break Energy (J / mm)	Displ. to Break (mm)
45 / 1	3.06	4056	8.44	13.35	428	11.47	19.34
45 / 2	3.056	4319	10.37	14.56	406	13.02	17.27
45 / 3	-	-	-	-	-	-	-
45 / 4	3.048	4257	10.23	15.60	479	13.54	18.49
45 / 5	3.06	4258	9.86	14.28	476	13.09	17.25
45 / 6	-	-	-	-	-	-	-
45 / 7	-	-	-	-	-	-	-
45 / 8	-	-	-	-	-	-	-
45 / 9	3.058	4370	10.60	14.54	498	14.15	17.80
45 / 10	-	-	-	-	-	-	-
45 / 11	3.064	4360	10.64	14.86	0	14.38	18.20
45 / 12	3.056	4369	10.47	14.54	0	13.22	17.25
45 / 13	3.054	2188	2.60	8.36	1977	3.36	9.49
45 / 14	3.054	4381	10.86	14.87	0	14.50	18.02
45 / 15	-	-	-	-	-	-	-
45 / 16	3.062	4324	10.60	14.68	0	13.97	17.76
45 / 17	3.062	3960	7.57	12.53	434	11.59	21.03
45 / 18	-	-	-	-	-	-	-
45 / 19	3.056	4269	10.48	14.64	116	13.94	18.03
45 / 20	3.064	4345	10.54	14.81	0	15.38	18.95
45 / 21	-	-	-	-	-	-	-
45 / 22	-	-	-	-	-	-	-
45 / 23	3.06	4347	10.69	14.82	0	15.85	19.16
45 / 24	3.064	4373	10.66	14.78	0	13.90	17.70
45 / 25	3.062	4168	8.99	13.69	279	11.51	19.60
45 / 26	3.052	3540	5.80	11.49	249	9.26	21.36
45 / 27	-	-	-	-	-	-	-
45 / 28	-	-	-	-	-	-	-
45/ 29	3.06	3560	5.98	11.43	201	10.18	22.86
45 / 30	3.056	3690	6.52	11.69	330	9.21	16.93
Average	3.058315789	4059.6842	9.0473684	13.658947	309.10526	12.395789	18.236316
Stand dev.	0.004435371	531.665	2.3156469	1.8006292	449.45336	2.8972522	2.6386512
Varience	0.00002	282667.67	5.3622205	3.2422655	202008.32	8.3940702	6.9624801
Maximum	3.064	4381	10.86	15.6	1977	15.85	22.86
Minimum	3.048	2188	2.6	8.36	0	3.36	9.49

Exp. No.	Thickness (mm)	Impact Property for ABS Lustran 640 Condition : Increase Holding Time					
		Load at Peak (N)	Peak Energy (J/mm)	Displ. to Peak (mm)	Load at Break (N)	Break Energy (J/mm)	Displ. to Break (mm)
46 / 1	3.06	4252	10.29	14.57	90	14.33	18.39
46 / 2	3.052	4344	10.63	14.72	0	15.50	18.79
46 / 3	-	-	-	-	-	-	-
46 / 4	3.06	4243	9.48	13.92	468	12.50	17.01
46 / 5	-	-	-	-	-	-	-
46 / 6	3.056	2419	3.16	8.68	2067	4.36	10.30
46 / 7	3.06	4331	10.43	14.82	0	15.67	19.25
46 / 8	-	-	-	-	-	-	-
46 / 9	3.058	4314	10.40	14.45	0	15.00	18.45
46 / 10	3.064	3760	6.98	12.18	229	11.49	22.76
46 / 11	3.06	4265	10.45	14.60	0	14.13	17.97
46 / 12	3.058	3368	5.58	11.06	1982	7.68	13.52
46 / 13	3.06	2252	2.78	8.25	2030	3.57	9.38
46 / 14	3.06	4339	10.46	14.60	0	14.95	18.42
46 / 15	3.06	4331	10.54	14.70	0	16.39	19.70
46 / 16	-	-	-	-	-	-	-
46 / 17	-	-	-	-	-	-	-
46 / 18	-	-	-	-	-	-	-
46 / 19	3.064	3994	7.58	12.90	0	8.59	14.33
46 / 20	-	-	-	-	-	-	-
46 / 21	3.062	4336	10.17	14.47	372	13.29	17.65
46 / 22	3.06	3709	6.49	11.81	397	11.59	21.71
46 / 23	3.062	3211	4.98	10.54	1958	7.49	13.43
46 / 24	3.058	4327	10.47	14.55	0	14.42	17.94
46 / 25	-	-	-	-	-	-	-
46 / 26	3.064	4317	10.17	14.45	473	14.69	18.59
46 / 27	3.062	3499	5.69	11.05	1851	6.96	12.50
46 / 28	3.062	4333	10.53	16.19	116	14.35	19.67
46/ 29	3.062	4336	10.48	15.42	0	14.28	18.78
46 / 30	3.054	4279	9.86	15.34	408	12.46	18.09
Average	3.059909091	3934.5	8.5272727	13.330455	565.5	11.985909	17.119545
Stand dev.	0.003053633	626.46535	2.622422	2.2082885	802.54059	3.8078173	3.4372199
Varience	0.00001	392458.83	6.877097	4.8765379	644071.4	14.499473	11.814481
Maximum	3.064	4344	10.63	16.19	2067	16.39	22.76
Minimum	3.052	2252	2.78	8.25	0	3.57	9.38

Exp. No.	Thickness (mm)	Impact Property for ABS Lustran 640 Condition : Decrease Holding Time					
		Load at Peak (N)	Peak Energy (J/mm)	Displ. to Peak (mm)	Load at Break (N)	Break Energy (J/mm)	Displ. to Break (mm)
48 / 1	3.06	4275	10.36	15.00	0	14.84	18.90
48 / 2	3.066	3830	7.14	12.29	448	11.77	21.37
48 / 3	3.068	4280	10.31	14.68	0	13.59	17.70
48 / 4	3.052	4032	8.47	13.89	526	12.95	22.34
48 / 5	3.058	2609	3.16	8.83	1837	3.98	9.94
48 / 6	3.064	4320	10.43	15.81	0	14.52	19.49
48 / 7	3.072	4246	10.34	14.63	0	15.17	18.88
48 / 8	3.068	4303	9.96	15.94	270	12.26	18.44
48 / 9	3.076	4327	10.43	14.71	40	14.47	18.40
48 / 10	3.084	4303	9.96	15.94	270	12.26	18.44
48 / 11	3.066	4355	10.51	14.74	0	13.95	17.95
48 / 12	3.068	4134	10.16	14.58	145	14.62	18.66
48 / 13	3.068	2038	3.94	10.48	243	7.12	19.18
48 / 14	3.058	4255	9.87	14.30	532	14.21	20.44
48 / 15	3.068	4171	9.24	13.87	339	11.68	17.27
48 / 16	3.07	3453	5.65	11.14	1798	6.86	12.57
48 / 17	3.056	4277	10.46	14.73	0	15.30	18.86
48 / 18	-	-	-	-	-	-	-
48 / 19	-	-	-	-	-	-	-
48 / 20	3.072	4265	9.92	14.37	482	13.13	19.06
48 / 21	3.052	4332	10.64	15.79	0	14.46	19.08
48 / 22	3.06	4372	10.55	14.70	0	13.08	17.13
48 / 23	3.048	4346	10.64	14.77	38	13.25	17.39
48 / 24	3.052	4304	10.45	15.01	1235	13.08	17.34
48 / 25	3.056	4352	10.77	14.75	0	15.3	18.55
48 / 26	3.054	3888	7.31	12.44	318	10.41	17.76
48 / 27	-	-	-	-	-	-	-
48 / 28	3.056	4330	10.46	14.77	0	14.67	18.43
48 / 29	-	-	-	-	-	-	-
48 / 30	3.072	4224	10.14	14.67	48	12.82	17.43
Average	3.063230769	4062.3462	9.2796154	14.108846	329.57692	12.682692	18.115385
Stand dev.	0.008783201	557.18392	2.1038659	1.7216209	519.55552	2.7971965	2.3876151
Varience	0.00008	310453.92	4.4262518	2.9639786	269937.93	7.8243085	5.7007058
Maximum	3.084	4372	10.77	15.94	1837	15.3	22.34
Minimum	3.048	2038	3.16	8.83	0	3.98	9.94

Exp. No.	Thickness (mm)	Impact Property for ABS Lustran 640 Condition : Increase Melt Temperature					
		Load at Peak (N)	Peak Energy (J / mm)	Displ. to Peak (mm)	Load at Break (N)	Break Energy (J / mm)	Displ. to Break (mm)
51 / 1	3.028	1954	4.96	12.25	248	7.17	19.46
51 / 2	3.02	3658	6.36	11.84	1285	7.46	13.32
51 / 3	3.03	3090	4.45	10.20	1766	5.65	11.78
51 / 4	3.03	3465	5.58	11.27	1344	6.73	12.79
51 / 5	3.036	4316	10.95	15.10	0	15.30	18.82
51 / 6	3.046	3950	7.67	12.81	1247	9.47	14.65
51 / 7	-	-	-	-	-	-	-
51 / 8	3.044	4179	8.87	13.67	1094	11.39	16.48
51 / 9	3.038	1944	5.11	13.56	69	7.46	19.66
51 / 10	-	-	-	-	-	-	-
51 / 11	3.042	4249	10.39	14.74	670	15.10	18.86
51 / 12	3.036	3270	4.88	10.57	1600	5.97	12.06
51 / 13	3.03	4308	10.70	14.90	0	13.99	17.76
51 / 14	3.03	3465	5.58	11.27	1344	6.73	12.79
51 / 15	3.04	4243	10.40	14.86	586	12.71	17.10
51 / 16	3.032	3723	6.42	11.71	1317	7.51	13.13
51 / 17	3.026	4306	10.66	14.90	0	13.44	17.58
51 / 18	3.044	4179	8.87	13.67	1094	11.39	16.48
51 / 19	3.036	4049	8.32	13.36	614	9.78	15.10
51 / 20	3.05	4041	8.39	13.32	1333	9.94	15.03
51 / 21	3.036	2365	2.67	10.59	1663	3.42	11.7
51 / 22	-	-	-	-	-	-	-
51 / 23	3.036	4308	10.65	14.90	0	13.22	17.40
51 / 24	-	-	-	-	-	-	-
51 / 25	3.034	2582	3.05	8.63	1597	3.82	9.74
51 / 26	-	-	-	-	-	-	-
51 / 27	-	-	-	-	-	-	-
51 / 28	3.036	3484	5.52	11.63	1542	6.72	13.14
51 / 29	3.04	4290	10.77	15.09	0	14.21	18.21
51 / 30	3.05	4080	9.8	14.68	10.44	12.63	17.47
Average	3.03625	3645.75	7.5425	12.896667	850.97667	9.63375	15.437917
Stand dev.	0.007443994	755.96758	2.6802064	1.867639	657.80429	3.6181521	2.8664218
Varience	0.00006	571486.98	7.1835065	3.4880754	432706.48	13.091024	8.2163737
Maximum	3.05	4316	10.95	15.1	1766	15.3	19.66
Minimum	3.02	1944	2.67	8.63	0	3.42	9.74

Exp. No.	Thickness (mm)	Impact Property for ABS Lustran 640 Condition : Decrease Melt Temperature					
		Load at Peak (N)	Peak Energy (J / mm)	Displ. to Peak (mm)	Load at Break (N)	Break Energy (J / mm)	Displ. to Break (mm)
53 / 1	3.06	2864	3.66	9.11	1340	4.46	10.22
53 / 2	3.058	4201	10.18	14.43	279	14.50	18.57
53 / 3	-	-	-	-	-	-	-
53 / 4	3.054	4164	10.06	14.36	636	14.65	20.07
53 / 5	3.06	2110	5.28	12.65	422	8.65	19.87
53 / 6	3.066	4226	9.70	14.09	515	12.50	16.72
53 / 7	3.074	4215	10.10	14.37	0	14.25	18.04
53 / 8	3.07	4235	10.12	14.36	0	14.8	18.55
53 / 9	-	-	-	-	-	-	-
53 / 10	3.06	4260	10.05	14.27	108	13.14	17.27
53 / 11	3.066	4211	9.96	14.62	403	13.30	17.65
53 / 12	-	-	-	-	-	-	-
53 / 13	3.056	4293	10.48	15.23	0	15.39	19.51
53 / 14	3.058	3355	4.95	11.17	1414	6.10	12.70
53 / 15	-	-	-	-	-	-	-
53 / 16	3.06	4263	10.15	14.21	173	13.24	17.28
53 / 17	3.06	4311	10.26	14.94	431	14.15	18.33
53 / 18	3.06	4199	9.54	14.05	603	12.38	16.89
53 / 19	3.058	4310	10.38	14.53	0	14.79	18.39
53 / 20	3.066	4339	10.40	14.56	128	13.98	17.00
53 / 21	3.036	2365	2.67	10.59	1663	3.42	17.96
53 / 22	3.054	4345	10.41	14.50	0	15.14	18.51
53 / 23	3.052	4306	10.51	14.65	111	14.88	18.67
53 / 24	3.054	4327	10.51	14.46	0	15.49	18.85
53 / 25	3.06	4313	10.51	14.59	0	15.29	18.89
53 / 26	3.06	4294	10.45	14.51	0	15.26	18.71
53 / 27	3.06	4282	10.35	14.64	0	14.58	18.47
53 / 28	3.054	4213	10.28	14.49	893	14.29	17.98
53 / 29	3.064	4221	10.06	14.38	93	14.32	18.22
53 / 30	3.05	4201	9.91	14.24	518	14.24	19.86
Average	3.058846154	4016.2692	9.2665385	13.923077	374.23077	12.968846	17.814615
Standard dev.	0.007203845	616.35701	2.2809892	1.4372996	477.55396	3.3769647	2.0993299
Varience	0.00005	379895.96	5.2029115	2.0658302	228057.78	11.403891	4.4071858
Maximum	3.074	4345	10.51	15.23	1663	15.49	20.07
Minimum	3.036	2110	2.67	9.11	0	3.42	10.22

VITA

Miss Busarin Intasian was born on February 6 , 1974 , in Nakhonnayok , Thailand. She received her Bachelor's Degree of Science in Industrial Chemistry from the Faculty of Science , King Mongkut 's Institute of Technology Ladkrabang in 1994. She pursed the Master's Degree in Polymer Science, in the Program of Petrochemistry and Polymer Science, Faculty of Science , Chulalongkorn University in 1997 and finished her study in 2000.